IDEA

Innovations Deserving Exploratory Analysis Programs

Highway IDEA Program

Development of a Fracture Mechanics-Based Asphalt Binder Test Method for Low Temperature Performance Prediction

Final Report for Highway IDEA Project 84

Prepared by:
Simon Hesp, Queen's University, Ontario Canada

February 2004

TRANSPORTATION RESEARCH BOARD
OF THE NATIONAL ACADEMIES

INNOVATIONS DESERVING EXPLORATORY ANALYSIS (IDEA) PROGRAMS
MANAGED BY THE TRANSPORTATION RESEARCH BOARD (TRB)

This NCHRP-IDEA investigation was completed as part of the National Cooperative Highway Research Program (NCHRP). The NCHRP-IDEA program is one of the four IDEA programs managed by the Transportation Research Board (TRB) to foster innovations in highway and intermodal surface transportation systems. The other three IDEA program areas are Transit-IDEA, which focuses on products and results for transit practice, in support of the Transit Cooperative Research Program (TCRP), Safety-IDEA, which focuses on motor carrier safety practice, in support of the Federal Motor Carrier Safety Administration and Federal Railroad Administration, and High Speed Rail-IDEA (HSR), which focuses on products and results for high speed rail practice, in support of the Federal Railroad Administration. The four IDEA program areas are integrated to promote the development and testing of nontraditional and innovative concepts, methods, and technologies for surface transportation systems.

For information on the IDEA Program contact IDEA Program, Transportation Research Board, 500 5th Street, N.W., Washington, D.C. 20001 (phone: 202/334-1461, fax: 202/334-3471, http://www.nationalacademies.org/trb/idea)

FOREWORD

by Simon Hesp, Principal Investigator

This report presents the progress obtained towards the development of an improved low-temperature grading method for asphalt binders. Because the proposed method is based on fundamental material properties, it should be able to predict performance for all binders irrespective of their source and/or modification method (polymer-modified, gelled, oxidized, or "engineered"). Additionally, the new method is an improvement over current specification systems as it better recognizes the importance of chemical and physical aging as well as fatigue cracking as potential aggravating factors in low-temperature failure.

The project work was divided into distinct tasks that were documented and discussed as they were completed. The intent was to provide the sponsoring agencies with a "work-in-progress" document, which by late 2003 became a comprehensive reference for the implementation of a simple and accurate method for the grading of asphalt binders for low-temperature performance. As this project progressed, major findings were presented at meetings and appeared as publications in the peer-reviewed asphalt literature.

The effort was jointly funded by the Charitable Foundation of Imperial Oil of Canada, the Ministry of Transportation Ontario, the National Cooperative Highway Research Program through their Innovations Deserving Exploratory Analysis (IDEA) program, the Natural Sciences and Engineering Research Council of Canada, Queen's University, and the University of Minnesota.

The major tasks towards the development of a fracture mechanics-based binder grading method were conducted at Queen's University in Kingston, Ontario. Graduate students Sushanta Dhar Roy, Serban Iliuta, and Hongcheng Xing were supervised by principal investigator Dr. Simon A.M. Hesp.

The SHRP bending beam rheometer tests (AASHTO M320) and direct tension tests (AASHTO MP1a) on a set of twelve asphalt binders used in various test sections in Ontario were carried out at the University of Minnesota in Minneapolis, Minnesota, and at the Imperial Oil Research Center in Sarnia, Ontario. The University of Minnesota work was performed by graduate student Arindam Basu under the supervision of co-principal investigator Dr. Mihai O. Marasteanu. The Imperial Oil work was supervised by Mary Gale.

This report documents all the results obtained and provides a short yet comprehensive analysis of the major discoveries.

As a result of the early findings, the Ministry of Transportation Ontario commissioned a new test road with seven sections, each containing a different asphalt binder. The construction of this pavement trial was completed in late 2003 on Highway 655 north of Timmins, Ontario. On January 9, 2004, the air temperature reached a record low of -43.9°C in Timmins. Hence, careful monitoring of this site should soon provide additional validation of the binder grading method developed through this research project.

January 18, 2004

CONTENTS

AUTHORS, ACKNOWLEDGEMENTS AND DISCLAIMER

This report was prepared by the principal investigator, Dr. Simon A.M. Hesp, at Queen's University in Kingston, Ontario. The co-principal investigator was Dr. Mihai O. Marasteanu at the University of Minnesota in Minneapolis, Minnesota.

The research reported herein was conducted under MTO Contract No. 9015-A-000190, "An Improved Low-Temperature Asphalt Binder Specification System," NCHRP-IDEA Contract No. 84, "Development of a Fracture Mechanics-Based Asphalt Binder Test Method for Low-Temperature Performance Prediction," and an Imperial Oil of Canada University Research Grant, "The Importance of Fracture Properties and Yield Stress in the Failure Behavior of Asphalt Mixtures at Low Temperatures." Additional financial support was provided through a Natural Sciences and Engineering Research Council of Canada research grant and by Queen's University and the University of Minnesota. All financial support is hereby gratefully acknowledged.

Liaisons for the Ontario Ministry of Transportation were Drs. Tony Masliwec and Kai Tam while for the NCHRP-IDEA program these were Drs. Inam Jawed and Edward Harrigan. Further guidance and support were kindly provided by Barbara Shannon of Imperial Oil of Canada and Dr. Keith Davidson of McAsphalt Industries.

Maureen Garvie of Kingston, Ontario, is hereby thanked for the excellent job she did at proofreading this report.

Parts of this report have been or soon will be published in the scientific asphalt literature (e.g., Roy and Hesp (2001a, 2001b), Basu et al. (2003), Hesp and Roy (2004), Hesp et al. (2004), Marasteanu et al. (2004)).

None of the sponsoring agencies necessarily concur with, endorse, or adopt the findings, conclusions or recommendations either inferred or expressly stated in subject data developed in this study.

An Improved Low-Temperature Asphalt Binder Specification Method

ABSTRACT

This report deals with issues related to the development of an improved low-temperature asphalt binder specification method. It examines the effectiveness and/or deficiencies of current Performance Graded Asphalt Cement (PGAC) specification testing to predict low-temperature performance. It documents the development of a new and apparently more accurate specification approach that avoids the problems of current methods.

The ability of various binder properties to predict transverse stress cracking in the field is assessed from a total of 17 pavement trial sections constructed in northern Ontario. The properties considered include those obtained from the bending beam rheometer and direct tension test as well as those from a more fundamental fracture mechanics-based test method. The results indicate that the currently used grading procedure does a reasonable yet not perfect job at predicting the ranking for most sections within each site but a poor job at the prediction of the onset of cracking.

Physical aging of the binder is indicated as a likely cause for early distress. Other deficiencies in current specification testing, such as inadequate chemical aging in the pressure aging vessel and the absence of true fracture mechanics-based failure tests in both the brittle and ductile states, are evaluated and recommendations are provided to address most problems.

The method as developed in this project was able to predict the onset of low-temperature cracking with much improved accuracy for five northern Ontario trial sections that showed early distress.

An Improved Low-Temperature Asphalt Binder Specification Method

SUMMARY

The research effort documented in this report focused on the development of an improved low-temperature grading test method for asphalt binders. The accuracy of the proposed fracture mechanics-based method, as well as the currently used AASHTO M320 (formerly MP1) and MP1a specifications, is evaluated with field distress data from a total of 17 pavement trial sections constructed in northern Ontario. The main outcome of this research is that a combination of factors is able to explain the early distress detected in a number of test sections. Physical aging, notch sensitivity, and in-service chemical aging of asphalt binders (above and beyond what is predicted by the pressure aging vessel), can explain, to a large extent, the early onset of transverse cracking. Fatigue cracking, which may start during short periods of freezing and thawing in spring, or during hot spells in summer, is also considered as a potentially aggravating factor since it can add to transverse cracking severity during subsequent low-temperature exposures in winter.

The need for improvement is best illustrated with two C-SHRP sections on Highway 631 near Hearst in northern Ontario, which were constructed in 1991 with binders of the exact same grade, but show a difference in transverse cracking severity of nearly a factor of twenty. Furthermore, two sections on Highway 118 near Bracebridge in northcentral Ontario, constructed in 1994 with binders of almost identical grade, are cracked by a more modest difference of 40 percent. This particular anomaly is believed to be mainly due to different traffic levels for the respective locations of the two sections. Finally, a PG 58-28 and both of the PG 58-34 sections constructed in 1996 as part of an SPS-9A site on Highway 17 in Petawawa in northeastern Ontario, which were exposed to minimum surface temperatures of approximately -27°C in their first winter and again in 2003, and hence should not have cracked, are damaged by a significant 169, 52 and 65 transverse cracks/km, respectively.

AASHTO M320 grading temperatures of nine available binders were determined according to standard protocol after one hour of isothermal conditioning at the grading temperature in the bending beam rheometer (BBR) bath as well as after 72 hours of conditioning. In addition, three binders were recovered from field cores after eight years of in-service exposure and similarly graded. AASHTO MP1a grading temperatures of the same twelve binders were also determined after one-hour and 72-hour conditioning periods. No major differences were found between the two grading methods; the MP1a critical temperatures were all within a few degrees of the M320 temperatures.

Although interim versions of the BBR low-temperature specification test protocol allowed for a determination of the grade temperature after both one-hour and 24-hour conditioning, the provision never appears to have found wide acceptance, for reasons that are not well documented. Two of the worst performing binders investigated in this project lost 10°C and 13°C in their grade temperatures after a 72-hour conditioning period whereas another (superior) binder lost only 3°C over the same period. These findings are in good agreement with those of Phillips (1999) who found in a laboratory study on 16 different binders losses ranging from a low of 1.5°C to a high of 6°C after a 24-hour conditioning period. These results indicate that physical aging can be a significant unknown factor, and hence its magnitude should be assessed in an improved low-temperature specification method.

The newly developed grading method limits the use of asphalt binders to a temperature at which they fail in a substantially ductile manner in the presence of a sharp notch. Ductility is defined by the level of plastic deformation in a test on a notched sample. An alternate approach limits the use of a binder to temperatures at which the fracture energy reaches 100 J/m^2 at either 0.01 or 0.001 mm/s rates of loading. The ductile-to-brittle transition temperatures determined in this manner are shifted by -10°C in order to account to some extent for loading rate effects. Additional field calibration efforts are currently underway and may eventually result in a small change in this shift factor. In addition to the determination of a simple grade temperature, the method also allows the user agency to set limits on the absolute fracture energies in the brittle and ductile states in order to reduce fatigue-related transverse and longitudinal cracking. Depending on the traffic levels, such limits may be set either high or low.

Special consideration is given to adequate chemical and physical aging of the asphalt before any performance testing is conducted. Binder aging in both the rolling thin film oven (RTFO) and pressure aging vessel (PAV) is done before grading, but it is recognized that these methods are not yet perfected; hence, provision is made for improved procedures. In addition, grading is done after one-hour and 24-hour conditioning at a specified temperature to assess the effect of physical aging. If the loss in grade temperature is significant, the user agency may only wish to accept the asphalt binder in a lower class.

The fracture grading results in this report were obtained on specimens in single-edge notched bending (SENB) as first described by Lee and Hesp (1994). The SENB test was refined so that it now requires only five grams of asphalt placed in between aluminum inserts, to accurately determine all relevant fracture mechanics-based failure properties. The introduction of a notch in the asphalt is facilitated through the insertion of a 25-µm thin Teflon® sheet that is removed just prior to testing. Fracture properties determined in a single test include the following: plane-strain fracture toughness, K_{Ic}; plane-strain fracture energy, G_{Ic}, in the brittle regime; generic fracture energy, G_f, in the ductile-to-brittle regime; and crack mouth opening displacement (CMOD).

The standard test method provides an option to use the compact tension (CT) geometry for which the load-line displacement and the crack mouth opening displacement are the same. This geometry has the advantage of making a separate CMOD measurement redundant; however, its drawback is that alignment becomes more critical. Current efforts are focussed on perfecting this test geometry.

Fracture mechanics-based properties were determined for all nine binders originally collected during construction of the test sections as well as for the three recovered binders that had been in service for eight years. Fracture toughness, K_{Ic}, fracture energies, G_{Ic} and G_f, and crack mouth opening displacements (CMOD) were determined at two rates of loading and various temperatures around the brittle-to-ductile transition point. Fracture tests were conducted on samples conditioned for 72 hours at a temperature 10°C warmer than the regular AASHTO M320 grade temperatures. It was found that the grading based on a 100 J/m^2 fracture energy limit was more critical than either of the AASHTO M320 or MP1a grading methods after both one-hour and 72-hour conditioning periods. While the limiting fracture energy temperatures were significantly warmer than those determined according to currently used practice, they came very close to the likely cracking onset temperatures for the five sections that showed early distress. It is anticipated that a practical grading test would determine a grade temperature after two different conditioning times (e.g. after two and 24 hours of physical aging) in order to predict the grade temperature after longer times which are more realistic in terms of actual field conditions (e.g., after 72 hours).

Fracture mechanics-based properties were also determined at 0°C for a limited set of four unaged binders used in test sections on Highway 118. At a 30 mm/min rate of loading in the double-edge notched tension test (DENT) the essential work of fracture, w_e, and plastic work of fracture term, βw_p, were found to vary a great deal between different binders. Essential works of fracture ranged from 3.9 $kJ.m^{-2}$ to 23.3 $kJ.m^{-2}$ while plastic works varied from 0.5 $MJ.m^{-3}$ to 2.7 $MJ.m^{-3}$ for only four binders tested. These data suggest that the fracture resistance of different binders during freeze-thaw periods in the spring can be a significant unknown factor, and hence its magnitude should be assessed in an improved low-temperature specification method.

The results of this research show that the physical aging and notch sensitivity effects can be substantial and that to a large extent they are able to explain the early failures reported in this study (and likely many of those reported in the literature). In addition, chemical aging due to both oxidation and volatilization, beyond what is predicted by the current laboratory aging methods, is evidently also an important factor in low-temperature failure. Furthermore, fracture properties at 0°C were found to vary a great deal between different binders. Hence, it is proposed to grade asphalt binders after appropriate chemical and physical aging in the presence of a sharp notch to replicate the absolute worst possible conditions as they may materialize at some point in the life of the pavement. In addition, lower limits should be set on the fracture energies in the ductile state to lessen fatigue distress during freeze-thaw cycles that can aggravate low-temperature cracking. Once the proposed grading system is implemented it is expected that the predicted performance will more closely match the observed performance and that unnecessary failures can be avoided.

Chapter **1**
INTRODUCTION AND SCOPE

1.1 Problem Statement

Soon after the United States' Strategic Highway Research Program (SHRP) ended in the early 1990s, it was realized that the binder grading methods developed with straight asphalts may not always be sufficient for the performance prediction of modified and specialty asphalt binders. With respect to the low-temperature grading test development effort, SHRP researchers recognized that "Ideally, it is necessary to determine the fracture mechanics parameters for neat asphalt cement as well as for hot-mix asphalt concrete" (Anderson et al. (1994)); however, due to a lack of time and resources, in the end only the bending beam rheometer (BBR) and the direct tension test (DTT) were developed and no direct comparison was ever made with more sophisticated fracture mechanics-based failure tests.

About the same time as the final SHRP reports were released, research at Queen's University had started on the fracture mechanics testing of binders in their brittle state (Lee and Hesp (1994), Morrison et al. (1994), Lee et al. (1995)). This early work recognized that binders of approximately the same SHRP performance grade could show enormous differences in their low-temperature fracture toughness and fracture energy. Furthermore, it was later discovered that notched binder specimens sometimes fail in a brittle fashion at much warmer temperatures than unnotched specimens (Hoare and Hesp (2000)). Hence, since these results were published, some (e.g., Ponniah and Hesp (1996), Ponniah and Kennepohl (1998), Hesp et al. (2000), Anderson et al. (2000 and 2001)) have suggested these differences in brittle fracture properties could perhaps explain the many anomalous results reported in the literature (e.g., Robertson (1995), Kandhal et al. (1996), Button and Hastings (1998), Anderson et al. (1998), Anderson et al. (1999), Abd El Halim et al. (1999 and 2001), Reinke and Dai (2001) and others).

The study reported herein aims at providing a more definitive answer by carefully determining the fracture properties of appropriately aged binders with field performance of corresponding test sections on Highway 118 in Bracebridge, Ontario, and on Highway 17 in Petawawa, Ontario. In addition, performance data from a trial on Highway 631 near Hearst, Ontario, which was constructed in 1991 as part of the Canadian SHRP program (C-SHRP), are reviewed to further illustrate the need for improvement.

1.2 Research Plan

The project set out first to refine the original fracture toughness test method as published in 1994 (Lee and Hesp (1994)) and then to validate the results obtained for binders with mixture and field data. The research program involved a number of distinct tasks: (1) development of a practical yield stress test; (2) development of a practical fracture toughness test; (3) crack surveying; (4) binder aging; (5) SHRP testing of asphalt binders; (6) fracture and yield stress testing of Highway 118 and Highway 17 binders; (7) fracture testing of field mixes; and (8) reporting.

For the development of a practical and accurate low-temperature binder specification method, some of the same guiding principles as those facing the SHRP researchers were used (Anderson et al. (1994)):

- the sample preparation needs to be easy;
- it must be possible to use a standard test apparatus to obtain reproducible results;

- it must be possible to conduct a large number of tests within a short time;
- it must be possible to evaluate the effect of parameters such as time of loading and temperature.

Since there were limited cracking data from the field, an additional set of experiments was conducted in the laboratory to validate the binder test results with those obtained in a true fracture test on the mix. Core samples were similarly tested in order to force sample failure under circumstances of temperature and level of tensile strain that may never be realized for the specific field locations.

1.3 Future Work

Since the test sections in both Bracebridge and Petawawa were designed at a time when the current state of knowledge was not yet available, the binders that were used are not ideally suited for field validation of the current low-temperature specification methods. In Bracebridge, the continuously graded, SHRP low-temperature grades ranged from approximately -23°C to -38°C whereas the high temperature grades ranged from +67°C to +75°C. In Petawawa, the low-temperature grades used ranged from -31°C to -40°C while the high-temperature grades were all kept close to +58°C. For the weather stations nearest to these test locations (i.e., Muskoka Airport and CFB Petawawa), the specified 98 percent confidence limits for the low-temperature grades are -32.5°C and -33.7°C, respectively (LTTPBind, v. 2.1 (1999)). Hence, it is unlikely that all of the sections will be challenged within a reasonable time thus confounding the effects of aging, fatigue and general deterioration with those of thermal cracking. A serious unknown factor for the Highway 118 site is the variation of traffic levels for the different test sections. Finally, what effect, if any, the fact that the Petawawa SPS-9A site was constructed over two years, with the binder course in 1996 and the surface course in 1997, has had on the premature cracking in this site is another unknown factor.

Although the Bracebridge and Petawawa sites may be interesting from a whole life cycle cost analysis perspective, they are not ideally suited for the validation of a single distress mechanism such as low-temperature cracking. The Petawawa site should become interesting from a high-temperature point of view since all its sections have a high-temperature grade close to +58°C.

To come to a definitive field validation of both the AASHTO M320 and MP1a approaches to low-temperature grading as well as the proposed fracture mechanics-based specification system, it was imperative that a new test site be constructed with a number of carefully chosen binders. All binders should possess a *single* SHRP grading that provides a reasonable degree of certainty that within the first few years of service the sections will all be exposed to a temperature that guarantees some transverse stress cracking. The onset of cracking and the severity can then be correlated with the limiting temperatures as provided by the various grading methods.

The Ministry of Transportation Ontario has just included such a test site within a large Superpave® contract for Highway 655 in the far north of Ontario. It has side-by-side seven sections containing binders with performance grades that are all within the -34°C to -36°C range, as measured according to AASHTO M320, but that have large variations in fracture properties. The project involved a design of two layers, 50-mm binder course and 40-mm surface course, with the same binder in both lifts on both lanes of each 500-m section. This major new trial pavement was successfully constructed by Miller Paving in late 2003. Since the air temperature in the Timmins area reached a record low of -43.9°C on January 9, 2004, it is expected that this effort will soon add to the information presented in this document. This well-designed test road will provide an ideal opportunity to determine which properties are best used for performance prediction.

Chapter 2
LITERATURE REVIEW OF LOW-TEMPERATURE ASPHALT BINDER SPECIFICATION DEVELOPMENT EFFORTS

2.1 Early Investigations of Failure in Asphalt Binders and Mixtures

Seminal investigations into the failure of asphalt binders and mixtures at Koninklijke-Shell Laboratories in Amsterdam focused on stiffness as the cardinal property in rutting, fatigue as well as in low-temperature fracture (Van der Poel (1954, 1955), Heukelom (1966, 1969), Hills (1974)). In one of these early papers on rheology and fracture in binders and mixes, Heukelom concluded from his experimental data (1966):

- "that Van der Poel's stiffness concept has provided a valuable means of simplifying the description of, not only rheological, but also fracture properties of asphalt cements and asphalt mixes.";
- "the modulus of asphalt cement is a measure of the rheological condition of the bitumen, on which the fracture properties depend. The effect of temperature and loading time on the fracture properties of road bitumens of various grade and origin is thus condensed in the stiffness as a single parameter."; and
- "Parameters for the fracture properties of mixes can be separated into the stiffness of the asphalt cement and a 'mix factor' which is independent of the above-mentioned variables, but dependent on the proportion of asphalt cement, grading of the minerals and compaction of the mix. A further study of these variables can be simplified by determining the value of the mix factor only, so that much superfluous laboratory effort can be saved."

Following these far-reaching suggestions, a large number of researchers (e.g., McLeod (1968), Fromm and Phang (1970), Readshaw (1974), Hills (1974), Deme and Young (1987)), as well as those involved in the SHRP program (Anderson et al. (1994)) and others, have thus focused their attention on stiffness as a binder specification parameter for failure at low temperatures. It is generally assumed that if the stiffness at a somewhat arbitrary loading time exceeds a limiting value, transverse cracking will occur in the road. It is not widely recognized, however, that the correlations made by Heukelom were only valid for unmodified binders. While modifiers were used only sparingly in the late 1960s, today the situation is different in that in some areas nearly half of all binders are modified (air blown, polymer-modified, gelled, "engineered," etc.) (Bardesi et al. (1999)). This development, which has slowly evolved over the last 30 to 40 years, was the main reason for the existence of the Strategic Highway Research Program (SHRP). The ultimate aim of SHRP was to find better ways to evaluate asphalt materials by using properties that are more accurate and reliable for performance prediction.

2.2 Bending Beam Rheometer and Direct Tension Specification Tests

The SHRP program developed two test methods for low-temperature performance grading of asphalt binders: the bending beam rheometer (BBR) and the direct tension test

(DTT) (Bahia et al. (1992), Anderson et al. (1994), Anderson and Dongré (1995)). The bending beam rheometer was developed to provide a measure of both the creep stiffness (S(t)) and the relaxation ability (m(t)) of an asphalt binder as a function of time. If a binder is too stiff, it will likely produce mixtures that give rise to high thermal stresses, given the fact that stress is directly proportional to stiffness. Such high-stress situations are unwanted, since they are commonly believed to lead to a high incidence of transverse stress cracking. The second parameter measured with the bending beam rheometer is the slope of the creep stiffness versus time curve, the so-called m-value. It reflects a binder's ability to reduce thermal stresses through viscous flow mechanisms. If the m-value reaches a certain limiting value (0.3 at 60 seconds loading time), the binder is said to be unable to relax thermal stresses, a characteristic that could also lead to a high incidence of transverse thermal stress cracking. The SHRP low-temperature binder specification based on the BBR is generally believed to do a reasonable job for unmodified binders, but its usefulness for modified binders is less certain (Kluttz and Dongré (1997), Dongré et al. (1997), Anderson (1999)).

The second binder test developed by SHRP researchers was intended to measure failure characteristics under realistic low-temperature and loading conditions. The direct tension test was specifically designed to test binders with a high stiffness (300 MPa < S(60) < 600 MPa) which were thought to give adequate low-temperature performance in the pavement. The reader is referred to other publications for a detailed discussion of the various hypotheses used in the development of the direct tension test (Anderson et al. (1994), Anderson and Dongré (1995)). However, the direct tension test does not appear to have found wide acceptance. Current efforts are directed toward combining the BBR with the DTT results in order to predict a so-called critical cracking temperature reflecting both the rheological and failure characteristics of a binder (Kluttz and Dongré (1997), Dongré et al. (1997), Bouldin et al. (2000)).

Since the SHRP program ended in 1994, reports have appeared that raise concerns about the ability of both the bending beam rheometer and direct tension tests to predict and/or rank the performance of asphalt binders, irrespective of formulation, production method, and modification level (e.g., Robertson (1995), Kandhal et al. (1996), Ponniah and Hesp (1996), Button and Hastings (1998), Anderson et al. (1998), Anderson et al. (1999b), Abd El Halim et al. (1999, 2001), Anderson et al. (1999a, 2000 & 2001), Hesp et al. (2000), Reinke and Dai (2001)). There is now much suspicion and some actual evidence that inferior binders are still able to pass the SHRP specification criteria while superior binders may not always be recognized as such. Hence there is a need for a comprehensive, material property-based specification system.

2.3 Critical Cracking Temperature

Recently Bouldin et al. (2000) proposed to control transverse cracking by specifying a limiting temperature at which the failure stress of the binder is reached due to thermal shrinkage in uniaxial tension. The approach largely follows the ideas of Hills (1974) from Koninklijke/Shell Laboratories in Amsterdam, who developed it for asphalt mixtures. The stiffness and relaxation data from the BBR is used to calculate the thermal stress buildup in the binder, which is then compared with the tensile strength as measured in the direct tension test, in order to get a critical temperature at which the binder would be expected to fail. The so-called "pavement constant" is introduced in the binder method in an attempt to scale the thermal stress developed to that in the asphalt concrete pavement (Bouldin et al. (2000)).

In a study on two unmodified and six modified asphalt materials, it was found that this pavement constant could vary between 3.4 and 16.7 (Roy and Hesp (2001a)). This was revealed through comparing the true stress buildup in a restrained cooling test on the binders with that in the corresponding mixtures. Such a large variation for only eight systems in what is supposed to be a constant naturally casts much doubt on the validity of this concept. The approach has nevertheless been adopted as a provisional standard under the MP1a designation by AASHTO, which was used in the present study to obtain MP1a grading temperatures for all available binders.

2.4 Thermal Stress and Failure in Asphalt Pavement Mixtures

When a pavement cools, a number of processes occur either successively or simultaneously. Only after a detailed understanding of these processes is obtained, can pavements be designed that will not fail due to exposure to low temperatures. Initially when a pavement cools, the asphalt binder is soft enough for any shrinkage stress that may occur to dissipate through viscous flow. However, upon further cooling, the asphalt binder stiffens, and at some temperature thermal stresses can no longer relax through viscous mechanisms. Eventually these thermal stresses can become so great that some measure of strength of the asphalt concrete may be exceeded, and this could result in the formation of large cracks transverse to the driving direction. However, the words "some", "may" and "could" are used here because at the present time it is unresolved which properties are critical. Furthermore, there is no direct evidence that large transverse cracks *always* occur in pavements that have been exposed to extreme temperatures.

Anecdotal evidence suggests that different scenarios are in fact possible and that there are pavements that have shown minimal thermal cracking even after 30 to 40 years in service. One documented test site on a road monitored for the Canadian part of the Strategic Highway Research Program (C-SHRP) provides a good example: Highway 57, approximately 50 km east of Toronto, Ontario, had four different overlays constructed on a severely cracked pavement (153 cracks/km) in 1990 (Frechette and Shalaby (1997)). The three unmodified sections (75 mm virgin HMAC, 100 mm virgin HMAC and RAP/HMAC asphalt) all cracked at the same places where there were underlying cracks in the original pavement soon after construction. In contrast, the 75 mm thick section made with a binder that was modified with 4 percent by weight of a styrene-butadiene polymer has shown superior performance in that only one transverse crack had reflected through some five years later. Whether this was due to the use of softer base asphalt, a tougher binder or some other as yet unidentified factor remains to be investigated.

Later in this report the results from another C-SHRP trial on Highway 631 west of Hearst, Ontario, will be reviewed. For this site there is one section which has been exposed to temperatures well below its SHRP grade temperature but it is only cracked to a limited degree. Such examples show that our understanding of low-temperature failure is still incomplete.

The important early publications by Fabb (1974) and Hills (1974), combined with later reports from Kim and coworkers (Kim and El Hussein (1995), El Hussein et al. (1998)), Shin and coworkers (Shin et al. (1996), Bhurke et al. (1997)), Fortier and Vinson (1998), and Hesp and coworkers (Hesp et al. (2000), Roy and Hesp (2001)), may provide some insight into an important detail of the failure mechanism that can explain the existence of pavements with a much lower tendency towards transverse stress cracking.

Fabb (1974) at the British Petroleum Company was the first to rigorously evaluate the thermal stress restrained specimen test (TSRST). He used the test, originally proposed by Monismith and coworkers (1965), to investigate the effects of such variables as aggregate type and gradation, filler and binder content, and additives on the failure behavior of asphalt mixtures at low temperatures. In considering a failure criterion for the TSRST, Fabb stated the following: "because it was considered that the cessation of stress increase indicated incipient failure, the temperature at which maximum stress was first attained was adopted as the failure criterion." Many research studies in later years adopted the same criterion or were silent on the issue of how to define failure. Fabb also noted that in his entire study there was very little variation in the failure stress and that the use of polymers does not "present a cure for this problem" (i.e., thermal cracking) because his "failure temperatures" did not change by more than a couple of degrees when various polymers were added to the straight bitumen. This finding was later confirmed by the work of others on different modified systems (e.g., Isacsson and Zeng (1998), Fortier and Vinson (1998), Hesp et al. (2000)), but the question of which failure criterion to choose in the TSRST is still unresolved.

Fortier and Vinson (1998) remark that in their work "several modified AC specimens displayed a low-temperature failure without apparent fracture. This behavior would appear to be advantageous for the performance of pavements in cold regions." Hesp et al. (2000) report on sophisticated thermal fatigue tests in which certain tough samples are taken to temperatures as low as -50°C without any apparent catastrophic fractures. In contrast, brittle binders did fail in such fashion.

At about the same time as Fabb published his TSRST findings, Hills from Koninklijke-Shell Laboratories in Amsterdam reported on the development of his so-called "glass plate" test (Hills (1974)). By cooling thin films of asphalt in a glass dish, he noted that fracture initiated close to the glass, when a cracking sound was heard, but further cooling was required to propagate the cracks to the free bitumen surface. Hence, these experiments suggest that, at least in Hills' glass plate test, debonding occurred before binder fracture ensued. More recent work by Shin and coworkers at the University of Michigan (Shin et al. (1996), Bhurke et al. (1997)), by Jacobs and coworkers at Delft University in the Netherlands (Jacobs (1995), Jacobs et al. (1996)), and by Kim and coworkers at the National Research Council of Canada in Ottawa (Kim and El Hussein (1995), El Hussein et al. (1998)) has confirmed that in real asphalt mixtures the failure process indeed often starts with yielding, soon followed by the development and propagation of cracks along the coarse aggregate interface. Although the primary reason for this to occur is the difference in thermal contraction between the binder (or mastic) and coarse aggregate, triaxial stress states that exist ahead of propagating cracks can also contribute substantially to the debonding process. The formation of these so-called "damage zones," as well as the loss of interfacial adhesion, has been observed in mixtures in the laboratory, and actual pictures exist in the asphalt literature (Jacobs (1995), Shin et al. (1996), Kim et al. (1997), Bhurke et al. (1997), El Hussein et al. (1998), Radovskiy (2000)).

The fact that cracks often form along the interface explains why Fabb and those after him did not see large effects due to the addition of polymers. Toughness may greatly be increased, but the change in interfacial integrity still occurs at about the same temperature as for unmodified systems, causing thermal stress to reach a maximum. Combined with Fabb's choice of a somewhat arbitrary failure criterion, this gives the impression that binder toughness does not matter when it comes to thermal cracking and that only stiffness influences the failure temperature.

The work reported herein aims at disproving this notion by carefully comparing stiffness (SHRP BBR) and strength (SHRP DTT, fracture toughness, fracture energy and crack opening properties) for a number of binders with known field performance. The very fact that failure often starts and progresses at the interface of the coarse aggregate suggests that it is toughness that is important (or perhaps interfacial toughness, which relates to binder toughness). It is not what happens in the early stages that should be a concern but rather what happens subsequent to the loss of interfacial adhesion. Secondary events can result in the formation of large transverse cracks and total disintegration of the road structure. Or, provided that the binder is tough enough to prevent microcrack coalescence and propagation, they can present a more favorable situation with only microcracking and a consequent reduction in thermal stress (Hesp et al. (2000)). For this reason, research at Queen's University started in 1994 with the aim of using fracture properties of the binder to predict more accurately the onset and severity of thermal cracking in pavement mixtures. Eventually this work may be able to explain why certain pavements fail sooner than expected and why others never fail through fracture.

2.5 Why Fracture Mechanics Tests?

Whereas creep stiffness as measured in the bending beam rheometer is a material property, the direct tension failure stress and/or strain in the brittle state are not, and so it is reasonable to assume that these properties are better replaced by a measure of toughness. Fracture toughness provides a measure of resistance to failure in the presence of severe tensile constraint and sharp cracks. Further, as this property is independent of sample size and geometry, it should be particularly useful for specification testing. Combined with the stiffness and/or yield stress, the toughness can provide a fundamentally sound specification system that is likely to do better than any of the currently available grading methods.

2.5.1 Fracture Mechanics Principles

The use of sophisticated fracture mechanics tests on asphalt mixtures has been well documented for many years (Ioannides (1997)). Since both fatigue and thermal distress involve a fracture process, many researchers have favored the use of advanced methods and theories, developed primarily for metals, composites and ceramics, applying these to better understand asphalt.

Studies on asphalt concrete have involved the use of fracture toughness (K_{Ic}) and fracture energy (J_{Ic}) parameters (e.g., Irwin (1977), Little and Mahboub (1985), Abdulshafi and Majidzadeh (1986), Dongré et al. (1989), Mahboub (1990), Ramsamooj (1991), Sulaiman and Stock (1995), Bhurke et al. (1997)) as well as more extensive R-curve methods (Mobasher et al. (1997), Marasteanu et al. (2002)), specific energy of damage approaches (Aglan et al. (1992)) and cohesive crack model approaches (Jenq et al. (1991, 1993)).

In the mid-1990s, research at Queen's University for the first time explored a very simple, notched three-point bend test to measure resistance to brittle fracture in both straight and various polymer-modified asphalt binders at low temperatures (Lee and Hesp (1994), Morrison et al. (1994), Lee et al. (1995)). Although tests on asphalt specimens had been done before in three-point bending at low temperatures (see, for example, Heukelom (1966)), the introduction of a sharp notch was first investigated in the work at Queen's University. Fracture toughness so measured, and as defined in the various ASTM standards on which these efforts were based, is defined as follows:

> *the resistance of a material to fracture in a neutral environment in the presence of a sharp crack under severe tensile constraint, such that the state at the crack front approaches plane strain, and the crack-tip plastic (or non-linear viscoelastic) region is small compared with the crack size and specimen dimensions in the constraint direction.*

The ASTM methods continue with a statement that:

> *A K_{Ic} value is believed to be a lower limiting value of fracture toughness. This value may be used to estimate the relationship between failure stress and defect size in service* (ASTM E 399 (1990) and D 5045 (1996)).

Hence, K_{Ic} is really a measure of *strength* in the presence of sharp notches rather than a measure of *toughness* (Harder (1992)). By combining K_{Ic} with the stiffness modulus, E, one does obtain a measure of toughness given by the fracture energy, G_{Ic}, which is also a true material property for brittle materials:

$$G_{Ic} = (1 - \nu^2)\frac{K_{Ic}^2}{E} \quad \text{(plane strain)} \qquad (2\text{-}1)$$

The plane-strain fracture energy, G_{Ic}, being a material parameter independent of specimen size and geometry, is ideally suited for the study of thermal cracking in binders and mixtures subjected to thermal shrinkage stresses. Unlike the properties derived from the SHRP DTT and other less commonly used methods (e.g., Fraass' fracture test, Hills' glass plate test), fracture energy is based on the fundamental principles of mechanics and conservation of energy. Only fracture mechanics-based parameters can separate those effects that are due to specimen geometry from those due to intrinsic material properties (e.g., see Mai et al. (2000) and references therein).

It should be recognized, however, that the situation in a pavement is still considerably more complex. Initially there exists three-dimensional constraint and hence plane-strain conditions but during the final stages of failure there must locally be conditions that resemble plane-stress states (for which the fracture toughness is not a material property independent of specimen geometry and size). Furthermore, the issue of the interface and what effect it has on the failure process must be considered. It may be possible to measure the interfacial fracture properties but that was beyond the scope of this project. Finally, many pavements also suffer from repetitive compressive loadings (i.e., fatigue) during periods of cold weather and, perhaps more importantly, during periods of spring thaw when the subgrade provides little support. The consequences of these added forms of distress are not clear at this time but there are reports in the literature of increased amounts of transverse cracking in truck lanes and truck hill climbing lanes as opposed to the passing lane (e.g., Deme (1996).

For the above reasons we have also investigated the generic fracture energy in the ductile-to-brittle transition regime, G_f, and the essential and plastic works of fracture in the ductile regime, w_e and w_p, respectively. User agencies can select to do a comprehensive fracture grading of an asphalt binder and set the limiting grade temperature depending on weather data, and adjusting the fracture energies in the brittle-to-ductile and fully ductile regimes depending on traffic levels.

2.5.2 Previous Results for Fracture Toughness Tests on Asphalt Binders

The first results on the plane-strain fracture toughness properties of regular and modified asphalt binders are given in papers by Lee and Hesp (1994), Morrison et al. (1994) and Lee et al. (1995). These early efforts were primarily aimed at using the *quantitative* fracture mechanics approach to better understand the effect of polymer-bitumen compatibility on fracture resistance. Lee et al. (1994) and Morrison et al. (1994) investigated the effects of polymer content and type, particle size, and bitumen source in polyethylene-modified systems on fracture properties such as fracture toughness, fracture energy and stiffness.

These early studies proved that the polymer's compatibility with the bitumen has enormous influence on fracture resistance as measured by K_{Ic} and G_{Ic}. For instance, Figure 2.1 shows the effect of polymer content and base bitumen on K_{Ic} in chlorinated polyethylene-modified systems. The data show not only an effect from the polymer content but also a significant effect from the bitumen penetration grade and source. (The 200-300 grade was from a different source than the other two grades, which were both from the same South American source.) The same polymer definitely does not provide the same performance benefit in different base asphalts.

Ponniah and Hesp (1996) were the first to suggest the use of binder fracture energy for performance grading at low temperatures. Their results will be discussed in more detail later.

Recent papers from Queen's University by Hoare and Hesp (2000) and Roy and Hesp (2001a, 2001b) have compared wider ranges of commercially more relevant polymer modifiers, and once again large differences were found in fracture resistance. Base bitumen, compatibility, polymer molecular weight and degree of crosslinking were all found to be important factors that influence the toughness of the binder.

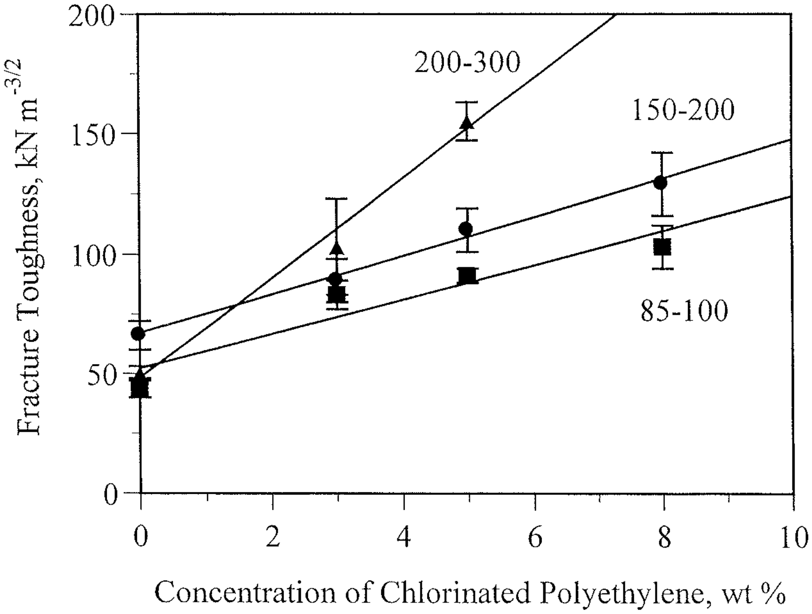

Figure 2.1 Effect of polymer concentration and bitumen grade and source on fracture toughness in chlorinated polyethylene systems (error bars give 90 percent confidence level). (Reproduced from Lee et al. (1995))

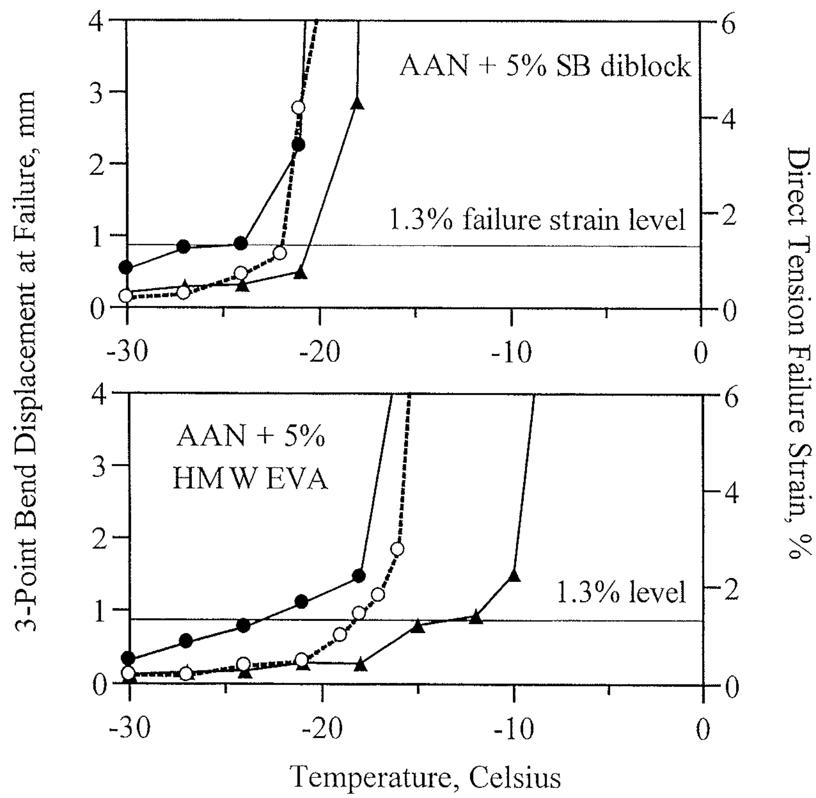

Figure 2.2 Effect of notching on the ductile-brittle transition in two modified binders. (Reproduced from Hoare and Hesp (2000))

To show the important difference between a notched and an unnotched test, Hoare and Hesp (2000) measured the ductile-brittle transition in bending, on notched and unnotched specimens, as well as in (unnotched) direct tension. Figure 2.2 shows results for AAN binder modified with 5 percent SB diblock and EVA copolymers. The results indicate that for performance grading it makes a big difference whether a sample is notched (solid triangles for three-point bending) or unnotched (solid circles for three-point bending and open circles for DTT). The SB diblock system loses only about 2-3°C due to notching, whereas the EVA system loses as much as 6-9°C. To put these differences in performance grading into perspective, Figure 2.3 provides the low-temperature statistics for the Bracebridge and Petawawa locations as obtained from the software program LTPPBind (1999). This indicates that an error of about 6°C in the performance prediction for the two binders could mean a reduction in confidence from 98 to 50 percent that in a given year a pavement would not be exposed to a temperature that causes damage due to thermal cracking. In other words, if these binders were used based on the unnotched performance grading, the EVA system would probably crack every other year while the SB system may perform close to what is desired (i.e., at a 98 percent confidence level).

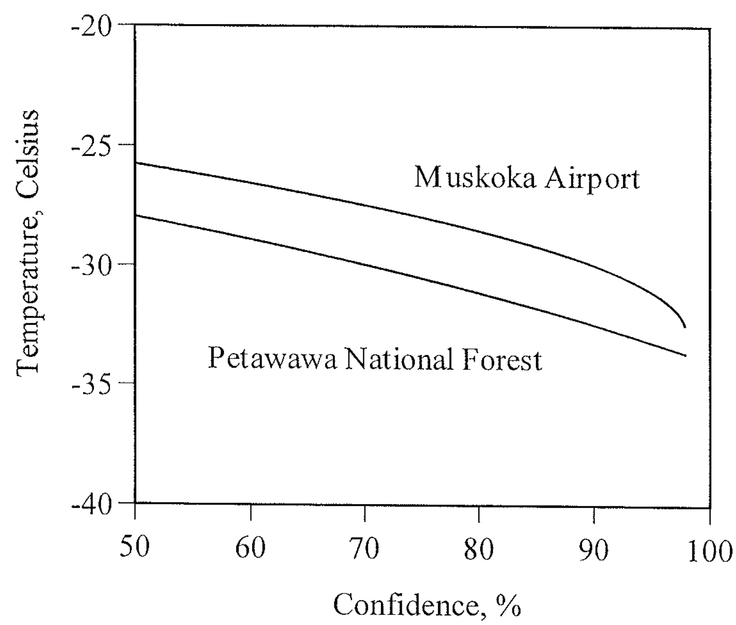

Figure 2.3 Low-temperature performance statistics for Bracebridge (i.e., Muskoka Airport) and Petawawa locations. (Reproduced from LTPPBind Software v. 2.1 (1999))

Garces et al. (1996) were able to use the toughness test to investigate mastics and were able to validate their data with the crack pinning theory as originally developed by Evans (1972) and later refined by Green et al. (1979). An understanding of this theory has already allowed for the design of mixtures with significantly improved rutting resistance (Hesp et al. (2001)).

The early results on polyethylene systems, as well as the later data with EVA, SBS, SB and other polymers, have since been confirmed by others (Sabbagh and Lesser (1998), Champion et al. (1999, 2000) and Anderson et al. (2000, 2001)). There is now consensus that binders with the same performance grades can have enormous variations in fracture properties in their brittle state. This finding, as exemplified in Figure 2.4, led to the current effort to investigate whether those differences have any influence on the onset and severity of thermal cracking.

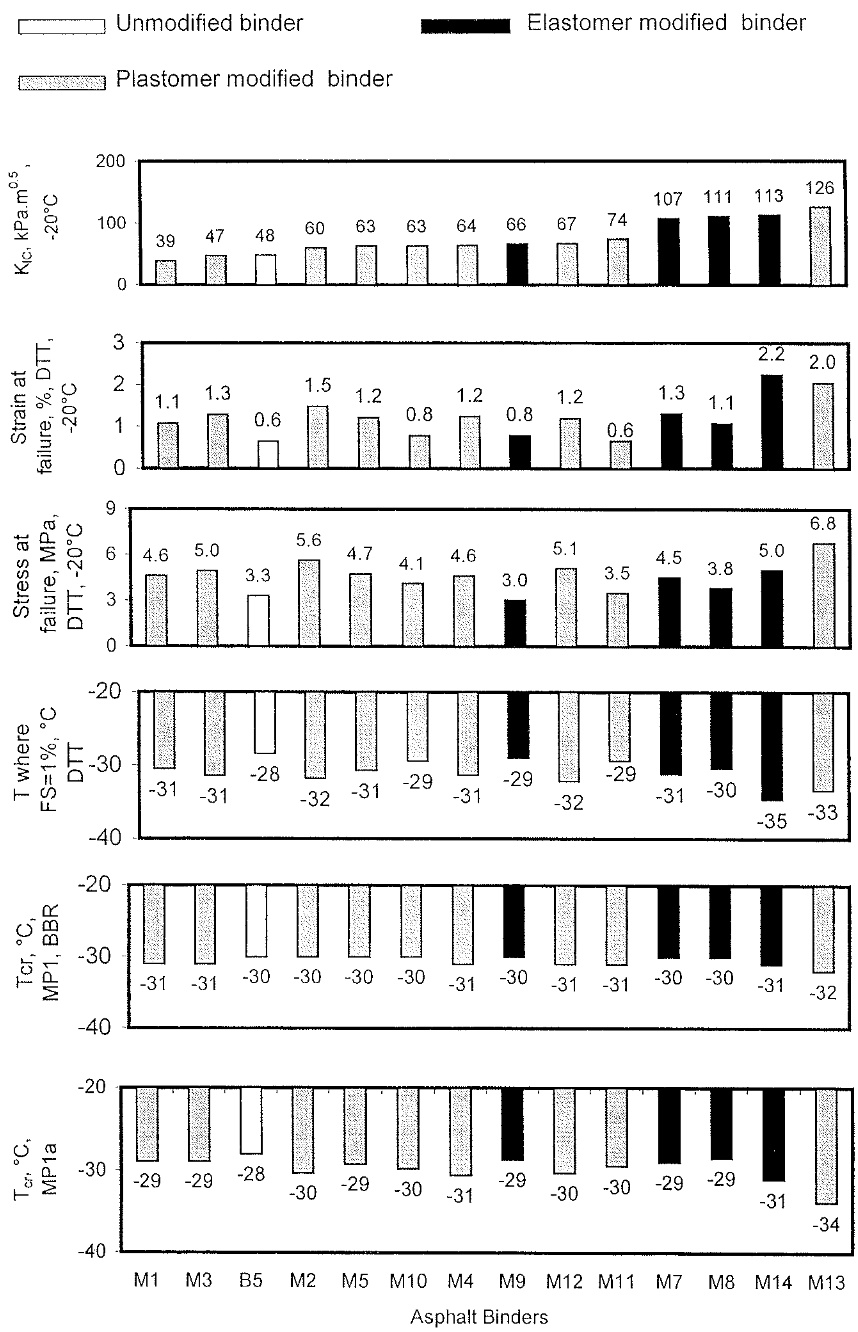

Figure 2.4 Low-temperature specification data in contrast with fracture toughness for a range of straight and modified asphalt binders. (Reproduced from Anderson et al. (2001))

Chapter 3
MATERIALS AND EXPERIMENTAL DETAILS

3.1 Materials

3.1.1 Materials for Test Development and Laboratory Validation Studies

The materials used in this part of the project were obtained from various sources (a detailed discussion of this work is published in Roy and Hesp (2001a, 2001b)).

3.1.1.1 Base Asphalts

The asphalt binders used in the laboratory validation study were obtained from the SHRP Materials Reference Library in Reno, Nevada, and from Golden Bear Oil Specialties in Oildale, California. The material obtained from Golden Bear was used as a substitute for the low asphaltene California Valley binder that had been used by SHRP (reference code AAG-2) but was no longer available. The pertinent properties for both AAG-2 and AAN binders are given in Table 3.1 (SHRP MRL (1994)).

3.1.1.2 Polymer Modifiers

All polymer modifiers were added at a level of 5 percent by weight to the binders. Diblock, linear triblock, and two different radial styrene-butadiene copolymers were obtained from various commercial sources. The tapered diblock SB polymer was reported to contain 25 percent styrene (17 percent in a pure polystyrene block with the remainder in the tapered part) whereas all three SBS polymers were reported to contain 30 percent styrene. The diblock SB had a molecular weight of approximately 75,000 g/mol, the linear SBS a molecular weight of approximately 200,000 g/mol and the two radial SBS polymers molecular weights in the 400,000 g/mol range. These three styrene-butadiene polymers are different by their molecular weights and ability to form a three dimensional network (i.e., number of styrene blocks within one molecule).

Table 3.1 Asphalt Binder Properties †

Binder	AAG-2	AAN
Source	California Valley	Bow River
SHRP Grade	58-16	58-16
Conventional Grade	AR-2000	85/100
Asphaltenes, %	5.0	15.7
Polars, %	51.0	33.9
Aromatics, %	35.3	40.1
Saturates, %	6.6	10.3

† SHRP MRL (1994)

One of the radial SBS modifiers came extended with 30 percent carbon black and 20 percent heavy oils so this material was tested at 10 weight percent in the AAN binder (5 percent SBS). The carbon black interacts with the asphaltene fraction in the AAN binder, making the remainder more compatible with the polymer modifier. All these styrene-butadiene polymers are frequently used for asphalt modification although not necessarily in AAN and AAG-2 base asphalts.

An ethylene-vinyl acetate (EVA) modifier was obtained from a commercial source. The vinyl acetate content was reported by the supplier to be 20 percent, and it had a high molar weight. The polymer is widely used in road paving but again not necessarily in the AAN base in which it was used in this study.

3.1.1.3 Aggregates

The aggregates and baghouse fines for the laboratory validation studies were collected from a quarry near Kingston, Ontario. The gradation matched a standard Ontario dense-graded surface mixture with a maximum aggregate size of 11 mm. All samples were made with limestone coarse aggregate and screenings (53.1 percent) and natural sand (46.9 percent) and a constant binder content of 6 percent by weight of the mixture.

3.1.2 Materials for Highway 631, 118 and 17 Test Sections

3.1.2.1 Test Section Binders

Binder samples used for the Highway 631 trial near Hearst, Ontario, were never kept. However, pertinent data are available in the literature (e.g., C-SHRP Technical Brief 19 (2000), Robertson (1995), and references therein). The data as compiled in these references are reproduced in Table 3.2. It appears that the performance grades for sections 1 (B) and 2 (A) were nearly the same after PAV aging (-33°C vs. -33.5°C). In contrast, the binder for section 3 (AA) had an advantage at -37°C. However, if the recovered binders are considered then it becomes evident that the binder in section 2 had an advantage (S(60s) = 104 MPa for section 631-2 vs. 175 MPa for section 631-1) and the binder for section 3 (AA) had a diminished edge. This could indicate problems with the PAV method to replicate field aging for this site.

Samples of the five modified binders from Highway 118 had been stored in well-sealed paint cans since 1994 in an office at Queen's University. Approximately 2.5 kg was available for each of the five binders. Unfortunately, no original binder samples were ever kept for the two unmodified control sections constructed with the 85-100 and 150-200 penetration grade asphalts.

One of the modified and the two control binders (85-100 and 150-200) had been supplied by Petro-Canada. The other four modified binders were supplied by Bitumar, Husky Oil, McAsphalt Industries, and Polyphalt. Source information is provided in Table 3.3 in alphabetical order. Conventional properties are provided in Table 3.4. Table 3.5 lists low- and high-temperature SHRP properties for each section as determined shortly after the construction in the summer of 1994 by Imperial Oil staff in Sarnia, Ontario.

In the summer of 2001, samples for four of the five binders used on the Petawawa site were obtained from McAsphalt Industries, which had supplied all five binders for this study. It was again unfortunate that no original binder samples were kept for the 85-100 penetration grade control section. However, it should be mentioned that recently larger quantities of all binder were discovered in the Materials Reference Library in Reno, Nevada and that these materials have now been transferred to Queen's University. The pertinent properties for the Highway 17 binders are listed in Table 3.6.

The Petawawa trial was designed to include two binders with known insufficient low-temperature performance for the location (the 85-110 grade control and a PG 58-28). A further two binders were selected with a grade right at the 98% confidence limit for that location of which one was polymer-modified and the other was not (PG 58-34P and PG 58-34). Finally, one additional section with an even lower limiting BBR temperature (PG 58-40) was chosen. Although not apparent, the PG 58-40P had a higher polymer content than the PG 58-34P. Both binders were modified with an SB diblock copolymer/sulfur system.

Table 3.2 Pertinent Binder Properties for Highway 631 C-SHRP Sections †

Section	SHRP Grade ‡	BBR on PAV residue			BBR on Recovered Binder		
		T, °C	S(MPa)	m-value	T,°C	S(MPa)	m-value
631-1 (B)	52-33	-18	140	0.373	-18	175	0.370
631-2 (A)	52-33.5	-18	131	0.396	-18	104	0.390
631-3 (AA)	46-37	-24	206	0.342	-18	133	0.360

† C-SHRP Technical Brief 19 (2000). ‡ Continuous grades according to AASHTO M320.

Table 3.3 Source Information for Highway 118 Binders †

Supplier	Product	Type of Modification
Bitumar	Ecoflex	Oxidized with Crumb Rubber
Husky Oil	Black Max	Radial SBS/Sulfur
McAsphalt Industries	Multigrade	SB diblock/S/Gel Process
Petro-Canada	Premium	Specialty Catalytic Process
Petro-Canada	85-100	Control Unmodified
Petro-Canada	150-200	Control Unmodified
Polyphalt	sPE	Stabilized Polyethylene

† Ponniah and Hesp (1996)

Table 3.4 Selected Conventional Properties for Highway 118 Binders †

Test Section	Pen ‡ @ 25°C, 0.1 mm	Pen ‡ @ 4°C, 0.1 mm	Viscosity @ 135°C, Pa.s
118-1	87	-	0.90
118-2	47	18	-
118-2A	85	31	-
118-3	66	22	0.91
118-4	87	48	1.35
118-5	66	30	0.80
118-6	39	-	2.02

† Imperial Oil (1994), ‡ Penetration on RTFO-aged residues.

Table 3.5 SHRP Properties for Highway 118 Binders †

Section	T(G*/sin δ = 2.2 kPa), °C	T(S = 300 MPa), °C	T(m = 0.3), °C	Low-Temperature Grade, °C
118-1	79.6	-34.8	-23.4	-23.4
118-2	-	-26.3	-26.7	-26.3
118-2A	-	-33.2	-31.5	-31.5
118-3	70.0	-35.4	-30.0	-30.0
118-4	74.7	-38.0	-40.3	-38.0
118-5	66.7	-34.5	-32.8	-32.8
118-6	75.3	-33.0	-25.2	-25.2

† Imperial Oil (1994). Relevant AASHTO methods are as follows: T240, PP1, TP1, and TP5.

Table 3.6 SHRP Properties for Highway 17 Binders †

Binder	G*/sin δ @ 58°C (10 rad/s, 2.2 kPa min)	T, °C	S, MPa (60 s, 300 max)	m-value (60 s, 0.3 min)
PG 58-28	3.820	-18	260	0.316
PG 58-34	5.821	-24	225	0.304
PG 58-34P	5.225	-24	266	0.307
PG 58-40P	2.308	-30	208	0.333

† McAsphalt Industries (1996). Relevant AASHTO methods are as follows: T240, PP1, TP1, and TP5.

3.1.2.2 Test Section Aggregates and Mix Designs

The Highway 631 test sections were constructed as part of the C-SHRP program to validate the SHRP BBR and DTT low-temperature specification method. The sections were constructed in 1991 on a new granular base. Details on the mix designs and aggregates used for these sections can be found in Anderson (1999).

The Highway 118 test sections were constructed with a dense-graded Ontario HL-4 surface coarse design with a maximum aggregate size of 19 mm. All sections were made with granite coarse aggregate (27.3 percent), limestone coarse aggregate (18.2 percent), natural sand (27.2 percent) and screenings (27.2 percent). The binder content for the control was selected at 5.2 percent by weight of the mixture to obtain an air voids content of 4.0 percent by volume. The amount of binder for each section was adjusted to obtain a constant air voids content for the entire site.

Mixture design for the Highway 17 sections followed conventional Marshall as well as Superpave® protocols. The Marshall design consisted of an HL-3 surface course with 5.7 weight percent of asphalt binder and a design air voids content of 4.0 percent. To prevent stripping, 0.5 weight percent of antistripping agent (Redicote 82-S) was added by weight of the binder. The Superpave® design consisted of a mixture of 45 percent coarse and 55 percent fine aggregate. The binder content was 5.2 percent by weight of the mixture and the design air voids content was 4.0 percent.

3.1.3 Field Core Samples

A total of 70 core samples (10 for each test section) were taken from the Highway 118 site in early May of 2002, after 8 years of in-service conditions. The approximate coring locations (in meters from the start of each section), the average core weights and the equivalent average core thickness for each section are provided in Table 3.7. In sections 1 and 2 the cores were taken throughout the section in order to prevent massive distress in any one location (both these sections had already severely cracked). In the remaining five sections the cores were taken clustered in two locations towards the beginning and end. All cores were spaced a minimum of 5 meters apart.

The average pavement thickness was within the MTO-allowed limits for a design thickness of 2 inches (5 cm) in all but section 4. The lift thickness in section 4 was below the 4 cm lower limit and hence this fact should be considered in future crack severity analysis. If the stiffness is proportional to the third power of the thickness then this section has only about *half* the stiffness of some of the thicker sections. However, the binder for this section has the lowest SHRP BBR and the highest DSR grades, hence it is unlikely that it will show much distress before the entire site is to be rehabilitated.

Immediately after cutting, cores were stored, separated from one another with very fine sand, in thick-walled plastic tubes to prevent damage during transportation to Queen's University (see Figure 3.1).

Table 3.7 Field Coring Locations, Weights and Thickness for Highway 118

Section	Coring Locations	Average Core Weight, kg	Equivalent Average Core Height †, cm
1	81, 97, 120, 143, 189, 198, 222, 236, 255, 262	1.88 ± 0.17	4.2 ± 0.40
2	9, 39, 84, 115, 160, 193, 232, 242, 262, 268	2.02 ± 0.16	4.5 ± 0.36
2A	4, 10, 15, 20, 25, 235, 240, 245, 250, 255	1.86 ± 0.11	4.2 ± 0.25
3 ‡	55, 60, 65, 70, 75, 195, 200, 210, 215, 220	2.00 ± 0.19	4.5 ± 0.43
4	55, 60, 65, 70, 75, 210, 220, 230, 240, 250	1.66 ± 0.08	3.7 ± 0.18
5	30, 35, 40, 45, 50, 160, 165, 170, 175, 180	1.88 ± 0.08	4.2 ± 0.18
6	15, 20, 25, 30, 35, 220, 230, 235, 240, 250	1.83 ± 0.06	4.1 ± 0.13

† Calculated from the weight by assuming a constant density of 2.442 g/cm^3. ‡ Little variation in thickness was found between the cores taken from the intersection and those at the beginning of section 3.

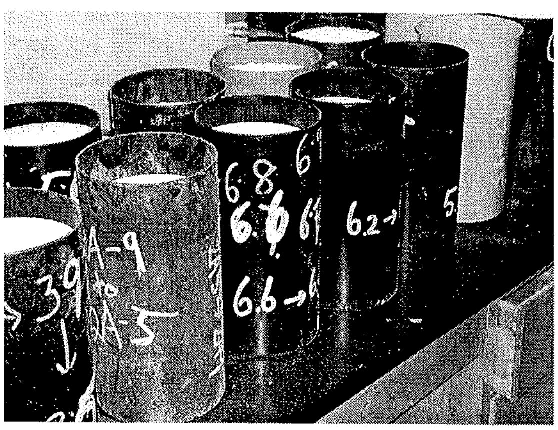

Figure 3.1 Tubes used for securing field core samples during transportation and storage.

A total of 60 core samples (10 for each test section) were taken from the Highway 17 site in November of 2002, after 5 years of field exposure. The cores were taken from two clusters in sampling areas at both the beginnings and ends just outside each monitoring portion for the test sections. The core heights were all within a narrow range around 130-mm which was the design thickness of the pavement.

Since Highway 17 is part of the Trans Canada Highway system its design calls for a much thicker pavement structure compared to what was acceptable on Highway 118. Hence, the Highway 17 site was constructed with two layers of either Superpave™ or conventional Marshall designs. In this study only the properties of the top 2 inches of asphalt concrete were tested.

3.1.3.1 Binder Recovery from Core Samples

For BBR and DTT grading, the binders were recovered from selected cores by extraction with toluene followed by a wash with tetrahydrofuran (THF). Asphalt concrete batches of approximately 2 kg were broken up and left to soak in approximately 2 L of toluene for at least 12 hours after which the solvent was removed from the coarse aggregate. A tall graduated cylinder was used for sedimentation of fine particulate matter before evaporation of the solvent. This procedure was repeated three times followed by a final wash with 2 L of THF. After sedimentation, the asphalt solution was carefully decanted and subsequently evaporated in a rotary evaporator. A final temperature of 150°C and aspirator pressure of 20 mm Hg were maintained for 1 hour to ensure complete removal of all solvent without hardening or oxidation of the binders.

3.2 Pavement Trial Details

3.2.1 Highway 631 C-SHRP Trial near Hearst, Ontario

The Highway 631 site is located some 63 km west of Hearst in northern Ontario, Canada, and was part of the C-SHRP program for the validation of the Superpave® low-temperature binder specification. Four sections, containing three different binders of two grades, were constructed in 1991 on a new granular base. Section lengths varied between 360 and 590 m. Three sections had a design thickness of 50 mm while a fourth section was 100 mm thick. In the early 1990s, the annual average daily traffic count (AADT) on these sections was approximately 300 with 25 percent truck traffic. In 1999, the AADT had increased to approximately 600 of which now 29 percent was truck traffic.

Two of the binders were continuously graded at PG -33 and PG -33.5 while the third was graded as a PG -37. The LTPPBIND™ grade required for this location is a PG -40 at 98 percent confidence, which reduces to a PG -34 by accepting a reduced 50 percent confidence. Hence, at -33°C it is very likely that the pavement will experience what are supposed to be damaging temperatures on a regular basis. The binder grading properties for this trial are given in Table 3.2.

3.2.2 Highway 118 near Bracebridge, Ontario

The sections on Highway 118, near Bracebridge, Ontario, were constructed in 1994 over a 7-km stretch of the westbound lane, between 16 and 23 km east of Highway 11. The sections were placed on a base consisting of pulverized asphalt concrete. Monitoring sections and design thickness were constant at 270 m and 50 mm, respectively.

The location for this trial was less than ideal since a traffic split occurs within the site. For 2000, the AADT for sections 1 and 2 was approximately 3450 with 5.8 percent truck traffic. The AADT for the remaining 5 sections was thought to be 1250 with 4.1 percent truck traffic. However, commuter traffic to and from Bracebridge coming from Conway Crescent, which meets Highway 118 towards the end of the monitoring portion for section 3, may have added to the latter numbers for both sections 3 and 2A to the west. Thus, the variation in traffic volumes and the lack of detailed data are serious unknown factors for this site.

The continuous AASHTO M320 grades for the five modified binders that were used varied between approximately -23°C to -38°C at the low end and between +67°C to +80°C at the high end (see Table 3.5). Unmodified binders were no longer available but 2.5-kg samples had been kept for each of the five modified materials. Modifiers included styrene-butadiene radial and diblock copolymers, polyethylene as well as two oxidized materials. For details on the binders used in this test road refer to Table 3.3 and Ponniah and Hesp (1996).

The continuous LTPPBIND™ grade required for this location is a PG 53-32 at 98 percent confidence, which reduces to a PG 46-26 by accepting a reduced 50 percent confidence. Thus at -23°C and -25°C it is likely that the pavement will experience what are supposed to be damaging temperatures just about every other winter whereas at -38°C it should never really be challenged.

3.2.3 Highway 17 SPS-9A Trial near Petawawa, Ontario

The Highway 17 trial, near Petawawa, Ontario, was part of the SPS-9A program. Six test sections, containing five different binders of four SHRP grades as well as an 85/100 penetration-graded binder, were constructed in 1996 on both lanes starting some 5.4 km west of the Petawawa River. The 65-mm thick binder course for this trial was constructed in late 1996 whereas a surface course of equal thickness was placed in June 1997.

In 1994, the AADT was approximately 5670 with 12 percent truck traffic. In 2000, this had increased to approximately 6000 with 14 percent truck traffic. These numbers were constant for the length of the project and split 50/50 for both lanes.

The penetration-graded asphalt was no longer available but 4.0-kg samples were kept for each of the four PG-graded materials. The SHRP grades used included: PG 58-40P (polymer-modified for both Marshall and Superpave™ designs), PG 58-34 (unmodified as well as polymer-modified for Superpave™ designs) and PG 58-28 (unmodified binder for Superpave™ design). The modifier used in the PG 58-34P and PG 58-40P grades was a styrene-butadiene copolymer. Straight PG 58-34 was obtained from a western Canadian source. Pertinent properties for these materials are listed in Table 3.6.

3.3 Experimental Methods

3.3.1 Infrared and Nuclear Magnetic Resonance Spectroscopy

Samples of unaged, RTFO-aged (AASHTO T240-97, 85 minutes at 163°C), PAV-aged (AASHTO PP1-98, 20 hours at 100°C and 2.09 MPa) and field-aged binder were analyzed by infrared (IR) and nuclear magnetic resonance (NMR) spectroscopy.

3.3.1.1 Sample Recovery for Spectroscopy

Asphalt binders were recovered for spectroscopic analysis from the field cores through extraction with dichloromethane (DCM). It was considered a preferred solvent because it has a low boiling point and a relatively low flammability (as compared with tetrahydrofuran (THF) and carbon disulfide (CS_2)). Samples were taken from within 2 cm of the top surface of two cores (one core from each end of a section).

Figure 3.2 shows how the cores were cut for sampling. Samples were broken up into small pieces and extracted with DCM until further addition of DCM could not remove any more binder from the aggregate. The DCM was removed by gentle evaporation.

3.3.1.2 IR Spectroscopy

Dichloromethane is not suitable for the quantitative IR analysis of oxidation products for two reasons. First, it does not free the ketone functional groups from possible hydrogen bonding interactions with organic acids (Petersen (1987)). Second, it has a number of interfering peaks in the IR regions of interest to study the oxidation of asphalt. Useful IR experiments were thus performed on evaporated residues that were re-dissolved in either dry THF or CS_2.

The THF solvent was used in an attempt to completely remove the interference of hydrogen bonding on the absorbance from ketones, carboxylic acids and other oxidation products in the carbonyl region of the IR spectrum. Tetrahydrofuran, a cyclic ether with a highly electronegative oxygen, frees up any bound carbonyl groups that may be present in the asphalt. This provides a more quantitative analysis of the amount of oxidation present (Petersen (1987)).

Spectra of binders re-dissolved in CS_2 were used to obtain information on possible polymer (i.e., butadiene) oxidation for three of the five Highway 118 binders and for two of the four Highway 17 binders.

The IR analysis focused particular attention on the carbonyl region around 1,700 cm^{-1}, the sulfoxide peak around 1,030 cm^{-1} and the 1,4-butadiene peak around 965 cm^{-1}, since that is where oxidative effects are expected to show up first (Petersen (1987)). Infrared spectra were taken on a Bomen MB-120 spectrophotometer at a resolution of 4 cm^{-1} with an average of 32 scans per sample. All spectra were taken with the pure solvent as background.

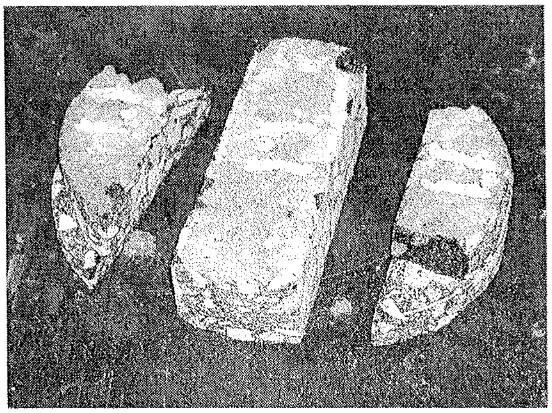

Figure 3.2 Cutting of field core samples for spectroscopic analysis (numbers are on the driving surface of the core).

The region of most interest for a typical IR spectrum of the asphalt binder from section 4 on Highway 118 is provided in Figure 3.3. The integrated area under the IR spectrum between 1,678 and 1,730 cm^{-1} and the maximum peak height in this region were recorded as indicators of the degree of asphalt oxidation. The height was determined from a baseline drawn between peak shoulders at 1,678 and 1,730 cm^{-1}. The sulfoxide peak was likewise analyzed between 1,004 and 1,050 cm^{-1} whereas the trans butadiene and styrene peaks were analyzed from 937 to 986 and 690 to 707 cm^{-1}, respectively.

3.3.1.3 NMR Spectroscopy

Recovered binders were also redissolved in either deuterated DCM for the ^{1}H NMR or deuterated chloroform for the ^{13}C NMR analysis. The NMR analysis considered both the aromatic and aliphatic hydrogen (^{1}H) as well as aromatic and aliphatic carbon (^{13}C) contents since it was expected that these are sensitive to hardening through volatilization (Jennings et al. (1993)). All NMR spectra were taken on a Brucker Avance spectrometer of which the specifics are provided in Table 3.9.

A typical ^{1}H NMR spectrum for a Highway 118 binder is provided in Figure 3.4 whereas the ^{13}C spectrum for the same sample is given in Figure 3.5. A significant amount of effort went into the acquisition of quality NMR spectra, especially from the samples that were recovered from the field.

For samples with solid, insoluble particles the integrations were found to be inaccurate. Filtration of the recovered DCM solutions through a 0.45 μm Teflon® filter cartridge was found to be almost impossible due to clogging of the filter pores whereas centrifugation for half an hour at 3000 rpm did remove a significant amount of solid material but had little positive effect on the resolution of the spectra. Finally, some improvements in resolution were obtained by filtering the solutions through a shallow bed of silica gel. This was effective at removing most of the particulate matter yielding spectra that could be integrated with a higher degree of confidence. However, this left the question of what was removed by the silica gel filtration? It may have been a sparingly soluble binder fraction that should have been included in the NMR analysis. Samples that were flushed out with more dichloromethane still rendered spectra with low resolution and large errors in the integrations. Hence, perhaps the low solubility materials had come through the silica gel with big amounts of solvent only to re-precipitate in the more concentrated NMR solutions. However, due to a lack of time and resources this issue was not further investigated.

The results of the spectroscopic analysis will be discussed in detail in section 4.1 of this report.

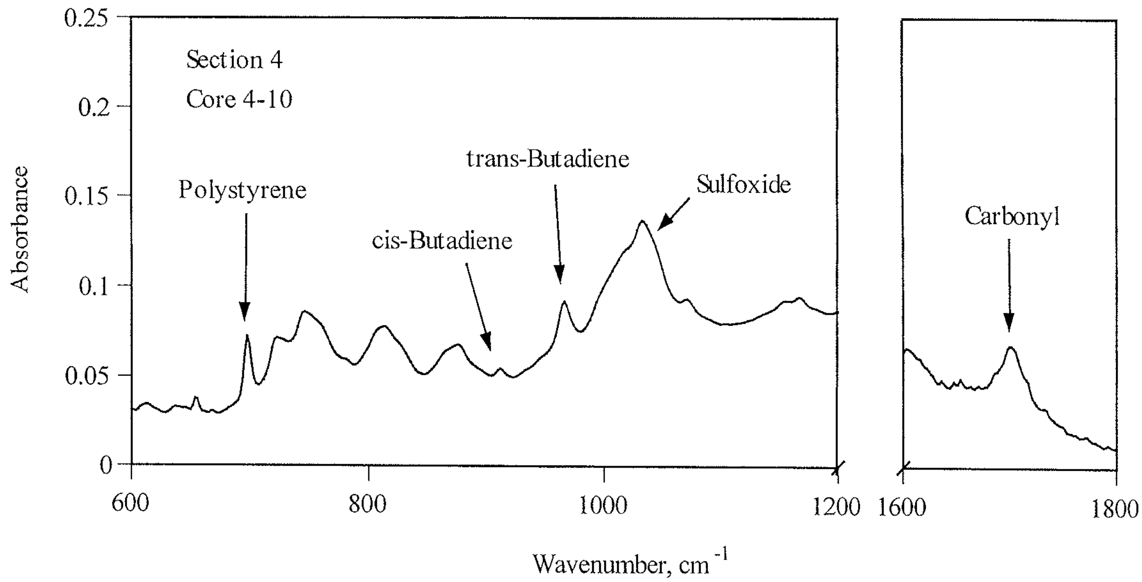

Figure 3.3 Infrared spectrum for a binder sample from section 4 on Highway 118. (CS_2 solvent-compensated.)

Table 3.9 Bruker Avance-300 Spectrometer Details

Parameter	^{1}H spectra	^{13}C spectra	^{13}C-APT spectra †
Sweep width, Hz	4195	18832	18832
Relaxation delay, s	1.0	3.0	4.0
Acquisition time, s	3.91	0.87	0.87
Number of scans	16	1000	1000
Integration limits, ppm			
Aliphatic ^{1}H	0-5	-5 to 66	-
Aromatic ^{1}H	6-10	110 to 160	-
Solvent	CD_2Cl_2	CD_3Cl	$CDCl_3$
Concentration, g/mL	0.04	0.5	0.5
Additive, g/mL	-	0.02 ($Cr(acac)_3$) ‡	-

† Attached proton test (APT) spectra were used to distinguish primary, secondary, tertiary and quaternary carbons. ‡ The chelated chromium compound was added to improve the relaxation of the carbon (see Jennings et al. (1993), SHRP-A-335).

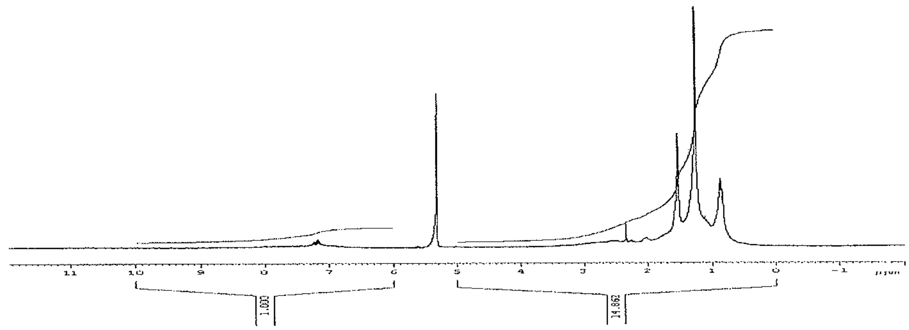

Figure 3.4 Typical ^1H NMR spectrum for binder from section 3 on Highway 118.

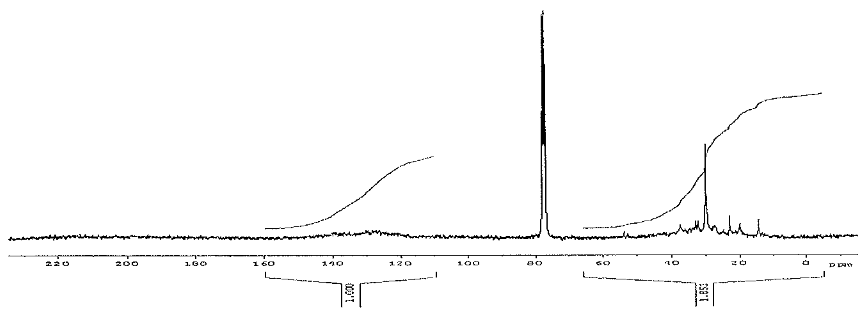

Figure 3.5 Typical ^{13}C NMR spectrum for binder from section 3 on Highway 118.

3.3.2 SHRP Binder Testing

All binders were tested according to the most recent SHRP protocols for the bending beam rheometer (AASHTO M320) as well as the direct tension test (AASHTO MP1a) at the University of Minnesota in the laboratory of co-principal investigator Professor Mihai Marasteanu. For a detailed discussion of the experimental design the reader is referred to Basu (2002) and Basu et al. (2003).

In order to investigate the effects of time-temperature superposition and physical aging, samples were tested for up to two hours in the bending beam rheometer both after one-hour and after three-day isothermal storage at the testing temperature. Direct tension tests were conducted on samples that were also stored for one hour and three days at their testing temperature.

From these data it is possible to obtain an indication of what effect the storage and loading times have on the SHRP low-temperature grading. Originally, the SHRP methods allowed tests to be conducted after both one hour and 24 hours of storage. Even though this option was abandoned shortly after it was proposed, at least one report existed in the literature prior to our study, which discusses the potentially significant effect of conditioning time on grading temperatures (Phillips (1999)).

3.3.3 Yield Stress Testing of Binders

The compressive yield stresses of binders were determined according to procedures that follow the examples of Kinloch et al. (1983) and Young and Beaumont (1977). In brief, cylinders of either two-inch high and one-inch in diameter or one-inch high and 0.5-inch in diameter were compressed between two Teflon®-coated metal platens at strain rates of 0.01 or 0.001 mm/s and various temperatures. The stress-displacement curve was used to determine a 2 percent offset yield stress. The reproducibility in the yield stress varied somewhat depending on the type of binder but was nearly always acceptable with only three samples tested. The stress-strain curve in compression was also used to determine a second value of Young's modulus, E_c, for each binder (second to the one determined in the three-point bend test, E_b).

Further discussion on the development of this test method is provided in Chapter 4.

3.2.4 Fracture Testing of Binders

A significant part of this project consisted of the refinement and validation of the fracture toughness test as originally developed by Lee and coworkers (Lee and Hesp (1994), Morrison et al. (1994) and Lee et al. (1995)). With only slight modifications, the original test was modeled on ASTM E 399-90 *Standard Test Method for Plane-Strain Fracture Toughness of Metallic Materials* (ASTM (1990), Lee and Hesp (1994)).

Two more recent methods that are pertinent to this work are ASTM D 5045-96 *Standard Test Method for Plane-Strain Fracture Toughness and Strain Energy Release Rate of Plastic Materials* (ASTM (1996)) and ASTM E 1290-93 *Standard Test Method for CTOD Fracture Toughness Measurements* (ASTM (1993)), which discuss the determination of fracture toughness (K_{Ic}) and fracture energy (G_{Ic}) in plastics and the crack tip opening displacement (CTOD) in metals. The CTOD method mentions that it is particularly relevant for the testing of "materials that exhibit a change from ductile to brittle behavior with decreasing temperature" (ASTM (1993)). Hence, this is why research at Queen's University is now focusing on the use of crack opening displacement properties in an improved binder specification test method. A limiting G_{Ic} or COD temperature will provide improved performance prediction because it is based on fundamental materials properties rather than properties that depend on specimen size and geometry (see for instance Figure 2.2 and Mai et al. (2000) and references therein).

The test method as originally developed uses a relatively large amount of binder (~55 g) for each sample and is conducted in three-point bending. Making it less compatible with current SHRP methodology and equipment. Furthermore, questions about notch sharpening, the effect of the notch angle, the fulfillment of plane-strain conditions, and the reproducibility needed to be investigated.

A final objective of this project was to investigate if the fracture energy (G_{Ic}) and the crack mouth opening displacement (CMOD) could be measured directly, preferably in a direct tension version of the fracture test, and if the CMOD value could then be used to calculate the crack tip opening displacement (CTOD) for specification purposes. By determining the CTOD in this manner one can circumvent the need for a separate yield stress tests thus further simplifying the binder grading system. By measuring in tension the compatibility with current SHRP DTT equipment would be further facilitated.

Discussions on the development of these test methods are provided in Chapter 4.

3.3.5 Fracture Testing of Mixtures

The asphalt mixtures were tested to complete failure in a newly developed critical crack mouth opening displacement (CMOD) test. This test was developed to investigate if it is possible to show differences in performance for mixtures that are made with different modified binders. As found in previous studies, both the SHRP low-temperature specifications and the TSRST are very insensitive to polymer modification (Fabb (1974), Kluttz and Dongré (1997), Hesp et al. (2000), Anderson et al. (2001)) and the TSRSTs do not often go to complete failure (Fabb (1974), Fortier and Vinson (1998), Hesp et al. (2000)). Hence, it was decided to test all the mixes in a fracture mechanics-based test that was modeled after ASTM standard test method E 1290-93 for CTOD fracture toughness measurements (ASTM (1993)).

Samples that measured approximately 80- by 45- by 12.5-mm with a 4-mm wide notch were taken to failure at a somewhat arbitrary crosshead speed of 0.01 mm/min (the slowest possible speed for the load frame used). The notch was cut with a diamond saw to a depth a_o, so that it would not end in the middle of a large aggregate particle. This presented a slight variation in the notch depths, although all were kept between a so-called a_o/W-ratio of 0.45 and 0.55, as is required in the ASTM standard (W is the sample depth and a_o is the original notch depth).

Although it is possible with certain assumptions to calculate an actual CTOD from the measured CMOD, in this project it was decided instead to compare the CMOD values obtained for different systems since these are all related to their CTOD through a constant (Ewalds and Wanhill (1985)).

Crack mouth opening displacements were measured with a clip-on gage (MTS model 632.02F-20) rated at a compressed force of only a few hundred grams. Failure loads were often much higher, and for that reason it was assumed that the clamping force had no significant effect on the crack opening process.

To validate the crack opening approach to binder grading in the laboratory, a set of binder CTOD's, as calculated from their respective fracture energies and yield stresses, were compared with measured CMOD's for the mixtures made with the same binders. Additional CMOD tests were done in three-point bending on samples cut from field cores that had been in the field for eight and six years, respectively.

3.3.6 Crack Surveying

Highway 631, because of its distant location, was visited on only two occasions both during the summer of 2003. Cracking data were obtained for all four sections and locations were determined from the south end of the test site with a distance-measuring wheel.

The field cracking data for Highway 118 were obtained at irregular intervals in 1997, 1998, 2001, 2002 and 2003. Distances were measured with a metric distance wheel and crack locations were recorded on a condition survey sheet and later transferred to a computer graphics program. The severity of the cracks was not recorded although a number of cracks were photographed so that comparisons can be made in years to come. It was noticed though that for the Highway 118 test sections the cracking severity correlated to some extent with the number of cracks in each section (e.g., section 118-1 not only had the most cracks but also the most severe cracks). Unfortunately, this site was not monitored as closely as hoped for due to staff reassignments at the Ministry of Transportation Ontario.

Temperature data are given in Chapter 4 and it appears from this information that most of the damage in sections 118-1, 118-2 and 118-6 occurred much later than the extreme low-temperature excursion during the winter of 1997. In future test roads it would be desirable to have the site visited several times each year at least after major low-temperature excursions like the one that occurred in the Bracebridge area during January 1997 and again during January 2003.

The Highway 17 test sections were monitored under the Long Term Pavement Performance Program (LTTP) at regular intervals and were visited three times for this project during Fall 2001, Spring 2002, and Spring 2003. It is anticipated that this road will be visited a few more times at regular intervals for several years to come until the differences between the various binders become established.

Chapter 4
RESULTS AND DISCUSSION OF RESULTS

4.1 Laboratory versus Field Aging

One important aspect of this project was to investigate to what extent the laboratory aging methods, rolling thin film oven (RTFO) and pressure aging vessel (PAV), were able to reproduce the 8 and 5 years of field aging for the Highway 118 and 17 binders. Since this is a validation study for different binder grading properties and methods, it is of utmost importance to determine that the observed differences in performance are in fact caused by differences in performance-based properties and are not exaggerated and/or confounded by some issue related to weaknesses in the laboratory aging methods. In the following sections, the use of infrared spectroscopy (IR) and nuclear magnetic resonance (NMR) are discussed with respect to the validation of the RTFO and PAV aging methods.

4.1.1 Infrared Analysis

Infrared analysis was used to learn about the relative degrees of oxidation in the various laboratory aging methods as compared to what has happened after eight and five years in the field. It is well known that oxidation leads to hardening of the binder and that this eventually accelerates the cracking process in the pavement. However, since each asphalt reacts differently to oxidation, it is impossible to predict a binder's relative change in performance from its oxygen content (Branthaver et al. (1993)). Performance properties depend on the intricate interactions between the constituents in each binder, and these are likely to vary a great deal among asphalts from different sources. But it is to be expected that two binders of the same source and with the same level and type of modification, one the PAV residue and the other recovered from the road, that have approximately the same degree of oxidation will have similar performance properties. Conversely, if such samples have very different levels of oxidation, then they are expected to show significant differences in their performance. For this reason IR was used as part of the validation process of the RTFO and PAV aging methods.

The IR results for the carbonyl monitoring are provided in Tables 4.1 and 4.2 for Highway 118 binders in THF and CS_2, respectively. The IR results for the sulfoxide peak heights are given in Table 4.3. Although both peak areas and heights were determined, there was no discernible difference between the trends in either. Hence, only the peak height data will be considered here.

The carbonyl data obtained in THF show that the level of oxygen uptake for the binders in the top 2.5 cm of the pavement appears to be anywhere from 2.5 to 4.2 times higher than what is predicted by the RTFO + PAV aging procedure. It is also interesting to note that the absolute oxidation levels are rather different for all five binders, with section 118-4 clearly having the lowest oxygen uptake. When considering the carbonyl and sulfoxide data obtained in CS_2 solutions, the differences between field and PAV-aged binders are less severe yet still significant. This may be due to the fact that CS_2 is less able to dissociate the acid functionalities in the oxidized binders.

The differences between the bottom 2.5 cm of the field cores and the RTFO + PAV residues is also less significant.

The overall conclusion we may draw from these results is that there appears to be much more oxidation in the field after eight years of exposure to oxygen (and water) from the environment than there is after a combined

RTFO + 20 hr PAV aging procedure at 100°C. This has important implications for the use of the RTFO + PAV aging method. However, the impact of this observation on the validation efforts in this project will be discussed in sections 4.5 and 4.7.

Table 4.1 Changes in Carbonyl Absorbance during Laboratory and Field Oxidation of Highway 118 Binders as Determined in THF Solutions

Section	Carbonyl Peak Heights in Absorbance Units				
	Unaged	RTFO-aged	PAV-aged	Field Core 1	Field Core 10
118-1	0.008	0.016	0.032	0.102	0.111
118-3	0.004	0.004 (0.007)	0.019 (0.022)	0.049	0.056
118-4	0.004	0.004 (0.006)	0.012 (0.014)	0.027 (0.028)	0.038
118-5	0.004 (0.004)	0.004 (0.008)	0.031	0.095	0.097
118-6	0.008	0.010	0.022	0.094	0.091

† Duplicates are given in brackets. Solvent was THF and concentration was kept constant at 1 g/10 mL.

Table 4.2 Changes in Carbonyl Absorbance during Laboratory and Field Oxidation of Highway 118 Binders as Determined in CS_2 Solutions

Section	Carbonyl Peak Heights in Absorbance Units				
	Unaged	RTFO-aged	PAV-aged	Field Core 1	Field Core 10
118-1	0.014	0.029 (0.029)	0.044	0.055 (0.084)	0.061 (0.087)
118-3	0.016	0.017 (0.020)	0.030	0.048	0.054
118-4	0.006	0.053 (0.052)	0.020	0.030	0.028
118-5	0.004	0.012 (0.012)	0.028	0.048 (0.085)	0.060
118-6	0.018	0.023	0.034 (0.037)	0.063	0.052

† Duplicates are given in brackets. Solvent was CS_2 and absorbance units are normalized for 1 g/10 mL.

Table 4.3 Changes in Sulfoxide Absorbance during Laboratory and Field Oxidation of Highway 118 Binders as Determined in CS_2 Solutions

Section	Sulfoxide Peak Heights in Absorbance Units				
	Unaged	RTFO-aged	PAV-aged	Field Core 1	Field Core 10
118-1	0.012	0.018 (0.016)	0.019	0.031 (0.032)	0.029 (0.027)
118-3	0.018	0.014 (0.020)	0.023	0.033	0.030
118-4	0.015	0.018 (0.014)	0.025	0.025	0.028
118-5	0.013	0.014 (0.016)	0.019	0.029	0.027
118-6	0.015	0.015	0.024 (0.020)	0.030	0.032

† Duplicates are given in brackets. Solvent was CS_2 and absorbance units are normalized for 1 g/10 mL.

A careful examination of the carbonyl and sulfoxide oxidation data in Tables 4.1 to 4.3 suggests that perhaps a doubling or tripling of the PAV aging time from 20 to 40 or 60 hours at 100°C might reduce the problem significantly. However, the infrared spectra yielded one additional piece of information that may make us think twice about such an easy solution.

The analysis revealed that as many as three of the five binders that were used on Highway 118 contained significant amounts of styrene-butadiene polymer. The binder for section 118-4 is marketed as an SBS-modified material but it came as somewhat of a surprise to also find butadiene and styrene peaks in the binders from sections 118-5 and 118-6.

Polystyrene is one of the most oxidation resistant commodity polymers available. Hence, it serves as a convenient internal standard in the infrared analysis if we make the reasonable assumption that little or nothing has oxidized under any of the laboratory or field conditions. Solutions made at the same concentration should show a relatively constant peak height at 700 cm^{-1} in the infrared spectrum, irrespective of the degree or type of aging. In contrast, the butadiene part of the styrene-butadiene polymer modifiers is much more susceptible to the negative effects of oxygen; therefore it deserves to be investigated to what extent the pressure aging vessel method is able to reproduce the in-service aging of the butadiene segments in the SB-type modifiers.

It is uncertain at present to what extent polymers in general improve performance. What is a certainty is that they add a significant amount to the cost of the binder. It is therefore important to know if the PAV aging method actually reflects what happens to the polymer in the road.

The heights for the polystyrene as well as the butadiene peaks for the infrared spectra on binders for sections 118-4, 118-5, and 118-6 are given in Figure 4.1. These results show that the combined RTFO/PAV procedure appears to do almost nothing to the butadiene functionality (in the times at the temperatures as required by the AASHTO RTFO and PAV protocols). This is in contrast to the results from Tables 4.1-4.3 that show the RTFO/PAV procedure is good for replicating at least a few years of in-service oxidation of the base asphalt. Hence, one would conclude that the polymer modifier is saved at the expense of the base asphalt for these three binders under the given conditions in the RTFO and PAV.

This would suggest that just a doubling or tripling of the PAV time might still not go far enough to replicate field exposure for six to eight years. However, such extended aging runs were investigated, and the results show that eventually the butadiene does get oxidized. The results of these experiments are described by Xing (2003). The impact of the limited 20-hour PAV procedure is less than what it appears to be in this study. A comparison of PAV and recovered binder properties sheds more light on this issue. Sections 4.2.2 and 4.5.3.2 present the results of this investigation.

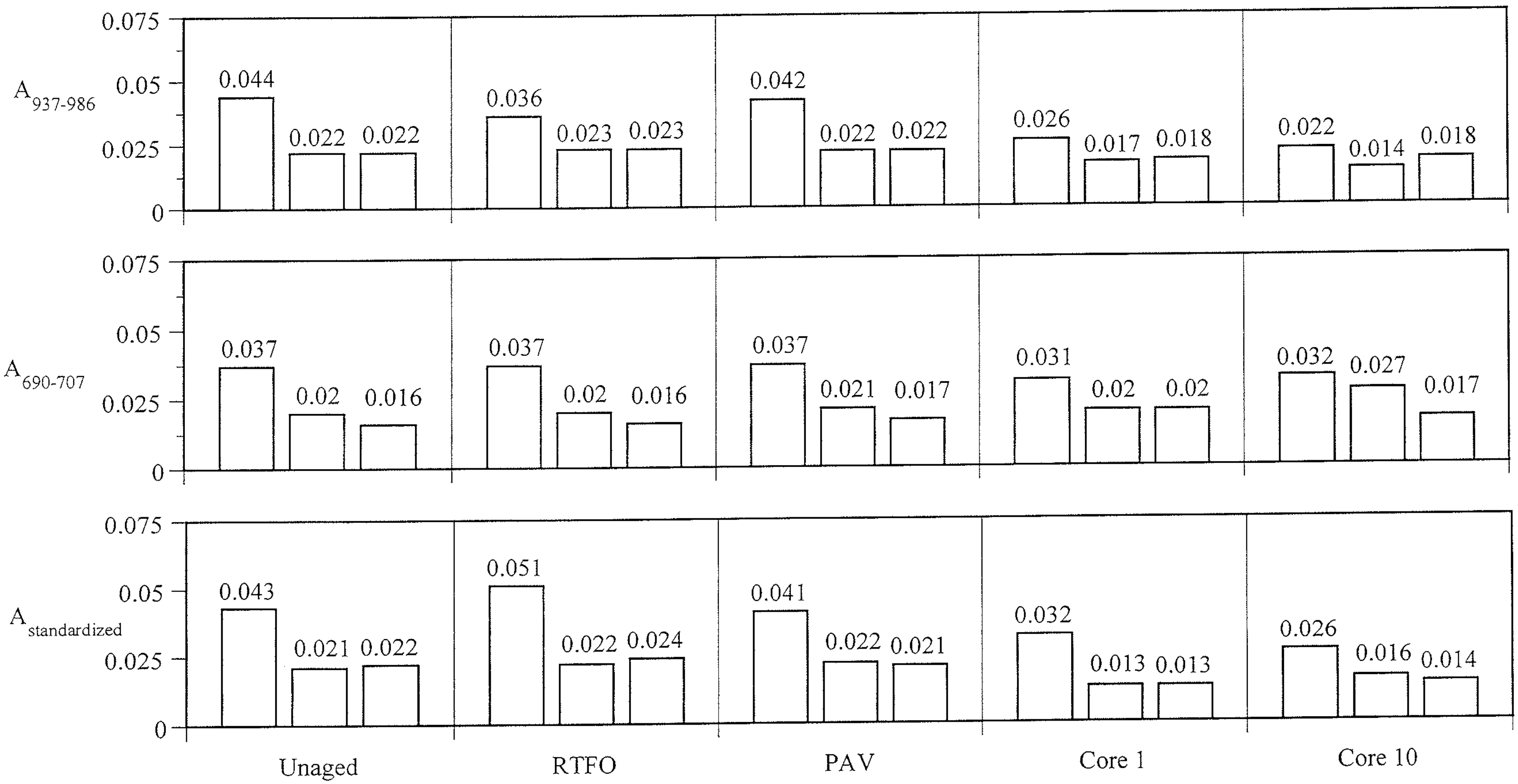

Figure 4.1 Infrared peak height data for binders from sections 118-3, 118-4, and 118-5, respectively. (The first series is for the butadiene absorbance, the second for the styrene, and the third for the butadiene corrected for variations in styrene peak height.)

4.1.2 Nuclear Magnetic Resonance Analysis

A small part of the SHRP program during the early 1990s focused on the use of nuclear magnetic resonance spectroscopy (NMR) for the analysis of asphalt binders and mixtures (Jennings et al. (1993), Pearson (1994)). Since then only a few studies have used this method for asphalt research, likely because of a lack of access to the specialized equipment as well as the general lack in expertise required to obtain meaningful results. Nevertheless, the use of NMR is promising not only because it can yield compositional data but it may also provide information on the rheological state of the binder within the mix without having to recover and disturb the binder with solvent. In this way an NMR spectrometer may be able to do what is impossible with, for instance, a dynamic rheometer, which requires properly recovered and reconstituted binder.

This study only focused on obtaining compositional data from solvent-extracted, service-aged binders to compare these with the same data obtained for the unaged, RTFO-aged and PAV-aged binders. Jennings and coworkers (1993) conducted similar experiments during the SHRP program but for unaged and laboratory-aged binders only. As far as we are aware, there are no reported studies that compare laboratory and field-aged binders by NMR or other spectroscopy methods.

The properties investigated in this project included the aromatic and aliphatic hydrogen contents as well as the aromatic and aliphatic carbon contents. It was hypothesized that these could be used to detect gross differences between the laboratory aging methods and the field-aged core samples. Such differences, if present, would have to be considered in any discussion on the relative frequency and severity of transverse cracks within the test sections on Highways 118 and 17. It is well known that fatigue cracking due to early embrittlement will confound any study of transverse cracking due to only low temperature exposure. If the PAV-aged materials show large differences from the field-aged samples, it would be prudent to take this into consideration when comparing the different sections as well as binder versus field data.

For comparison, the aromatic hydrogen and carbon contents as reported by Jennings and coworkers (1993) are given in Tables 4.4 and 4.5 for a number of the SHRP core asphalts. The NMR data for the Highway 118 binders are given in Tables 4.6 and 4.7.

It should be noted that the TFO aging process is not of the same severity as the RTFO aging, and that the POV (oxygen) aging is more severe than the PAV (air) aging. Furthermore, the degree of aging in these methods also depends on the time as well as the amount of material that is used and how it is introduced. Hence, the results from the SHRP program are given for an approximate comparison only.

The results presented in Tables 4.4 and 4.5 show that there are differences between the aromatic hydrogen and carbon contents for the various aging methods but that these differences are insignificant compared to the errors as found in the samples recovered from the field cores as given in Tables 4.6 and 4.7. Considerable time and effort were expended to obtain better NMR spectra, but in the end these data were the best we could get on state-of-the-art equipment. Hence, this part of our project was considered a failure. This may explain why there are no similar investigations published in the asphalt literature.

Unfortunately, it was beyond the scope of this project to further explore the numerous available methods in NMR spectroscopy for the analysis of these samples.

Table 4.4 Changes in Aromatic Hydrogen Contents during Laboratory Aging
(Reproduced from Jennings et al. (1993))

Asphalt	Percentage Aromatic Hydrogen		
	Unaged	POV-aged	TFO/POV-aged
AAA-1	7.3	6.9	7.4
AAB-1	7.6	8.1	7.7
AAC-1	6.4	7.3	7.8
AAD-1	6.8	6.5	6.6
AAF-1	8.7	9.4	9.6
AAG-1	7.3	8.5	8.3
AAK-1	6.8	7.2	7.0
AAM-1	6.5	8.0	6.9

POV= Pressure Aging Vessel (Oxygen) and TFO = Thin Film Oven Aging

Table 4.5 Changes in Aromatic Carbon Contents during Laboratory Aging
(Reproduced from Jennings et al. (1993))

Asphalt	Percentage Aromatic Carbon		
	Unaged	POV-aged	TFO/POV-aged
AAA-1	27.9	20.3	28.6
AAB-1	31.2	27.8	31.3
AAC-1	27.8	21.8	28.1
AAD-1	23.4	22.1	24.4
AAF-1	32.8	29.4	30.1
AAG-1	29.0	30.0	26.0
AAK-1	26.2	30.6	27.2
AAM-1	25.6	29.5	26.7

POV= Pressure Aging Vessel (Oxygen) and TFO = Thin Film Oven Aging

Table 4.6 Changes in Aromatic Hydrogen Contents during Aging of Highway 118 Binders

Section	Percentage Aromatic Hydrogen †				
	Unaged	RTFO-aged	PAV-aged	Field Core 1	Field Core 10
118-1	6.3	6.8 (6.7)	6.3 (6.7)	5.9 (5.1)	5.5 (3.9)
118-3	5.3 (5.7)	5.9 (6.1)	6.9	6.5 (4.6)	8.5 (4.2)
118-4	6.6	6.6 (6.5)	6.5	6.2	6.2
118-5	6.8	6.9	6.9	6.5	6.2
118-6	6.0	6.2	6.6	6.0 (5.6)	7.3 (5.6)

† Duplicates are given in brackets.

Table 4.7 Changes in Aromatic Carbon Contents during Laboratory and Field Oxidation of Highway 118 Binders

Section	Percentage Aromatic Carbon †				
	Unaged	RTFO-aged	PAV-aged	Field Core 1	Field Core 10
118-1	38.8	38.9 (33.8)	41.0	41.5 (32.4)	40.3 (31.9)
118-3	36.3	35.1	34.7	32.1 (31.9)	32.7
118-4	35.8 (37.4)	37.7	37.1	34.8	37.9
118-5	40.4	41.9	34.7	32.0	29.2
118-6	38.0	36.3	35.2	31.1 (35.5)	31.2 (33.9)

† Duplicates are given in brackets.

4.2 SHRP Specification Testing

Highway 118 and 17 binders were tested at the University of Minnesota and at Imperial Oil Research Center in Sarnia, Ontario, to determine their SHRP grades.

Samples were tested in the bending beam rheometer (BBR) for two hours after both one-hour and three-day conditioning at the grading temperatures. Properties determined included creep stiffness, S, and m-value at both storage and loading times. Samples were also tested in the direct tension tester (DTT) to determine their failure strain, ε_f, and failure stress in tension, σ_f, also after one-hour and three-day conditioning and at a single strain rate as specified by the AASHTO MP1a protocol.

4.2.1 Highway 118 Binders

The complete University of Minnesota results for the BBR and DTT investigations on Highway 118 binders are documented by Basu (2002). Further discussions are provided in Basu et al. (2003) and Marasteanu et al. (2003). Binders were also graded by Imperial Oil in 1994 and 2003. The reproducibility of the BBR data was generally found to be excellent, while for the DTT data there was a considerable amount of scatter (Basu (2000)).

Selected results are summarized in Figure 4.2, which provides the BBR limiting temperatures after both one-hour and three-day conditioning (Basu (2002), Basu et al. (2003), Imperial Oil (1994, 2003)) as well as the MP1a (BBR+DTT) grades for one-hour and three-day conditioning and a so-called pavement constant (PC) of 18. (For a discussion of the pavement constant, see Bouldin et al. (2000) or Bouldin and Dongré (2000) and for a critique of it, see Hesp et al. (2000) and Roy and Hesp (2002a).) Figure 4.2 also provides the critical temperatures according to a limiting strain criterion ($T(\varepsilon_f = 1\%)$) after both one-hour and three-day soaks.

Finally, Tables 4.8 and 4.9 provide the observed stiffness and m-values after both one-hour and three-day conditioning at the grading temperature (T_1) as well as at the pavement design temperature (T_1-10). These tables contain only data obtained at the University of Minnesota.

The aim of this part of the project was to investigate what effect, if any, storage time and loading time have on the BBR and DTT limiting temperatures. At this moment it is unclear what both should be for a pavement that cools during a winter night. However, it is obvious that the one-hour conditioning and 60-second loading time are both a compromise to facilitate rapid specification testing.

Originally, the BBR method allowed tests to be conducted after both one-hour and 24-hour conditioning. Even though this option was abandoned shortly after it was proposed, to the best of our knowledge, only a single paper by Phillips (1999) reports what effect this can have on binder grading. The results in this study show there are significant effects due to physical aging. For section 118-1, for instance, the limiting m-value grade loses almost 10°C after three days of conditioning. (Note that the numbers in Figure 4.2 are rounded.) This is a significant amount and should in some way show up in the onset and severity of cracking. These findings are in good agreement with those of Phillips (1999) who found in a study on 16 different binders losses ranging from a low of 1.5°C to a high of 6°C after a 24-hour conditioning period.

An inspection of the data in Figure 4.2 shows that for these binders the MP1a critical temperatures are not very different from the M320 temperatures. The biggest difference for the one-hour conditioning time is 6°C for section 118-1. However, on average, after one-hour conditioning the MP1a temperatures are 2.4°C lower than the M320 temperatures for this set of five binders, which is not insignificant in the context of low-temperature weather statistics as provided in, for instance, Figure 2.3. Comparing the three-day data, the conclusions are similar, although for these the average difference is only 0.6°C with MP1a still providing the lower temperatures. One should note that in the MP1a method it is possible to select any pavement constant (i.e., fitting parameter), and therefore a higher value would bring the M320 and MP1a data even closer together.

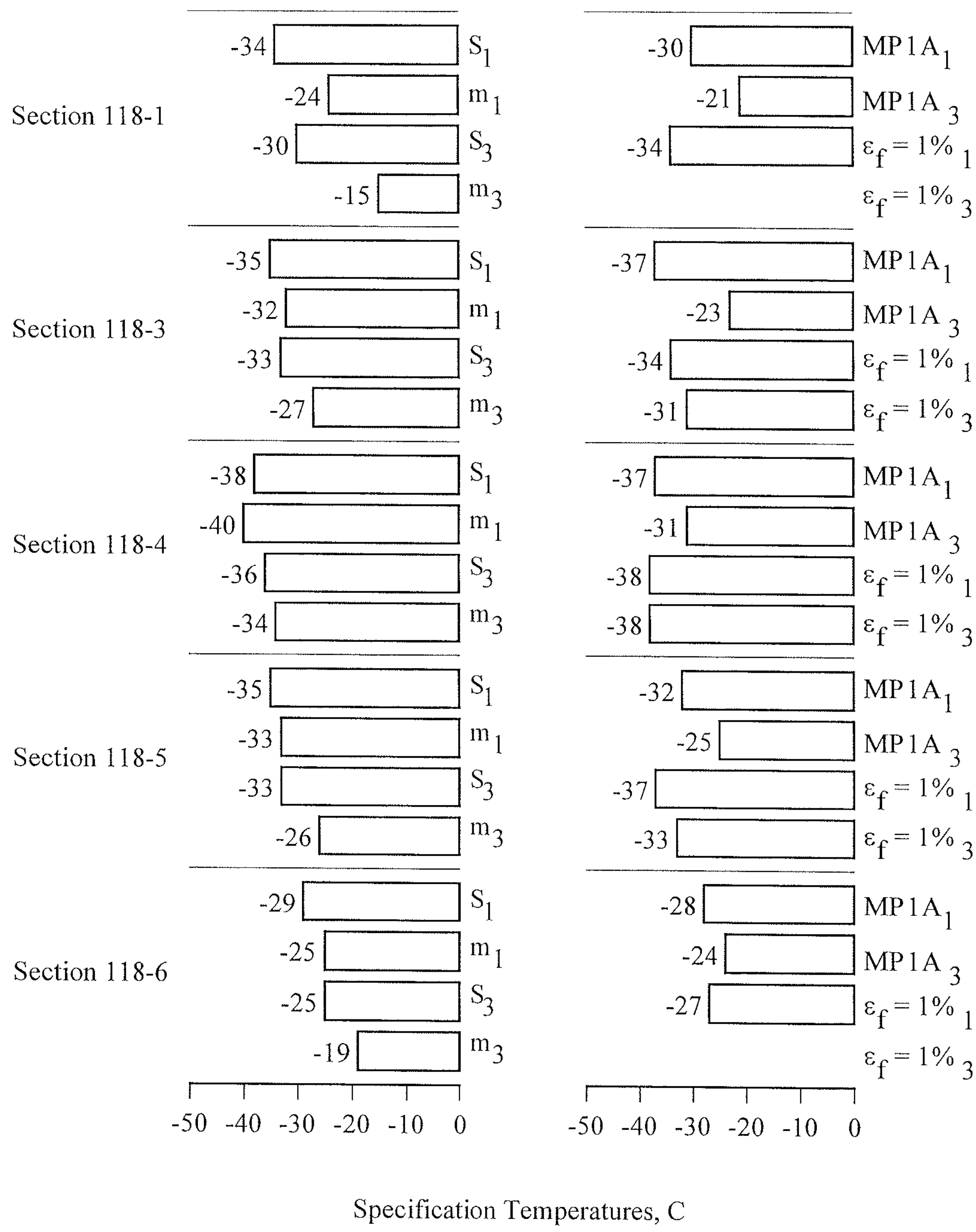

Figure 4.2 Specification temperatures for Highway 118 binders. (S_1 and m_1 are 60 s limiting stiffness and m-value temperatures - 10 after one hour of isothermal conditioning at the grading temperatures whereas S_3 and m_3 are the same after three days of conditioning. Similarly, MP1a and ε_f specification temperatures are also given for one-hour and three-day conditioning, respectively. Numbers on columns are rounded to the nearest degree.)

Table 4.8 Summary of University of Minnesota Stiffness Data for Highway 118 Binders

Section	PG	T_1, °C	S, MPa @ T_1, 60 s		T_1-10°C	S, MPa @ T_1-10°C, 2 hr		Differences, %	
			1 hour	3 days		1 hour	3 days	1 hour	3 days
1	70-22	-12	89	117	-22	55	100	-38	-15
3	64-28	-18	122	167	-28	82	162	-32	-3
4	70-34	-24	170	222	-34	116	214	-32	-4
5	64-28	-18	126	180	-28	76	153	-40	-15
6	70-22	-12	131	158	-22	83	154	-37	-3

Table 4.9 Summary of University of Minnesota m-Values for Highway 118 Binders

Section	PG	T_1, °C	m-Value @ T_1, 60 s		T_1-10°C	m-Value @ T_1-10°C, 2 hr		Differences, %	
			1 hour	3 days		1 hour	3 days	1 hour	3 days
1	70-22	-12	0.312	0.271	-22	0.400	0.320	28	18
3	64-28	-18	0.337	0.287	-28	0.404	0.328	20	14
4	70-34	-24	0.355	0.297	-34	0.426	0.342	20	15
5	64-28	-18	0.342	0.285	-28	0.417	0.340	22	19
6	70-22	-12	0.326	0.280	-22	0.393	0.319	21	14

Finally, the results from Tables 4.8 and 4.9 show that the time-temperature superposition for the stiffness works reasonably well after three-day conditioning, with errors ranging from 3 to 15 percent, but less so after only one-hour conditioning, with errors ranging from 32 to 40 percent. By using the master curves, this can be converted to an error in the stiffness grading temperature of less than 0.7°C after three-day conditioning to a higher, yet still acceptable, 3°C after one-hour conditioning (Basu et al. (2003)). The application of the time-temperature superposition principle for the m-value does not appear to improve after three-day isothermal conditioning. This is because the stiffness master curve not only shifts with time and temperature but also rotates (becomes flatter). It is doubtful whether the superposition principle can account for this rotation. For further details on this issue the reader is referred to Phillips (1999) and Basu et al. (2003).

How the above observations relate to field performance will be discussed in section 4.6. However, the data do show that the issue of which test method to select for performance grading is an important one. For instance, the binder in section 118-1 is expected to perform well for temperatures as low as -34°C according to the failure strain criterion after one-hour conditioning. In contrast, according to the limiting m-value after three-day conditioning, this would only be -15°C. A potential error of nearly 20°C, in the context of typical weather statistics such as those given in Figure 2.3, can have serious consequences. Depending on which method is correct, one either has a pavement that fails on several occasions in its first winter, or one pays too much for a grade that is 20°C too generous.

Hence, the current research effort is important in that it will contribute to a better understanding of which properties are truly critical for low-temperature performance grading of asphalt binders. It has been a hypothesis in this study that only true fracture mechanics properties such as fracture energy, G_{Ic} or G_f, and crack opening displacement, COD, on appropriately aged and conditioned samples can succeed where the currently used specification methods fail.

4.2.2 Recovered Highway 118 Binders

The binders of sections 118-1, 118-4 and 118-6 were recovered according to the procedure described in section 3.1.3.1, and tested according to AAHTO M320, MP1a, and fracture mechanics-based methods. The SHRP properties are discussed here while the fracture properties will be dealt with in section 4.5.3.

Figure 4.3 compares the various limiting temperatures for the PAV residues with those for the recovered binders. A number of interesting observations may be made with respect to these results. First, it appears that the PAV procedure does a reasonable job at predicting the limiting SHRP temperatures for these three binders since the correlation between the data plotted in Figure 4.3 is reasonable (slope = 1.00 and r^2 = 0.75). These findings are in agreement with the results of Robertson (1995) who found that the stiffness at -18°C of the recovered material correlated strongly with that of the PAV materials (slope = 0.98 and r^2 = 0.88). This would not have been expected in light of the spectroscopic results presented in section 4.1, which showed very significant chemical differences between PAV and recovered materials (see Tables 4.1-4.3 and Figure 4.1). However, when the individual sections are considered in Figure 4.3, it must be noted that the scatter can be quite large. This could still have been a result of an error in the individual measurements or in the recovery procedure and may not necessarily have been the fault of the pressure aging vessel procedure. The issue becomes clearer when the fracture data for these three binders are compared later in this report. Such a comparison will show one weakness of the PAV procedure that is not easily revealed by any of the current binder grading methods.

4.2.3 Highway 17 Binders

The results of the BBR and DTT investigations for Highway 17 binders are provided in Figure 4.4 and the effects of time-temperature superposition are given in Tables 4.10 and 4.11.

Similar comments to those made for the Highway 118 binders can be made with respect to the data for Highway 17 binders. The three-day versus one-hour physical aging appears to take away as much as 13°C from the limiting m-value temperature for the PG 58-28 control binder used in Petawawa. In contrast, the PG 58-40 binder with a significant amount of SB-type modifier loses only about 2°C in the limiting m-value temperature and 4°C in the M320 grade temperature after three-day conditioning.

The data in Tables 4.10 and 4.11 show again that the time-temperature superposition works best for stiffness after three days of conditioning and that it does not work very well for the m-value. Once more, master curves can be used to show that these errors convert into errors in grading temperatures of between 1.5 and 2.3°C for data after one-hour conditioning and between 0.4 and 1.5°C for three-day conditioning (Basu et al. (2003)).

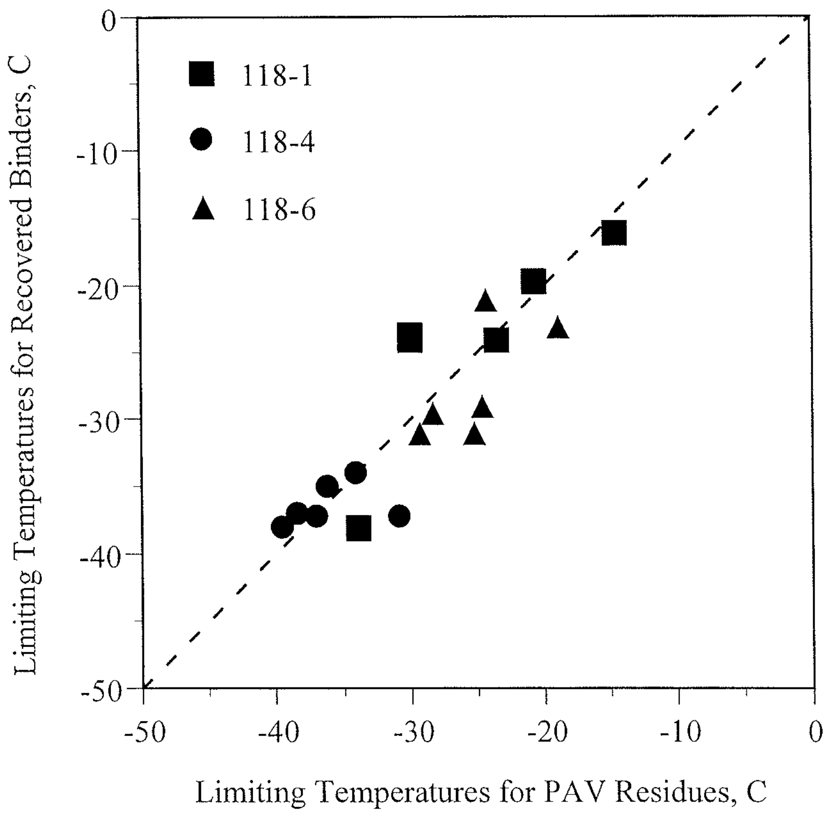

Figure 4.3 Comparison of limiting S, m and MP1a temperatures obtained on PAV residues with those obtained on recovered samples.

One final question that needs to be answered, however, is what relevance a two-hour conditioning time has with respect to low-temperature failure in regular as well as modified asphalt pavements. The loading time in a typical road structure is often much longer and it appears that this number is taken from the limited studies of Readshaw (1974), Hills (1974) and Deme and Young (1987). (These studies all used unmodified binders and never considered the m-value but rather focussed solely on stiffness as a grading property.) If time-temperature superposition works, then the consistent use of 60-seconds, two hours or any other loading time should all give the same performance ranking. However, since we see from the experimental results in this study that not insignificant errors can be made with shifts from 60 seconds to two hours, this raises the question of how large the differences in ranking become when even longer loading times are considered. This question has to be addressed in future studies.

If and how any of these SHRP data can be reconciled with field performance data from Highways 118 and 17 will be discussed in section 4.7 of this report.

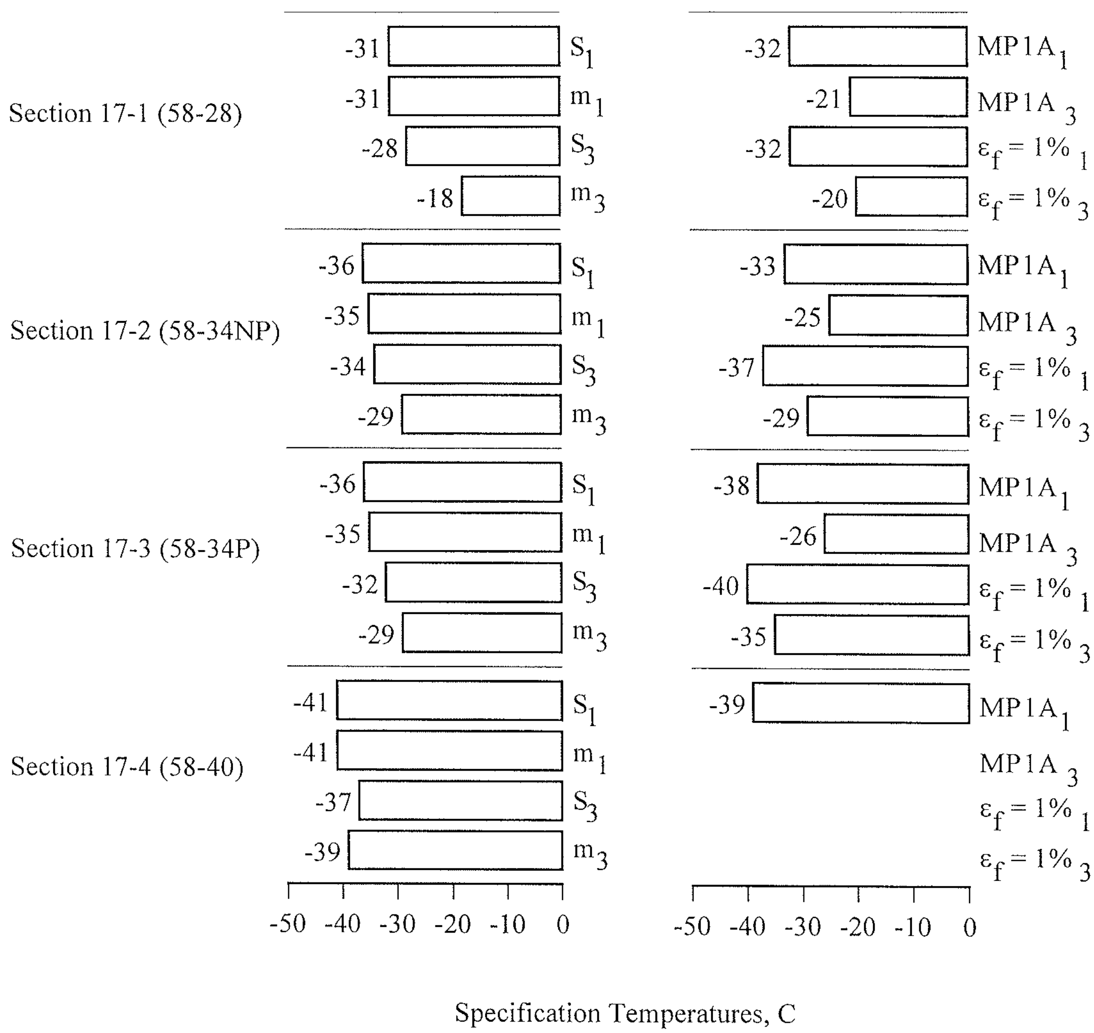

Figure 4.4 Specification temperatures for Highway 17 binders. (S_1 and m_1 are 60 s limiting stiffness and m-value temperatures - 10 after one hour of isothermal conditioning at the grading temperatures whereas S_3 and m_3 are the same after three days of conditioning. Similarly, MP1a and ε_f specification temperatures are also given for one-hour and three-day conditioning, respectively. Numbers on columns are rounded to the nearest degree. Some tests for section 17-4 could not be completed due to the binder detaching from the inserts in the DTT.)

Table 4.10 Summary of University of Minnesota Stiffness Data for Highway 17 Binders

Section	T_1, °C	S, MPa @ T_1, 60 s		T_1-10°C	S, MPa @ T_1-10°C, 2 hr		Differences, %	
		1 hour	3 days		1 hour	3 days	1 hour	3 days
58-28	-18	216	316	-28	158	328	-27	4
58-34	-24	255	372	-34	174	357	-32	-4
58-34P	-24	231	302	-34	158	286	-32	-5
58-40	-30	279	400	-40	211	366	-24	-9

Table 4.11 Summary of University of Minnesota m-Values for Highway 17 Binders

Section	T_1, °C	m-Value @ T_1, 60 s		T_1-10°C	m-Value @ T_1-10°C, 2 hr		Differences, %	
		1 hour	3 days		1 hour	3 days	1 hour	3 days
58-28	-18	0.328	0.231	-28	0.381	0.299	16	29
58-34	-24	0.305	0.246	-34	0.370	0.277	21	13
58-34P	-24	0.308	0.260	-34	0.391	0.308	27	18
58-40	-30	0.314	0.283	-40	0.369	0.314	18	11

4.3 Development of a Yield Stress Test Method for Asphalt Binders

4.3.1 Theoretical Background on Yielding in Asphalt Binders

To study the effect of temperature and rate of loading on the low-temperature yield properties for asphalt binders, it was decided to consider a theory originally developed to describe mathematically the process of flow in solids. (The theory is sometimes referred to as the "absolute rate theory" or "chemical rate theory," since it originated from arguments on chemical kinetics, or the "Eyring theory" after its best known advocate (Tobolsky and Eyring (1943).) In order to obtain a yield stress for specification purposes at very low loading rates (i.e., long loading times, reflective of what happens in a real pavement) and low temperatures, it would be convenient if this could be determined through measurements at shorter loading times and perhaps warmer temperatures. The approach as developed by Eyring and others may provide a practical way of doing this. Although the rate theory has received extensive attention in the general scientific literature, relatively few studies have been reported on asphalt materials (Herrin and Jones (1963), Herrin et al. (1966), Jacobs (1995), and Jacobs et al. (1996)).

Herrin and coworkers were the first to use the absolute rate theory to describe the deformation behavior of asphalt binders in two excellent papers from the early 1960s (Herrin and Jones (1963), Herrin et al. (1966)). They realized that "it combines the work of the mathematician, the physicist and the chemist to provide an explanation for the behavior of a material (i.e., asphalt) on a structural level and to relate the rate of shear to the shear stress, temperature and some basic properties of the material." The basic properties the authors refer to are the activation energy and so-called "flow units" of viscous flow in the asphalt material. The latter is now more commonly referred to as an activation volume for viscous flow. However, if and how it relates to the molecular dimensions and forces within the solid is less clear (Ha Anh and Vu-Khanh (2001)).

It should be noted that Herrin studied how shear rates, ranging from 10 to 10^{-5} reciprocal seconds, related to shear stresses, ranging from 2 to 30×10^4 dynes per square centimeter, first on a single asphalt binder at temperatures between 12 and 60°C (Herrin and Jones (1963)) and in a subsequent paper, on a further six different binders at temperatures ranging from 0 to 50°C (Herrin et al. (1966)). As the efforts in this work relate to low-temperature fracture, the yield behavior at higher strains and lower temperatures and rates of loading are studied.

A relatively straightforward discussion of how the theory relates to yielding in polymers is provided by McCrum and coauthors (McCrum et al. (1997)); hence their representation of the theory is briefly summarized here. Eyring's equation relates shear stress to rate of movement. Using a statistical approach for thermally activated flow, in which the activation volume, V*, passes an energy barrier, ΔH, to reach a vacant site at some distance, Eyring obtained the following relationship for the (random) jump rate in the absence of any externally applied shear force (McCrum et al. (1997)):

$$\text{random jump rate} = \alpha \exp\left[-\left(\frac{\Delta H}{RT}\right)\right] \qquad (4\text{-}1)$$

where α is a constant and ΔH is the barrier height which an average activation volume needs to surpass before reaching the vacant site. Eyring realized that the application of a shear stress allows this jump rate to be modified. (Figure 4.5 gives a graphical representation of this.) The rate in the direction of the externally applied shear stress is now increased, whereas the rate of return is decreased (McCrum et al. (1997)):

$$\text{forward rate} = \alpha \exp\left[-\left(\frac{\Delta H - \sigma_S V^*}{RT}\right)\right] \qquad (4\text{-}2)$$

$$\text{reverse rate} = \alpha \exp\left[-\left(\frac{\Delta H + \sigma_S V^*}{RT}\right)\right] \quad (4\text{-}3)$$

The net flow rate is then given by the following equation:

$$\text{net rate} = \alpha \left\{ \exp\left[-\left(\frac{\Delta H - \sigma_S V^*}{RT}\right)\right] - \exp\left[-\left(\frac{\Delta H + \sigma_S V^*}{RT}\right)\right] \right\}$$

(4-4)

which is further simplified by making the following reasonable assumptions (McCrum et al. (1997)):

- after application of an external stress the reverse flow can be neglected with respect to the forward flow;
- the net jump rate is proportional to the imposed strain rate; and
- the prevailing shear stress in tension is the maximum shear stress, which at yielding conditions is equal to half the yield stress, σ_y (McCrum et al. (1997)).

Including these simplifications and after further rearrangement, the final form of the well-known Eyring equation is then given by (McCrum et al. (1997)):

$$\frac{\sigma_y}{T} = \left(\frac{2}{V^*}\right)\left[\left(\frac{\Delta H}{T}\right) + 2.303R \log\left(\frac{d\varepsilon_y / dt}{d\varepsilon_o / dt}\right)\right]$$

(4-5)

where: σ_y is the yield stress, Pa
T is the absolute temperature, K
V^* is the activation volume, m^3
ΔH is the activation enthalpy, $J.mol^{-1}$
ε_y is the strain rate at yield, $m.m^{-1}.s^{-1}$
and ε_o is a constant.

The above relationship shows that by measuring the yield stress at various temperatures and strain rates, it is possible to determine both the activation volume and activation energy. Once these are obtained, it is possible to use the theory to predict the yield stress at other temperatures and strain rates. This is only achievable, however, if the flow mechanism does not change significantly within the time/temperature range considered (i.e., V^* and ΔH stay constant).

In this study the Eyring theory was used to determine activation volumes and energies for a number of straight and modified asphalt binders in their brittle regime. The ultimate aim was to combine the yield stress with a measure of fracture toughness at an appropriate loading time in order to more successfully control low-temperature fracture. This can be done by specifying a limiting crack tip opening temperature at which different binders should show equal performance. The word "should" is used here because interfacial strength and aggregate fracture issues will still need to be considered which, obviously, can never be predicted by measuring binder properties alone.

More recently, Jacobs and coworkers at Delft University of Technology in the Netherlands have used the absolute rate theory to describe fatigue failure in asphalt concrete (Jacobs (1995) and Jacobs et al. (1996)). In fatigue the backward jump (i.e., the healing of microcracks) plays an important role, and consequently the reverse jump rate cannot be neglected. Moreover, the presence of voids as well as the fine and coarse aggregate complicates any theoretical analysis. What this project aims to accomplish (i.e., to develop an improved, simple and accurate specification test method for low-temperature grading of asphalt binders) is a much less ambitious goal. For a more in-depth review of the theory as it applies to fatigue and other types of failure in heterogeneous materials, and for a discussion of the historical developments in this field, the reader is referred to the excellent dissertation by Jacobs (1995).

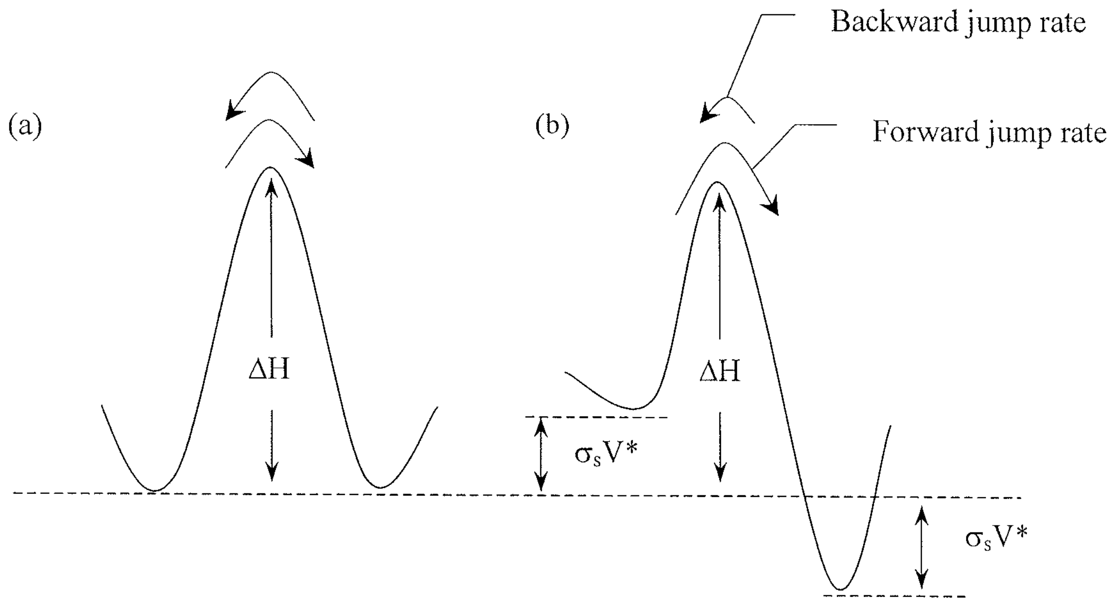

Figure 4.5 Schematic of the flow process as described by Eyring. (a) Before stress is applied with equal jump rates. (b) After stress is applied with segments preferentially jumping in the forward direction. (Reproduced from McCrum et al. (1997))

4.3.2 Yield Stress Test Development

A practical compressive yield stress test was developed in order to study the effect of strain rate and temperature on low-temperature yield properties. In this effort the examples of Kinloch et al. (1983) and Young and Beaumont (1977) were followed. Since it is impossible to determine the desired yield stress in tension in the brittle temperature regime, a surrogate yield stress was determined in compression. It is expected that there will be differences between the two yield stresses, but for practical reasons we assumed, for the moment, that these difference are small and have little effect on the theoretical analysis. (This point will be discussed further in section 4.5.2 on the development of a fracture test.)

Samples measuring either half an inch in diameter and one inch in height, or one inch in diameter and two inches in height, weighing approximately 3.2 grams and 25 grams each, respectively, were prepared by pouring the hot asphalt binder into silicone molds of the desired dimensions. Since the cavities had to be slightly overfilled to compensate for shrinkage upon cooling, the specimens were flattened with a hot metal plate before testing. Figure 4.6 shows the silicone mold used.

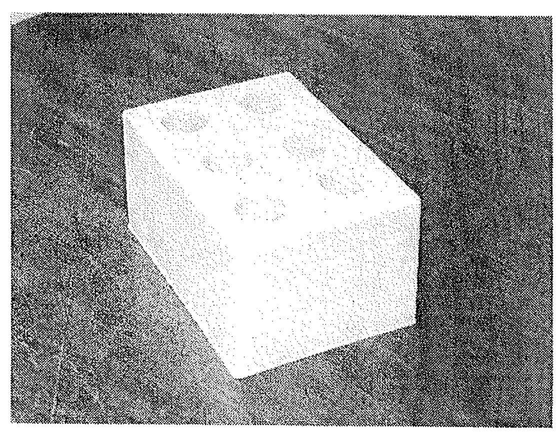

Figure 4.6 Silicone mold design for yield stress specimen casting.

After storing the samples for a sufficient amount of time at low temperatures to lessen the effects of physical aging, they were compressed between two flat metal plates in a temperature-controlled chamber. The crosshead displacement rate was varied between 0.003 and 2.5 mm.s^{-1}, resulting in strain rates that varied between approximately 10^{-1} and 10^{-4} reciprocal seconds. Yielding occurred gradually in this method, so a 2 percent offset yield stress was chosen as a reasonable approximation of the true yield stress.

Samples that had been compressed to a large degree were found to have a crown with excessive deformation on either top or bottom. However, the not unreasonable assumption was made that the 2 percent offset yield point would have been reached well before the start of this uneven yielding process. Future validation of this assumption is an option and if a problem arises, a compression sleeve may provide a solution.

4.3.3 Findings and Discussion of Findings on Yield Behavior in Asphalt Binders

4.3.3.1 Reproducibility of the Yield Stress Determination

As this project endeavored to develop an accurate and improved low-temperature grading test method it was considered prudent to pay some attention to the reproducibility of the data. Figure 4.7 gives an example of the reproducibility in one particular set of experiments and provides a graphic illustration of how the 2 percent offset yield stress is determined. As is obvious from this data, the attainable reproducibility is excellent and the determination of the yield stress is easily accomplished by drawing a line parallel to the initial tangent to the load-displacement curve.

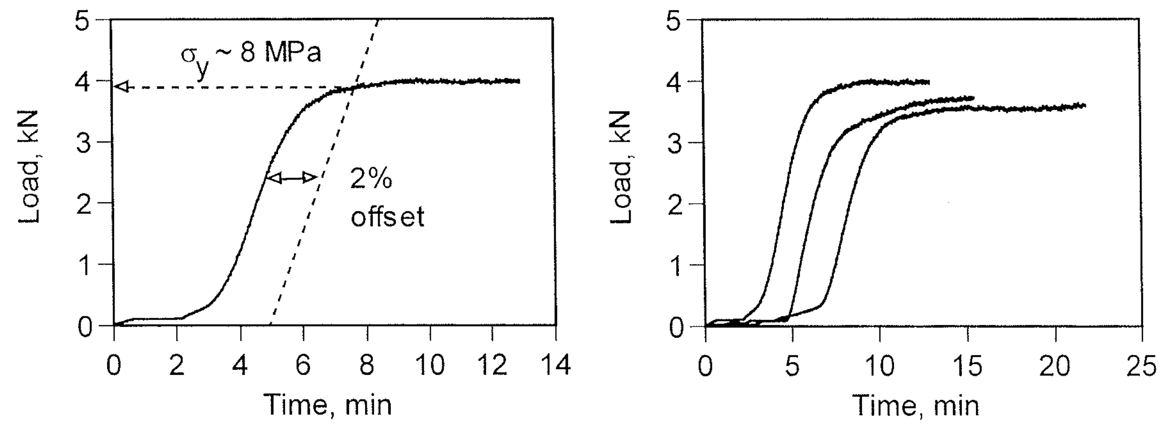

Figure 4.7 Reproducibility of the yield point determination. (Hesp and Roy (2002))

Not all of the yield stress determinations were as reproducible as those depicted above, but then again the test method was still being fine-tuned. It was found that the main sources of error result from misalignment of samples between the compression platens and from variability in the sample preparation and storage routines. Certain samples started to crack shortly after yielding ensued but before the 2 percent offset yield stress was reached in which case the maximum load was used to determine an approximate yield point.

4.3.3.2 Activation Volumes and Energies

By plotting the yield stress over temperature as a function of the logarithm of the strain rate (equation 4-5), it is possible to determine the activation parameters of the Eyring theory. The activation volumes were determined for a total of 10 systems (six polymer-modified, two unmodified, and two filled systems) at two temperatures for each system.

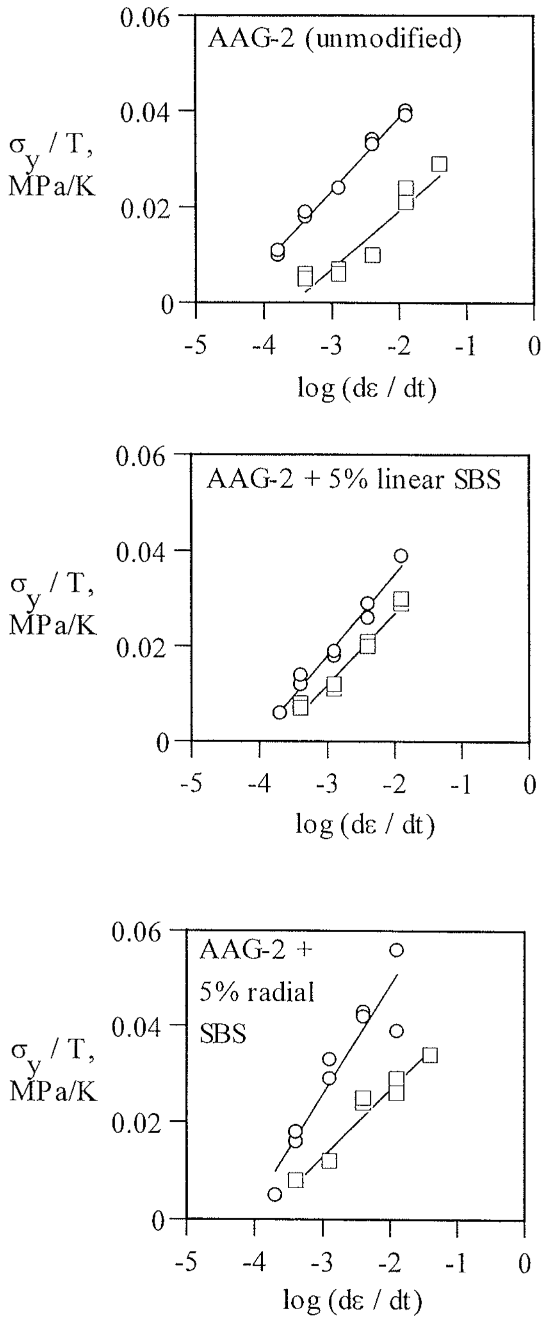

Figure 4.8 Yield stress data for AAG-2. (circles for -24°C and squares for -12°C) (Reproduced from Hesp and Roy (2004))

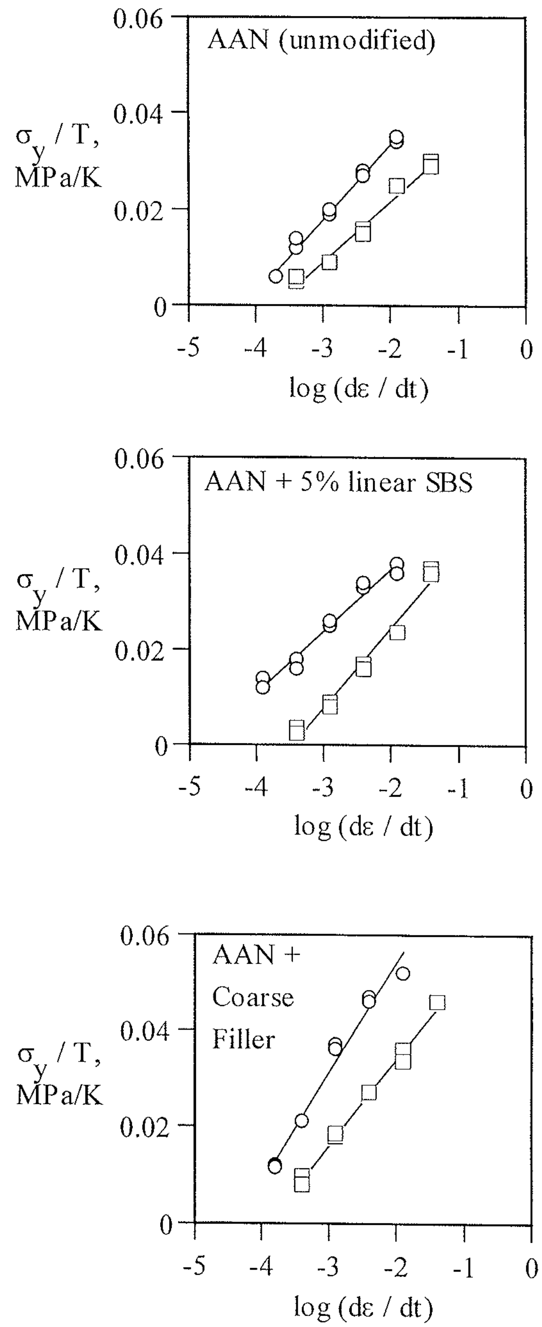

Figure 4.9 Yield stress data for AAN. (circles for -24°C and squares for -12°C) (Reproduced from Hesp and Roy (2004))

Figures 4.8 and 4.9 provide the Eyring plots for a number of representative samples, while Table 4.12 presents the activation volumes as determined from the slopes of the curves. When considering the data plotted in Figures 4.8 and 4.9, a number of observations can be made. The only sample that showed a typical Eyring plot (i.e., two parallel lines with a relatively constant activation volume and activation enthalpy) was the AAG-2 + 5%

linear SBS. This also happens to be the most compatible system: a relatively low molecular weight polymer in a binder that has a low asphaltene content. For this system it is possible to calculate an activation enthalpy for viscous flow, $\Delta H = 42$ kJ.mol^{-1}, from the distance between the two straight lines (McCrum et al. (1997)). Although the exact meaning of this number is unclear, it is not far off from typical activations energies that are reported in the polymer literature (McCrum et al. (1997), Ha Ahn and Vu-Khanh (2001)). For all the other samples, however, it is apparent that such an analysis would generate parameters that vary with both temperature and strain rate.

Table 4.12 Activation Volumes

Binder	T, °C	V*, nm^3
AAG-2	-12	5.3
	-24	4.1
AAG-2 + SBS triblock	-12	3.7
	-24	3.7
AAG-2 + SBS radial	-12	4.6
	-24	2.3
AAN	-12	5.1
	-24	4.1
AAN + SB diblock	-12	5.3
	-24	3.3
AAN + SBS triblock	-12	3.8
	-24	4.9
AAN + SBS radial	-12	8.7
	-24	4.7
AAN + EVA	-12	3.5
	-24	4.1
AAN + fine filler	-12	2.7
	-24	2.1
AAN + coarse filler	-12	3.6
	-24	2.5

Before continuing with further discussions, it is worthwhile to quote a statement made by Schmidt during the discussion that followed Herrin's 1966 presentation on the activated rate theory as applied to asphalt binders:

> *Sometimes one takes too seriously models that have been created for the convenience of the mathematical treatment. I would like to point out that "flow units" are this sort of convenience and not suggested as a model of the actual case. (Schmidt (1966)).*

This statement goes to the heart of the matter in that it is not proven that the schematic as given in Figure 4.5 for the derivation by Eyring is in fact describing the process as it occurs during yielding in asphalt binders. The actual situation appears to be considerably more complex, with several processes occurring at the same time or under different conditions of temperature and rate of loading (micro-cracking, shear band formation, diffuse yielding, interfacial fracture, etc.). These types of situations have been analyzed using modified Eyring equations by other researchers in the polymer field (Jacobs (1995)) but go beyond the scope of the present effort. Hence, only a number of somewhat general yet useful observations will be made from the data as presented in Figures 4.8 and 4.9 and in Table 4.12.

Putting the graphs for AAG-2 and AAN at -12 and -24°C side by side shows that at -12°C both binders possess nearly equal yield properties, while at -24°C the yield stress of the AAG-2 is much higher, irrespective of loading rate. This shows that AAN is the better binder with a less sensitive temperature response. The free volume, which makes the flow process possible, probably collapses much faster in AAG-2 than in AAN, yielding higher activation energies for the AAG-2 system.

Comparing the behavior of AAN and AAN + 5% linear SBS, it appears that the addition of polymer increases the yield stress but that this effect is stronger at lower temperatures. It also appears that only for the linear SBS in AAN the activation volume increases with a reduction in temperature. This anomalous behavior may be directly linked to the superior fracture performance (i.e., G_{Ic} or strength in the presence of a notch) of this particular binder (see Roy and Hesp (2001a and 2001b) and section 4.4 in this report) and could be caused by subtle interactions between the polymer domains and certain bitumen components. A recent paper by Anh and Vu-Khanh (2001) reporting on a yield and fracture study of polystyrene (PS) blended with ethylene propylene rubber (EPR) suggests that there appears to be an "implicit correlation between yielding and fracture behavior." The observations in our work on asphalt systems appear to be in good agreement with their findings in PS/EPR blends.

If straight AAN is compared with the filled AAN systems, it is noticeable that the yield stress increases significantly due to the presence of filler. This makes sense since the filler particles inhibit the flow process. However, what is not readily apparent but what follows from an analysis of the data in Table 4.12 is that the activation volume seems to decrease by a large amount due to the addition of filler. This suggests that the filler introduces a large number of small flaws (i.e., micro-cracks) in the matrix, thus facilitating the flow process at longer loading times. The slopes of many of the straight lines in Figure 4.3.3.1 and 4.3.3.2 also give the impression that negative yield stresses should be possible provided that low enough loading rates are applied. This is obviously impossible and can only be explained if the flow process occurs due to a mixture of viscous flow and the formation of microcracks or voids within the matrix. It would be interesting to refine the experimental technique and to accurately determine yield stresses at much slower rates of loading. Since the load frame used for this work was not able to apply such low rates, these experiments will have to wait until later.

Questions related to if and how the results as presented in this section should be used in a low-temperature binder specification scheme will be discussed in section 4.5 on the development of the fracture energy and CTOD test methods.

4.4 Validation of the Binder Crack Opening Displacement Property as a Performance Indicator for Low-Temperature Failure in the Mixture

The crack opening displacement concept was validated in laboratory mixture tests in order to evaluate a large number of well-controlled, modified binders made with the same base asphalt under well-controlled laboratory testing conditions.

Binder samples were tested at various rates of loading and test temperatures in three-point bending and in compression to determine their fracture energies and compressive yield stresses. The ratio of these, G_{Ic}/σ_{cy}, provides a measure of the critical crack tip opening displacement (CTOD) of the binder. (For further background, see sections 4.3 and 4.5.4.)

The CTOD property, binder stiffness, and binder fracture energy were subsequently compared with the crack mouth opening displacements (CMOD) as measured in the mixture tests at low temperatures. The CMOD property in the mixture is considered to be the most realistic performance-based property for low-temperature cracking since it provides a measure of strain tolerance in the presence of large flaws. Details of this study are presented in Roy and Hesp (2001a), while a summary is provided herein.

4.4.1 Fracture Tests on Binders

Tables 4.13 and 4.14 give an overview of all the values of stiffness, fracture toughness and energy, yield stress, and CTOD obtained at three temperatures and two strain rates for the binders as described in section 3.1.1.

It is clear from the data in Tables 4.13 and 4.14 that the binders studied demonstrated a wide range in their low-temperature fracture toughness and energy as well as compressive yield stress values. As this study is not the first to report on this fact, the results did not come as a total surprise. However, the magnitude of the differences found was impressive, and for that reason it was decided to investigate whether the very high toughness values can somehow translate into a better resistance to thermal cracking for the mixture.

Table 4.13 Binder Fracture Properties at -24°C and a Loading Rate of 0.01 mm/s

Binder	E_c, MPa	E_b, MPa	K_{Ic}, kN.m$^{-3/2}$	G_f or G_{Ic}, J/m^2	σ_{cy}, MPa	G_{Ic}/σ_{cy}, µm
AAN	111	235	69	28	4.5	6
AAN + diblock SB	70	212	136	131	3.7	35
AAN + EVA	168	198	68	25	7.9	3
AAN + linear SBS	31	58	181	736	1.2	613
AAN + radial SBS	38	101	127	232	1.5	154
AAG-2	174	293	62	16	> 5.1 (a)	< 3
AAG-2 + linear SBS	41	186	120	127	1.5	85
AAG-2 + radial SBS	200	317	137	73	7.0	10

Note: Young's moduli used to calculate G_{Ic} (i.e., K_{Ic}^2/E) and CTOD (i.e., $K_{Ic}^2/\sigma_{cy}E$) were averages from the load-displacement data obtained in the compression and three-point bend tests. (a) These samples failed in a brittle mode in the compression test; hence, the yield stresses are larger than the quoted failure stresses. E_c = Young's modulus as measured in compression; E_b = Young's modulus as measured in bending; K_{Ic} = fracture toughness; G_{Ic} = fracture energy; σ_{cy} = compressive yield stress; Binder AAN is a Bow River binder; Binder AAG-2 is a low asphaltene California Valley binder; SB = styrene-butadiene; EVA = ethylene vinyl acetate; SBS = styrene-butadiene-styrene.

Table 4.14 Binder Fracture Properties at -30 and -40°C and a Strain Rate of 0.001 mm/s

Binder	E_c, MPa	E_b, MPa	K_{Ic}, $kN.m^{-3/2}$	G_f or G_{Ic}, J/m^2	σ_{cy}, MPa	G_{Ic}/σ_{cy}, μm
AAN	158	242	76	29	> 9.4 (a)	< 3
AAN + diblock SB	115	190	106	74	6.0	12
AAN + EVA	236	180	54	14	> 9.4 (a)	< 2
AAN + linear SBS	68	115	167	304	2.4	127
AAN + radial SBS	82	136	116	123	3.2	38
	54	306	139	107	5.8	19
AAG-2	94	167	59	26	> 12.5 (a)	< 2
AAG-2 + linear SBS	110	271	106	59	2.3	26
AAG-2 + radial SBS	172	271	132	78	5.9	14

Note: Young's moduli used to calculate G_{Ic} (i.e., K_{Ic}^2/E) and CTOD (i.e., $K_{Ic}^2/\sigma_{cy}E$) were averages from the load-displacement data obtained in the compression and three-point bend tests. The radial SBS-modified AAN samples (containing 3 percent processing oil) never failed at -24°C or -30°C in a catastrophic fashion so the "toughness" values are based on the peak stresses reached. For this reason it was also tested at -40°C where it did fail in a catastrophic fashion (second listing in Table 4.14). (a) These samples failed in a brittle mode in the compression test at the given crosshead displacement rate; hence, the yield stresses are larger than the quoted stresses that were determined at a somewhat slower strain rate. E_c = Young's modulus in compression; E_b = Young's modulus in bending; K_{Ic} = fracture toughness; G_{Ic} = fracture energy; σ_{cy} = yield stress in compression; Binder AAN is a Bow River binder; Binder AAG-2 is a low asphaltene California Valley binder; SB = styrene-butadiene; EVA = ethylene vinyl acetate; SBS = styrene-butadiene-styrene.

The results are interesting in several respects. First, as expected, most of the binders appeared stiffer at the lower temperature and strain rate. Only a few of the samples were less stiff at -30°C and 0.001 mm/s than at -24°C and 0.01 mm/s, and this depended somewhat on whether the modulus was considered in bending or in compression. This either suggests that the time-temperature shift factors must be quite different for these binders or, alternatively, it could be that these two binders experienced some degree of damage in the form of micro-cracking during the compression test. Although this issue deserves further study, it is better left for a later time.

A further observation relates to the relative performance of the various polymer-modified binders. Although BBR and DT performance grades were not determined on these samples, going by the work of Anderson et al. (2000, 2001 and Figure 2.4) and other reports in the literature (Kluttz and Dongré (1997), Hesp et al., 2000), it is reasonable to assume that the modifiers would have had little if any effect on the performance grades as measured by the SHRP tests. In contrast, if all the systems studied in this project are considered, it becomes apparent that the low-temperature fracture and yield properties differ widely depending on the asphalt source and the modifier type. How these differences relate to mixture performance will now be discussed.

4.4.2 Fracture Tests on Mixtures

The crack mouth opening displacement results along with the sample dimensions (i.e., a_o and W) are given in Table 4.15. The data show that this true failure test is able to reveal a wide range in performance differences for different regular and modified mixtures. This would not have been predicted by either of the SHRP binder specifications (BBR and BBR + DTT) or necessarily the TSRST (e.g., see Fabb (1974) or Hesp et al. (2000)). In contrast, the binder fracture properties G_{Ic} and CTOD do appear to give a reasonable correlation with the mixture performance in this test.

With only a few samples tested at just one somewhat arbitrary strain rate, it would be unwise to draw any final conclusions. However, these initial results are encouraging in that they are able to provide insights into important aspects of the low-temperature failure process. Systems that failed in a catastrophic mode as opposed to those that showed stable crack growth in the mixture are identified with high accuracy by their low binder CTODs. Further, the toughest modified binder provided a critical mixture CMOD that was nearly four times as high as for its unmodified control. This ought to result in improved low temperature cracking resistance and may even prevent it altogether.

Figure 4.10 gives representative crack opening curves for two tested samples. The AAG-2 and AAN specimens as well as the brittle EVA specimens all broke in the catastrophic fashion as shown (abrupt increase in CMOD with a simultaneous decrease in load), whereas nearly all the tough SBS systems failed in a more gradual fashion (stable crack growth due to a rising R-curve followed by catastrophic failure). The arrows in Figure 4.10 indicate the CMOD at which the maximum load was reached and, for this particular AAG-2 specimen, where a so-called "pop-in" event occurred (an abrupt increase in CMOD followed by subsequent arrest).

In fracture mechanics, these CMOD values are just two of several that are used to calculate critical CTODs. The other points that are often reported are those at which the load versus CMOD curve first deviates from linear (onset of stable growth) and at which a first plateau is reached. Which of these is used as the critical CTOD depends on the application of the material and is usually agreed upon between user and producer of a particular material or part. However, in asphalt mixtures, the very occurrence of stable crack growth is beneficial, and hence the maximum load or pop-in values are selected in this study as critical properties for performance prediction.

Once more, the importance of field trials needs to be emphasized. The failure mechanisms are not yet fully understood to unequivocally state that just one particular binder property is able to describe the entire low-temperature failure process. The effects of the large aggregate interface, construction and subgrade flaws, loading time and temperature, moisture damage, aging, and associated traffic may all change the outcome to some extent from what is predicted with simple laboratory tests on small samples. Then again, bad experiences with materials similar to AAG-2 as well as with other equally brittle systems have for some time already alerted users that not all binders of the same SHRP low-temperature grade perform in the same way. Hence, this gives a strong indication that a low G_{Ic} or CTOD value could be used to screen out such undesirable materials.

Table 4.15 Critical Crack Mouth Opening Displacements for Asphalt Mixtures

Asphalt Mixture	T, °C	a_o, mm	W, mm	a_o /W	CMOD, μm	Crack Growth
AAN	-30	18.8	36.0	0.52	17	Catastrophic
	-30	18.1	37.3	0.49	9	Catastrophic
AAN + diblock SB (a)	-40	22.1	43.1	0.51	22	Catastrophic
	-40	22.8	45.0	0.51	14	Catastrophic
AAN + EVA	-30	20.6	39.4	0.52	16	Catastrophic
	-30	20.7	38.2	0.54	18	Catastrophic
AAN + linear SBS	-30	21.9	45.0	0.49	42	Stable
	-30	22.9	45.0	0.51	44	Stable
AAN + radial SBS (a)	-40	20.1	38.2	0.53	31	Stable
	-40	19.8	38.1	0.52	25	Stable
AAG-2	-30	22.9	43.6	0.53	15	Catastrophic
	-30	21.4	40.1	0.53	14/22	Pop-In/Catastrophic
	-30	20.6	42.1	0.49	13/26	Pop-In/Catastrophic
AAG-2 + linear SBS	-30	19.8	41.0	0.48	27	Stable
	-30	18.9	42.1	0.45	13	Catastrophic
	-30	21.3	42.0	0.51	15	Stable
	-30	20.6	40.3	0.51	38	Stable
AAG-2 + radial SBS	-30	20.5	43.6	0.47	27	Stable
	-30	21.3	44.9	0.47	19	Catastrophic

Note: (a) These two systems did not show any strength at -30°C and so were tested at -40°C instead. Binder AAN is a Bow River binder; Binder AAG-2 a low asphaltene California Valley binder; SB = styrene-butadiene; EVA = ethylene vinyl acetate; SBS = styrene-butadiene-styrene.

In Figure 4.11 the average mixture CMOD from Table 4.15 is plotted versus the binder stiffness in compression and bending, the fracture energy, and the calculated binder CTOD from Table 4.14. It is apparent that there is little correlation between the mixture CMOD and the binder stiffness in either compression or bending. Quite the opposite, there appears to be a reasonable relationship between the binder fracture energy or critical crack tip opening displacement and the mixture CMOD. It should be noted, however, that this is not a straight-line relationship in that the benefit of increasing the binder toughness appears to level off. This is because for higher toughness binders and mastics the failure process shifts more predominantly to the large aggregate interface where binder toughness is of less importance.

These are encouraging results that point towards both G_{Ic} and CTOD as being useful parameters for the prediction of low-temperature cracking severity. There is still, however, the remote possibility that none of these properties has much to do with the low-temperature cracking process as it occurs in the pavement. Hence, it is imperative that these ideas are tested in well-designed field trials such as the one just constructed on Highway 655 near Cochrane, Ontario. This trial has side-by-side seven different asphalt binders that all have an AASHTO M320 grade within the narrow -34°C to -35°C bracket. Hence, careful monitoring will allow the ideas presented in this section to be validated with actual field performance data.

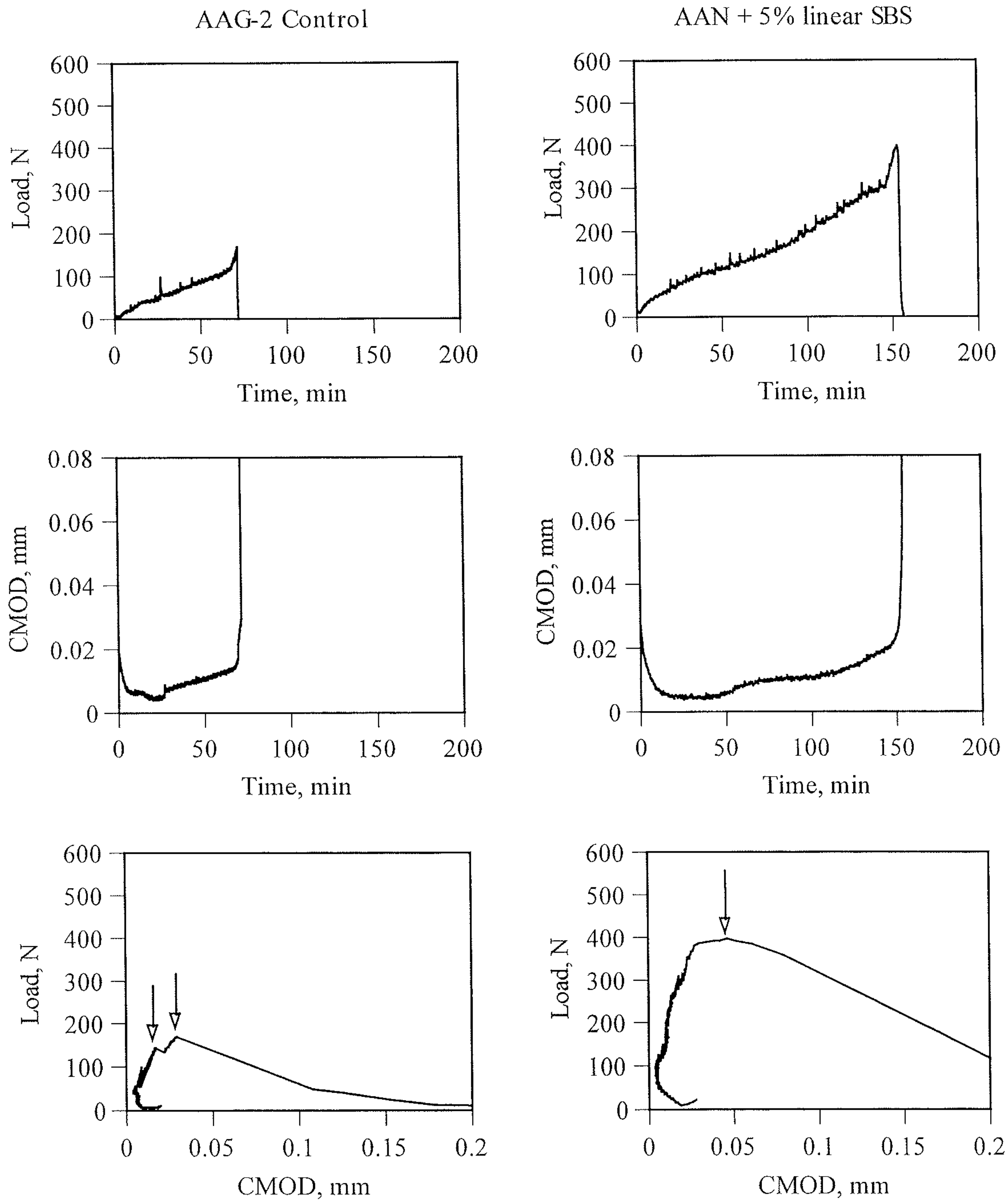

Figure 4.10 Representative crack mouth opening displacement results for AAG-2 control and AAN + 5% linear SBS mixtures at -30°C and strain rate of 0.01 mm/min.

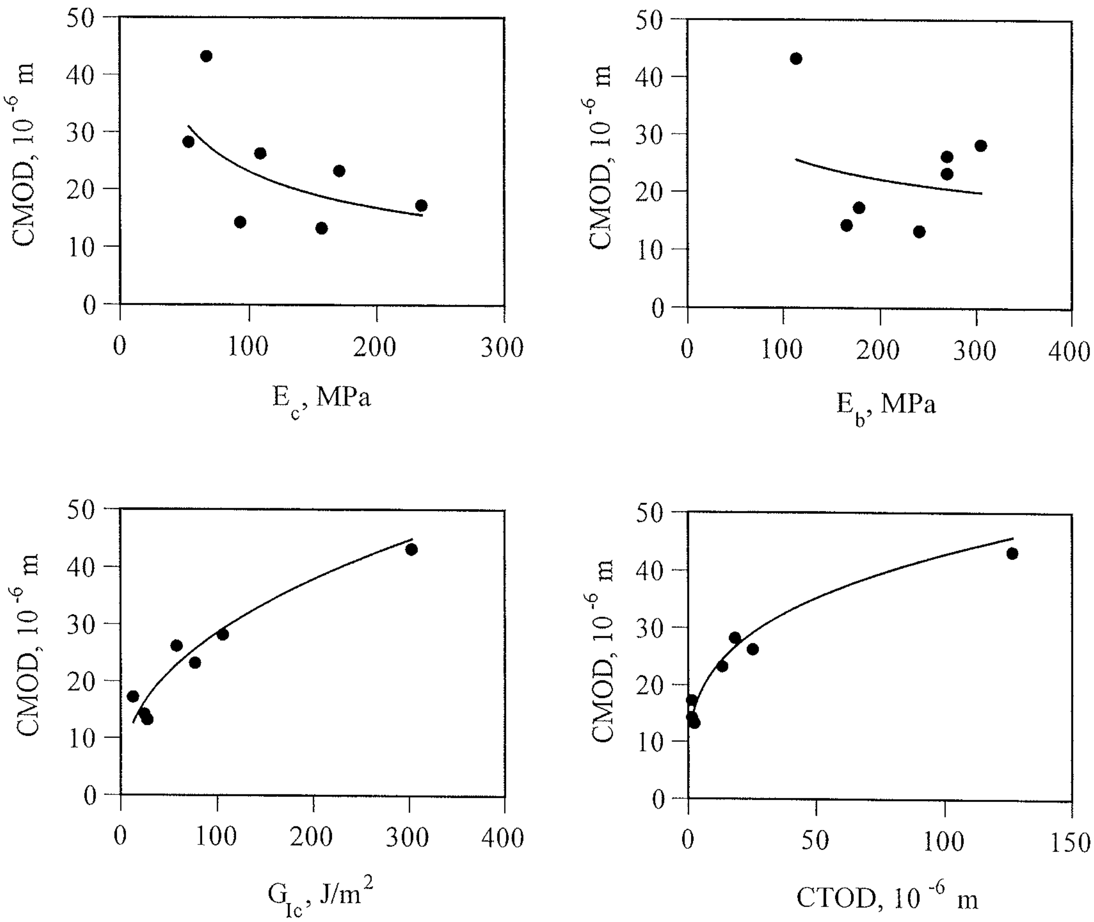

Figure 4.11 Correlation between mixture CMOD and various binder properties.

4.5 Development of an Improved Binder Grading Method Based on Fracture-Mechanics Principles

4.5.1 Background on Fracture Testing

The basic requirements for conducting a valid fracture test on a brittle material are outlined in various ASTM methods (e.g., ASTM (1990, 1993, 1996)). These methods all find their basis in the Griffith theory for failure in brittle solids, which allows one to calculate the maximum permissible flaw size for a given stress level and fracture energy or, if the maximum flaw size is known, to calculate the fracture energy from a fracture test at a given rate of loading (Griffith (1921)). A short discussion on the basic principles underlying the Griffith theory, following the arguments of Ewalds and Wanhill (1985), Broek (1997), McCrum et al. (1997) and others, and how these principles relate to failure in asphalt under thermal stress, is given in Roy and Hesp (2001b).

Griffith (1921) was the first to consider the process of fracture from an energy balance point of view (Ewalds and Wanhill (1985)). His basic premise was that a crack only propagates if the total energy of the system is lowered. Hence, instability occurs at a stress level, σ_f, for which the total strain energy released exceeds that which is required for the formation of two new fracture surfaces:

$$\frac{\pi\sigma_f^2 a}{E} = 2\gamma_e \qquad (4\text{-}6)$$

where E is Young's modulus, a is half the length of an ideally sharp crack, and γ_e is the elastic surface energy (Ewalds and Wanhill (1985)). Irwin (1948) and Orowan (1952) slightly modified Griffith's equation by including a plastic surface energy term, γ_p, for the plastic work done during the fracture process:

$$\frac{\pi\sigma_f^2 a}{E} = 2(\gamma_e + \gamma_p) \qquad (4\text{-}7)$$

Combining the two surface energy terms allows the Griffith equation to be used for materials that exhibit a limited degree of plastic deformation upon failure. In this relationship the left-hand side gives the released strain energy under critical conditions, G_c, whereas the right-hand side gives the resistance to fracture, R. For thick sections (i.e., plane-strain conditions exist), an additional $(1-\nu^2)$ term is included in equation 4-7, where ν is Poisson's ratio, and G_c then becomes G_{Ic}.

$$G_{Ic} = \frac{\pi\sigma_f^2 a(1-\nu^2)}{E} = 2(\gamma_e + \gamma_p) = R \qquad (4\text{-}8)$$

G_{Ic} is known as the plane-strain fracture energy, and it is found to be a material property (i.e., independent of specimen size and geometry) with much use for performance prediction in brittle failure (e.g., see Ewalds and Wanhill (1985), Latzko et al. (1984), Mai et al. (2000)).

Fracture energy can also be related to the total strain energy released upon fracture, U, and the specimen dimensions B and W in the following manner:

$$G_{Ic} = \frac{U}{BW\varphi} \qquad (4\text{-}9)$$

where U is the area under the stress strain curve, B is the specimen thickness, W is the specimen height, and φ is a tabulated correction factor that is dependent on the specimen compliance (see Mai et al. (2000), ASTM (1996), and references therein). In other words, equation 4-9 shows that it is possible to measure the fracture energy directly from a single test on a notched fracture specimen without having to resort to equation 4-8, which requires separate determinations of Young's modulus and Poisson's ratio. The fracture energy so determined should be close to if not the same as the one determined through equation 4-8.

An instructive way to consider the fracture process under a constant load condition is to give a picture of equation 4-8 graphically as energy versus crack length. (See Figure 4.12 reproduced from Ewalds and Wanhill (1985).) For a high stress σ_1 the critical crack length is low at a_1, whereas for a lower stress σ_2 the critical crack length is higher at a_2.

Figure 4.12 also shows that after the instability condition has been reached, the strain energy release rate, G, depends on whether the condition is constant load or so-called "fixed grips" (i.e., constant strain or full restraint) (Ewalds and Wanhill (1985)). Due to the growing crack in the sample, the stiffness of the sample can decrease, and hence for fixed grips conditions the strain energy release rate, $\partial G/\partial a$, decreases when the crack develops. This is an important detail for low-temperature failure in asphalt concrete, and it helps to some extent to explain why certain cracks in a pavement do not progress completely across the entire width of the road. Because of the slow stable crack growth that occurs just prior to catastrophic transverse cracking (for instance, in the form of localized yielding and blunting of cracks, interfacial failure, or the breaking of small aggregate particles), and due to regular fatigue cracking at more moderate temperatures, a significant decrease in stiffness can occur. It was proposed by Hesp et al. (2000) that for very tough binder systems this kind of relaxation may be enough to avert catastrophic failures totally and yield asphalt concrete that can readily be cooled to very low temperatures without showing any signs of serious damage. However, it should be noted that $\partial G/\partial a$ for the fixed grips condition remains positive and that G remains larger than R; hence, there must be more to this issue to explain the very existence of transverse cracks that do not reach the entire distance across the road. To understand this further, we have to consider a rising R-curve, which will be discussed later.

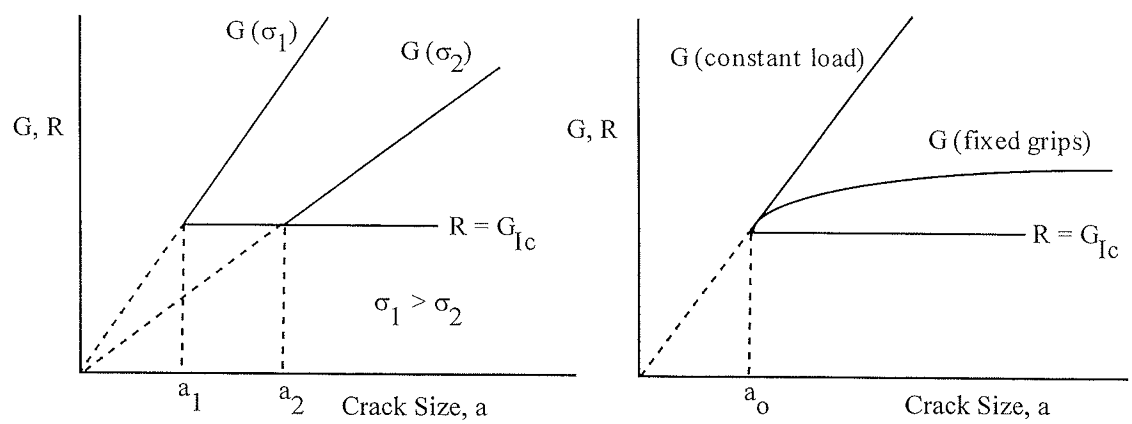

Figure 4.12 Graphical representation of the energy balance approach for plane strain fracture. G = strain energy release rate; R = resistance to fracture; σ_1 and σ_2 are stress levels; G_{Ic} = plane strain fracture energy. (Reproduced from Ewalds and Wanhill (1985))

Before proceeding, however, it is important to note that the fracture energy, G_{Ic}, gives a good indication of the performance of a particular binder at low temperatures under a worst-case scenario of plane-strain fracture. In the past, fracture energy has been used to successfully rank the five different specialty and polymer-modified binders of the Highway 118 test sections according to their failure behavior in a conventional restrained cooling test (Ponniah and Hesp (1996)). Furthermore, it has been possible to use fracture energy arguments to show why a particularly tough SBS-modified system never failed when taken in thermal fatigue cycles down to temperatures as low as -60°C, although this was not predicted by any of the SHRP tests (Hesp et al. (2000)). It is only when one deals with very tough binders that performance may even be better than what is predicted by G_{Ic} alone.

It has been observed with tough materials or under less severe conditions (higher temperatures and/or thinner sections under less constraint), that the situation as depicted in Figure 4.12 changes. The resistance to fracture can increase with the crack length, resulting in a so-called "rising R-curve." Figure 4.13 gives an example for constant load conditions. It shows that the strain energy release rate, G, is once again given by a straight line, but now R increases with crack length. This situation leads to a limited degree of stable crack growth at some stress level below the catastrophic failure stress. When the stress reaches σ_1 where G equals R for a crack size a_o, the crack can grow by a minimal amount, but when it does, the rising R-value soon catches up. It is only when the stress reaches a value σ_c, at which G equals R and $\partial G/\partial a$ equals $\partial R/\partial a$, that the point of no return is reached and catastrophic failure ensues at a crack length a_c.

If in addition to a rising R-curve there is also a limited degree of the fixed grips condition, the entire cracking process may in fact become beneficial to reduce thermal stresses and hence avert catastrophic failures. However, it is obvious that these conditions are considerably more complicated and that a simple failure criterion such as G_{Ic} starts to become somewhat elusive. Nevertheless, fracture energy is a useful parameter for the ranking of asphalt binders at low temperatures. A tougher binder means a larger $\partial R/\partial a$ value, and that promotes the stable crack growth phase. Furthermore, larger starting cracks or cracks that have already grown to some extent during a previous low-temperature cycle will show a more extended phase of stable crack growth (larger difference between a_o and a_c). Hence, the use of tough modified binders should show up as a reduction in the number and average length of low-temperature cracks in the pavement. Rising R-curves have in fact been observed in laboratory tests on asphalt mixtures (e.g., Figure 9 in Mahboub (1990), Figures 11-13 in Mobasher et al. (1997), Marasteanu et al. (2002)).

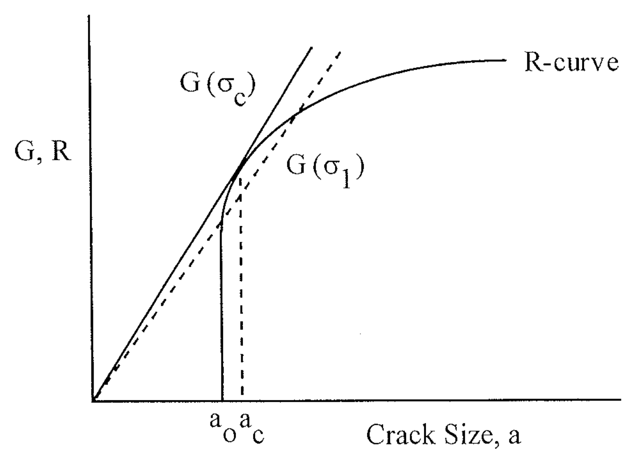

Figure 4.13 Graphical representation of a rising R-curve and stable crack growth. G = strain energy release rate; R = resistance to fracture; σ_1 and σ_2 are stress levels; a_o = crack size where stable crack growth starts; a_c = crack size at which catastrophic failure occurs. (Reproduced from Ewalds and Wanhill (1985))

A discussion on the origins of the rising R-curve is beyond the scope of this report. For further details, the interested reader is referred to the papers by Mahboub (1990) and Mobasher et al. (1997).

In order to avoid the entire problem of defining a failure criterion that is based on a Griffith approach (i.e., K_{Ic} or G_{Ic}) with a perfectly sharp crack tip, Wells (1962) decided to consider the failure strain at the tip of a somewhat blunted crack as a parameter to rank materials according to their fracture resistance. He argued that due to the high stress intensity factors at the tip of the crack, the material there must locally yield and blunt the crack before fracture occurs. Hence, he made the reasonable assumption that the *crack tip plastic strain* at failure can be used as an accurate failure criterion. The parameter that is now known as the critical crack tip opening displacement or CTOD has, since Wells first introduced it in 1962 been widely used for the ranking of various materials that show an appreciable degree of crack tip plasticity before failing (Ewalds and Wanhill (1985), Anderson (1995)). Later researchers have refined Wells' ideas, and the CTOD concept has evolved as a design parameter that can be used to calculate actual failure strains in the presence of cracks (Ewalds and Wanhill (1985), Latzko (1984), Anderson (1995), Broek (1997)).

If the assumption is made that the shape of the yielded zone ahead of the crack tip can be described by a so-called Dugdale model (details can be found in Ewalds and Wanhill (1985)), then it can be shown that the critical crack tip opening displacement under plane-stress conditions relates to the fracture energy and yield stress of the material according to the following simple relationship:

$$\mathrm{CTOD} = \frac{G_{Ic}}{\sigma_y} = \frac{K_{Ic}^2}{E\sigma_y} \quad \text{(plane-stress)} \quad (4\text{-}10)$$

where σ_y is yield stress, E is Young's modulus, and K_{Ic} is fracture toughness.

For plane-strain conditions (i.e., thick sections), it is found that the CTOD is about half of what it is for the plane-stress condition (Ewalds and Wanhill (1985), Anderson (1995):

$$\mathrm{CTOD} = \frac{G_{Ic}}{2\sigma_y} = \frac{K_{Ic}^2}{2E\sigma_y} \quad \text{(plane-strain)} \quad (4\text{-}11)$$

It is important to realize, however, that both depend on the ratio of two material properties, namely G_{Ic} and σ_y. The G_{Ic} (or K_{Ic}) can be measured in a straightforward three-point bend test, while for the σ_y a surrogate value in compression, σ_{cy}, must be used. Since the yield stress for brittle materials cannot be measured in tension (the specimen will fracture before it yields), it must be assumed that the compressive value is highly correlated with the yield stress in tension (Kinloch et al. (1983), Young and Beaumont (1977)).

This project was started by comparing the CTOD of pure binder with the failure characteristics in the asphalt mixture (see section 4.4). This approach has been able to provide a useful failure criterion for brittle failure in filled epoxy systems (Gledhill et al. (1978), Young and Beaumont (1977)) and has been studied to only a limited extent in failure of asphalt concrete (Jacobs (1995)). Thus it was decided to explore the technique for performance grading of polymer-modified and specialty asphalt binders. It may become exceedingly complex (and in the end not worth the effort) to go much further than to evaluate whether this simple concept can be used to develop a simple and more accurate grading system for asphalt binders than what is currently used.

The use of more complex J-integral and C*-integral techniques may not be warranted, since, as pointed out by others (Ewalds and Wanhill (1985), pp. 158-159), "it may be highly conservative (i.e., inefficient) to use J_{Ic} as a measure of the fracture resistance to be expected in practice… this is because the R-line for many materials has a very steep slope, and only a few millimeters of stable crack extension give J values two or three times J_{Ic}." Translated into more simple language, this means that asphalt binders and mastics are unlikely to crack when ductile, unless, of course, large construction flaws or subgrade problems are already present. Even then, the significant degree of fixed grips conditions that prevail in any shrinking pavement will limit the amount of cracking until brittle conditions are attained. The CTOD concept has been successfully used with materials that show appreciable crack tip plasticity yet do not require the use of J- or C*-integral methods (Ewalds and Wanhill (1985), Latzko et al. (1984), Anderson (1995)).

4.5.2 Fracture Toughness and Fracture Energy Test Development

4.5.2.1 Sample Preparation and Sample Size

The first objective with respect to the refinement of the fracture toughness test method was to reduce the sample size and arrive at an acceptable sample preparation method. Issues similar to those which faced the SHRP researchers and their successors presented themselves in this project.

A single rolling thin film oven (RTFO) run produces anywhere between 200 and 250 g of RTFO-aged binder from eight tubes; this material is then further aged in the pressure aging vessel (PAV). Hence, it would be prudent to design a complete grading scheme that uses less than the ~200 g of binder that comes from the PAV to determine a low, intermediate, and high temperature grade for each binder.

The original fracture studies published in the mid-1990s used a Dow Corning RTV silicone rubber mold to cast binder samples measuring 175-mm x 25.4-mm x 12.7-mm, with a sharp 90° starter notch, 5-mm deep, on a single side in the middle (see Figure 4.14). This design had a number of drawbacks. First of all, the RTV silicone rubber is rather hard, which made it difficult to remove the sample from the mold. Hence, recent molds have been made with Dow Corning HiSil III, which is a softer silicone rubber, making it much easier to remove the samples after cooling.

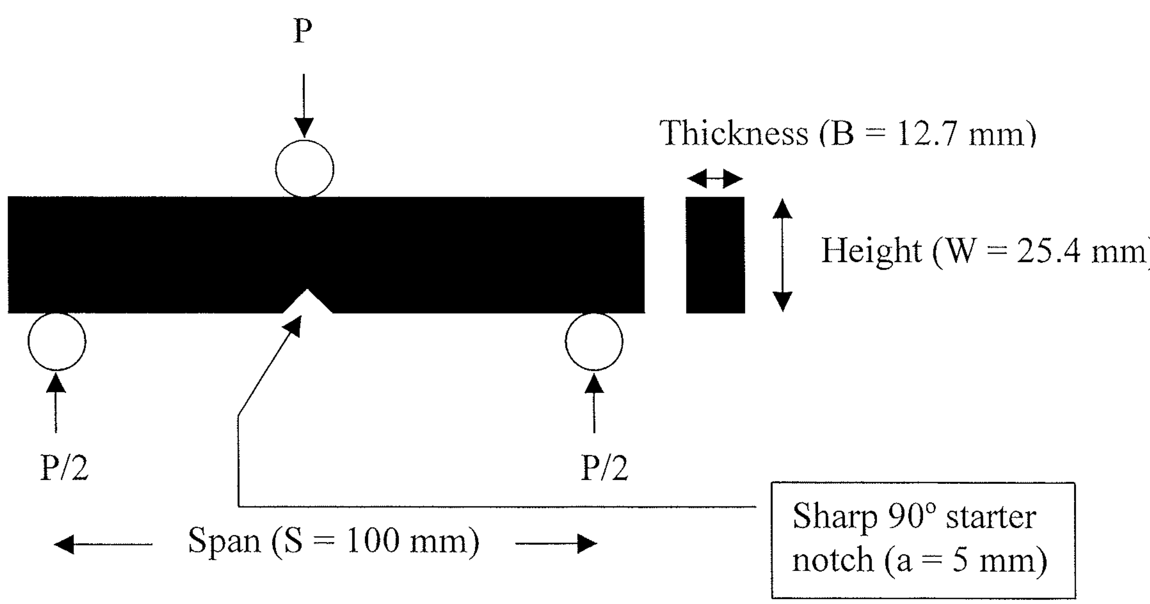

Figure 4.14 Schematic of the original fracture toughness test method (not to scale). (Reproduced from Lee and Hesp (1994))

The second drawback of the original design related to the approximately 55 g of material required for the casting of a single fracture specimen. Using such large specimens for grading purposes would create problems, since only a limited amount of material is produced after PAV aging. To this end, the design was altered with inserts that facilitate using a mere ~2.5-5 g for a single fracture specimen. This project first explored the use of plastic (polycarbonate) inserts but finally settled on aluminum inserts, since these are much easier to clean. Figures 4.14-4.17 provide pictures of old designs and some of the new ones that were considered in this study.

A further problem with the mold design related to the reproducibility of the dimensions for the samples as taken from the mold after cooling. When asphalt binder specimens cool, there is always a certain amount of shrinkage causing both deviation and variation in the desired dimensions. The thickness, B, is poorly controlled in molds such as those shown in Figures 4.14 and 4.15, since these are both filled with the samples positioned on their sides. The ligament thickness, W-a, is poorly controlled in molds as designed according to Figures 4.16 and 4.17, since in these molds the samples are positioned on their bottoms.

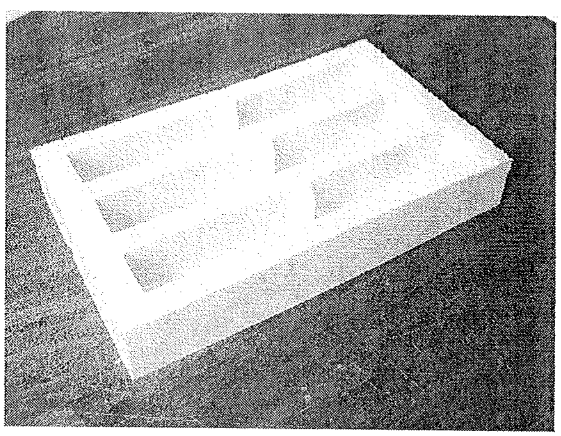

Figure 4.14 Original silicone mold design for specimen casting without inserts (W = 25.4 mm, B = 25.4 mm, 45° angle, a = 12.7 mm).

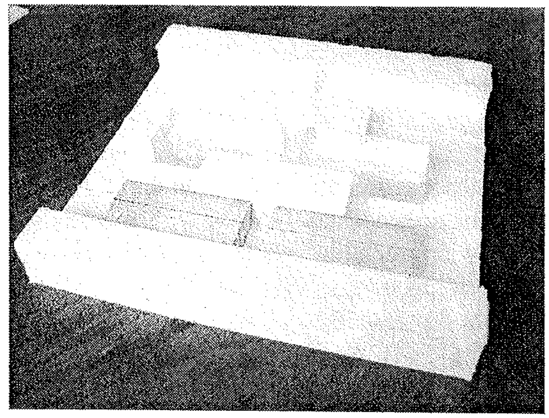

Figure 4.15 Alternative method for casting with plastic or aluminum inserts (W = 25.4 mm, B = 12.7 mm, 90° angle, a = 5.0 mm).

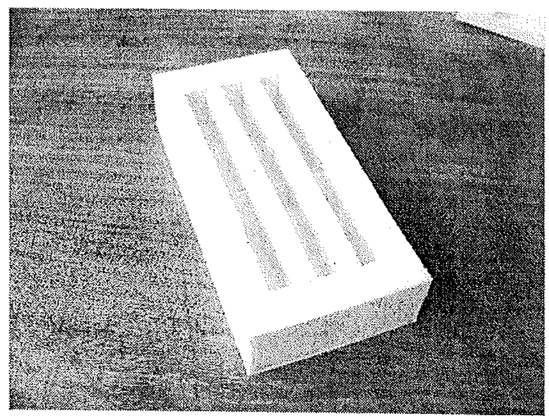

Figure 4.16 Alternative method for casting specimens with or without inserts (W = 25.4 mm, B = 12.7 mm, 45° angle, a = 12.7 mm).

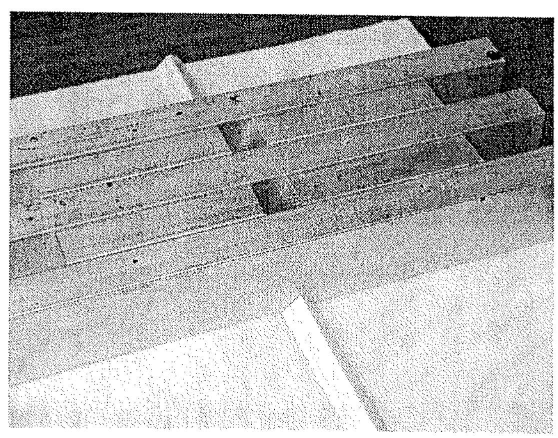

Figure 4.17 Alternative method for casting binder specimens with inserts (W = 25.4 mm, B = 12.7 mm, 90° angle, a = 5.0 mm).

Furthermore, in all of these designs it would be necessary to pour the asphalt binder very carefully so that it just fills the mold, or to trim excess binder in cases when of overfilling. For these reasons a slightly modified mold system was chosen which is able to produce samples with tightly controlled dimensions without having to trim excess binder.

The new designs position the samples with their backs on a sheet of overhead transparency film. The notch is introduced by inserting either an angled silicone strip or a narrow piece of transparency film from the top through a series of six to 10 sets of sample inserts arranged side by side and separated by overhead transparency or Teflon® film. Once the samples are cooled enough, the silicone notch and transparency films are removed, and the samples are ready for testing. This particular technique for preparing the samples guarantees the most accurate control of important dimensions such as notch depth, a, sample height, W, and sample thickness, B. The design assures that these dimensions are in no way dependent on how far the sample cavity is over- or under-filled (within reasonable limits). Figures 4.18 and 4.19 show how these molds are assembled, while Table 4.16 shows typical results for failure load and fracture energy on a series of seven AAN binder samples as prepared with the mold as depicted in Figure 4.18.

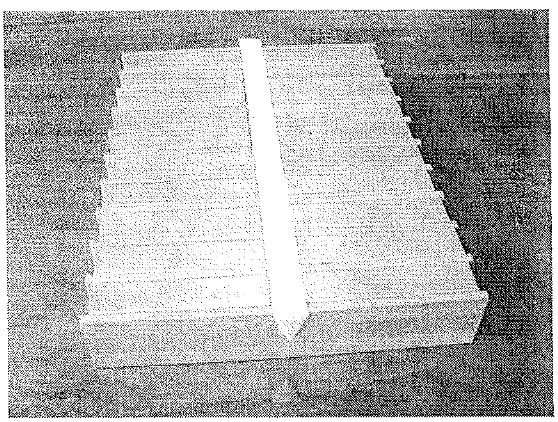

Figure 4.18 Mold design with a 45° angle groove notch (12.7 mm deep).

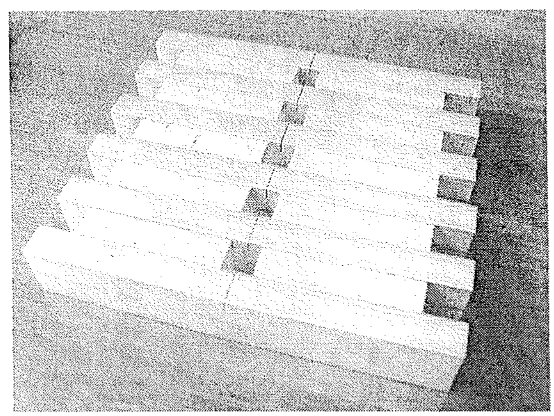

Figure 4.19 Mold assembly with a thin slit notch (5 mm deep, 25 μm wide).

Table 4.16 Fracture Results for 5 g Binder Samples Tested with Aluminum Inserts †

Sample	Dimensions	Failure Load, N	Fracture Energy, J/m^2
1		14.7	6.5
2		15.7	6.9
3	W = 25.4 mm	16.1	9.1
4	B = 12.7 mm	13.3	6.7
5	a/W = 0.5	16.6	7.3
6		14.2	5.4
7		11.7	7.3
Average:		14.6	7.0
Standard Deviation:		1.7	1.1

† Tests were all done at -27°C and a 0.01 mm/s crosshead speed.

4.5.2.2 Effect of Razor Sharpening the Notch

Regular samples as taken directly from a silicone mold were tested, and the results obtained were compared with those for samples sharpened with a new razor blade just prior to testing. These experiments were done to investigate what effect, if any, the sharpness of the notch has on the failure properties. A frequent criticism of fracture tests is that it would require too much time and effort for the preparation of a sufficiently sharp notch to make the test valid and reproducible. The result of this comparison is given in Table 4.17.

Although the error in the 10-mm notch depth sample data is rather high (in part due to the fact that these specimens were made with the old silicone mold design), the overall conclusion to be drawn from this set of data is that there is no significant effect due to razor sharpening of the notch. This is not a totally unexpected outcome, since the toughness of these materials is low, and it is likely that the samples when made are already damaged (i.e., sharpened) to an extent that further sharpening is of little significance.

Table 4.17 Effect of Razor Sharpening the Notch on Failure Loads †

Sample	a = 10.0 mm		a = 12.7 mm	
	Regular	Razor Sharpened	Regular	Razor Sharpened
1	15.0	14.0	12.3	14.7
2	19.0	18.1	16.0	16.9
3	21.5	21.2	13.9	15.9
4	15.9	13.6	13.7	17.5
5	23.7	11.0	13.9	17.8
6	16.6	21.6	17.0	14.0
7	18.0	23.7	17.7	14.2
8	22.4	12.2	14.5	17.4
9	21.1	20.1	17.4	14.2
10	23.6	16.2	15.9	12.9
11	22.2	27.8	13.2	17.8
12	17.1	19.7	15.6	17.3
13	20.9	27.2	17.5	16.6
14	18.5	23.0	15.5	14.7
15	16.4	16.0	16.1	14.3
16	14.6	15.1	14.6	
17	16.3	19.2	14.3	
18	15.4	13.5	17.8	
19	21.6	10.9	19.5	
Average:	18.9	17.9	15.6	15.7
Standard Deviation:	3.1	5.1	1.7	1.9

† Samples were tested without inserts at -24°C and 0.01 mm/s.

4.5.2.3 Plane-Strain Condition

Finally, the effect of sample width on the toughness was investigated to ascertain the plane-strain condition. If the size has no effect on toughness, then there exists what are called "plane-strain conditions." Testing under plane-strain conditions means that the toughness so obtained is a true material property independent of size and geometry. Failure loads in such tests can be used to calculate a valid K_{Ic} and G_{Ic} according to the various published procedures (e.g., equations 4-8 and/or 4-9, ASTM (1990, 1996)). In this set of experiments a few minor surprises were found, which are discussed next.

Table 4.18 provides the fracture data for samples with 0.5-, 0.75- and 1.0-inch thickness. To ascertain plane-strain conditions, one often does a series of tests on samples with varying thickness, B, height, W, or ligament thickness, W-a (Cayard (1990)). If plane-strain conditions are met, then the toughness measured remains constant. If toughness changes with thickness, then either mixed-mode or plane-stress conditions exist, and the measured value is not a material property.

So, if the plane-strain conditions are satisfied, the expected failure loads for samples 1.5 and 2 times wider are simply 1.5 and 2 times higher than those of a 0.5-inch sample. However, the results as presented in Table 4.18 are quite different in that at both temperatures the 0.5 inch results are much higher than the 0.75 and 1.0 inch results (i.e., the 0.5 inch wide samples appear tougher). The fracture energy should be relatively constant in the brittle regime under plane-strain conditions so it was a surprise to find that it is not constant with a 50 percent notch depth. Hence, we can conclude that at these two temperatures the ligament thickness of 12.7 mm (i.e., W-a) allows for mixed-mode (i.e., partial plane-stress) conditions, and the toughness increases for thinner samples. These results contrast with those obtained in an earlier investigation with 20 percent notch depth specimens where the sample dimension did not have an effect on the determined fracture properties (Hoare and Hesp (2000)).

The fact that the 50 percent notch in a 0.5 inch thick sample does not provide plane-strain was surprising but should not pose problems since the COD method allows for substantial yielding and therefore should be able to deal with any measurement as long as there is no bulk yielding with plastic collapse. A further comment that can be made about these tests is that they were done on unaged samples. The results probably would have been different had the AAN been aged in which case the plane strain-plane stress transition would likely have been reached at widths below 0.5 inch.

However, if the specification scheme is supposed to measure the CTOD in the ductile-brittle temperature range as well as the fracture energy in the brittle regime, then it is probably better to stick with a shorter notch in the 20-25 percent range. Such shorter notches will guarantee a more brittle failure over a wider temperature range compared to the 50 percent notch depth as used to obtain the data in Table 4.18.

4.5.2.4 Reproducibility of the Fracture Test

The reproducibility of the fracture test is generally excellent, with coefficients of variations in the 10-15 percent range. Although the numbers in Tables 4.16-4.18 are not perfect, it should be noted that a rather brittle sample was used for these experiments and that the large sample sizes were difficult to accommodate on the three-point bend fixture. Further, difference between results in Table 4.16 and in Table 4.18 may well be explained by differences in temperatures and times for which the binder samples were heated before preparation of fracture beams or by differences in storage conditions of such beams before testing. The SHRP protocol requires that samples be stored at the test temperature for one hour plus or minus five minutes, which is far too short a period to be meaningful (see section 4.2 on SHRP test results). It has not yet been decided how to standardize the sample preparation and handling protocol for fracture testing since this will only happen after broad consultation with users of the method.

Table 4.18 **Plane-Strain and Mixed-Mode Conditions in Samples with 50 Percent Notch**

Sample	Dimensions, inch	Temperature, °C	Failure Load, N	Fracture Energy, J/m²
1	B = 0.50	-24	17.0	22.5
2	Mixed-Mode		13.3	10.9
3			12.3	16.3
Averages:			**14.2**	**16.6**
4	B = 0.75	-24	10.8	3.2
5	Plane-Strain		8.6	2.9
Averages:			**9.7**	**3.1**
6	B = 1.00	-24	16.2	10.2 †
7	Plane-Strain		15.9	5.5
Averages:			**16.1**	**7.9**
8	B = 0.50	-30	12.3	9.3
9	Mixed-Mode		14.8	14.0
10			15.9	11.0
Averages:			**14.3**	**11.4**
11	B= 0.75	-30	12.3	4.1
12	Plane-Strain		11.0	3.2
13			11.1	6.1
Averages:			**11.5**	**4.5**
14	B = 1.00	-30	12.1	2.5
15	Plane-Strain		15.9	7.5
16			10.6	2.0
Averages:			**12.8**	**4.0**

Note: Samples were made with a 45° notch. Tests were done at 0.01 mm/s loading rate. Fracture energy calculated according to ASTM D 5045-96 from the area under the curve (i.e., equation 4-9). † This number is suspect and ideally a few additional samples should have been tested.

The above results should also be placed in their correct context. Tests have been conducted at Queen's University since 1994, and fracture energies so determined have ranged anywhere from 10 to 300 J/m² for samples of nearly the same SHRP performance grade. Hence, even though the errors appear large in some instances, the enormous variations in fracture energy should make it easy to show statistically significant differences between binders.

4.5.3 Fracture Specification Properties of Test Section Binders

4.5.3.1 Fracture Properties of Highway 118 Asphalt Binders

Unaged and RTFO-Aged Materials

The fracture toughness, K_{Ic}, and fracture energy, G_f or G_{Ic}, were measured on both unaged and RTFO-aged materials at -24°C and -30°C at both 0.001 and 0.01 mm/s in three-point bending. Binders were conditioned before testing for three days at -24°C to avoid problems with physical aging. Samples for this set of experiments were cast with aluminum inserts in a silicone mold similar to the one shown in Figure 4.15. (Later designs had not yet been optimized when these samples were tested.) The specimen thickness, B, was measured after the sample had failed in order to account for variations in failure load due to errors in thickness. The notch depth, a, was kept constant at 10 mm, and the sample height, W, was kept constant at 25.4 mm (a/W = 0.394). The number of samples tested for each individual temperature and strain rate varied between two and five.

Fracture toughness was calculated from the failure load and sample dimensions according to the relationship given in ASTM method D 5045-96 (ASTM, 1996):

$$K_{Ic} = \frac{P_f S}{B W^{3/2}} \times \left(\frac{3}{2} \sqrt{x} \frac{\left[1.99 - x(1-x)(2.15 - 3.93x + 2.7x^2\right]}{(1+2x)(1-x)^{3/2}} \right) \tag{4-12}$$

where: P_f is the failure or peak load, S is the span (100 mm), B is the sample thickness (nominal 12.5 mm), and x = a/W (0.394).

The fracture energy was calculated from the area under the load-displacement record according to equation (4-9):

$$G_{Ic} = \frac{U}{BW\varphi} \tag{4-9}$$

where: U is the area under the load-displacement curve in Joules and φ is a correction factor for the sample compliance (φ = 0.331 for a/W = 0.394 (ASTM D 5045-96)).

Given the low loads that are generally required for failure in asphalt binders it was deemed unnecessary to correct the fracture energy for system compliance, loading-pin penetration, and sample compression before fracture (ASTM D 5045-96). However, the validity of this assumption may need to be checked at some later date with very tough and ductile binders.

Although the application of the above relationships is strictly valid only in the linear elastic regime, the results for ductile failure are also reported here, but these may not be true material properties. In spite of that, they still provide a measure of the resistance to fracture. The results in Table 4.18 also suggest that some of the data obtained for this set of tests with a 10-mm notch may in fact be mixed-mode toughness values. Hence, G_f is used to indicate that some of these values may be generic fracture energies rather than true plane-strain fracture energies.

Table 4.19 gives the average fracture toughness and fracture energy values obtained for the five Highway 118 binders under the above-stated conditions. Figure 4.20 provides a comparison of fracture properties K_{Ic} and G_f (or G_{Ic}) for the binders from sections 118-1 and 118-6, with AASHTO M320 (BBR) performance grades of -23.6°C and -24.7°C, respectively.

The data are interesting in several respects. Large variations in both K_{Ic} and G_f are observed for binders that have nearly the same performance grades under the AASHTO M320 or MP1a system (see, for instance, Figure 4.20). In addition, some binders of different performance grades appear to have similar fracture energies in the brittle state. There are also some results that are not easy to understand. For example, the unaged binders for sections 118-4 and 118-6 have *lower* fracture energies at the 0.001 mm/s strain rate at -24°C and -30°C, respectively. This is counterintuitive and clearly needs further investigation. It may be due to a violation of the requirement for plane-strain conditions and plastic collapse (Cayard (1990)). The ligament (W-a) for these tests on unaged samples was smaller than what is desirable, and excessive deformation may have reduced the failure load by a large amount (ASTM (1996)). However, if and how these results can be reconciled with field performance data will be discussed in section 4.7 of this report.

Table 4.19 Average Fracture Properties of Unaged and RTFO-Aged Highway 118 Binders

Section	Aging	T_l, °C	dε/dt, mm/s	K_{Ic}, kN/m$^{3/2}$	G_f or G_{Ic}, J/m^2
118-1	Unaged	-24	0.01	60	10.0
			0.001	64	35.2
		-30	0.01	56	6.7
			0.001	49	7.1
	RTFO	-24	0.01	67	8.0
			0.001	79	23.3
		-30	0.01	61	7.4
			0.001	50	6.2
118-3	Unaged	-24	0.01	97	22.6
			0.001	109	102.7
		-30	0.01	82	10.6
			0.001	72	12.1
	RTFO	-24	0.01	111	34.4
			0.001	102	64.8
		-30	0.01	111	25.4
			0.001	82	15.1
118-4	Unaged	-24	0.01	260	1129.3
			0.001	31	16.8
		-30	0.01	85	21.1
			0.001	103	38.5
	RTFO	-24	0.01	188	195.3
			0.001	85	112.5
		-30	0.01	154	62.6
			0.001	82	28.4
118-5	Unaged	-24	0.01	157	90.0
			0.001	118	96.2
		-30	0.01	102	18.0
			0.001	102	32.8
	RTFO	-24	0.01	98	21.2
			0.001	82	29.5
		-30	0.01	79	10.9
			0.001	72	8.6
118-6	Unaged	-24	0.01	99	18.4
			0.001	112	31.8
		-30	0.01	119	15.3
			0.001	20	3.2
	RTFO	-24	0.01	116	23.2
			0.001	104	34.0
		-30	0.01	133	19.1
			0.001	119	30.3

Estimated errors are 10-15% in fracture toughness and 20-30% in fracture energy.

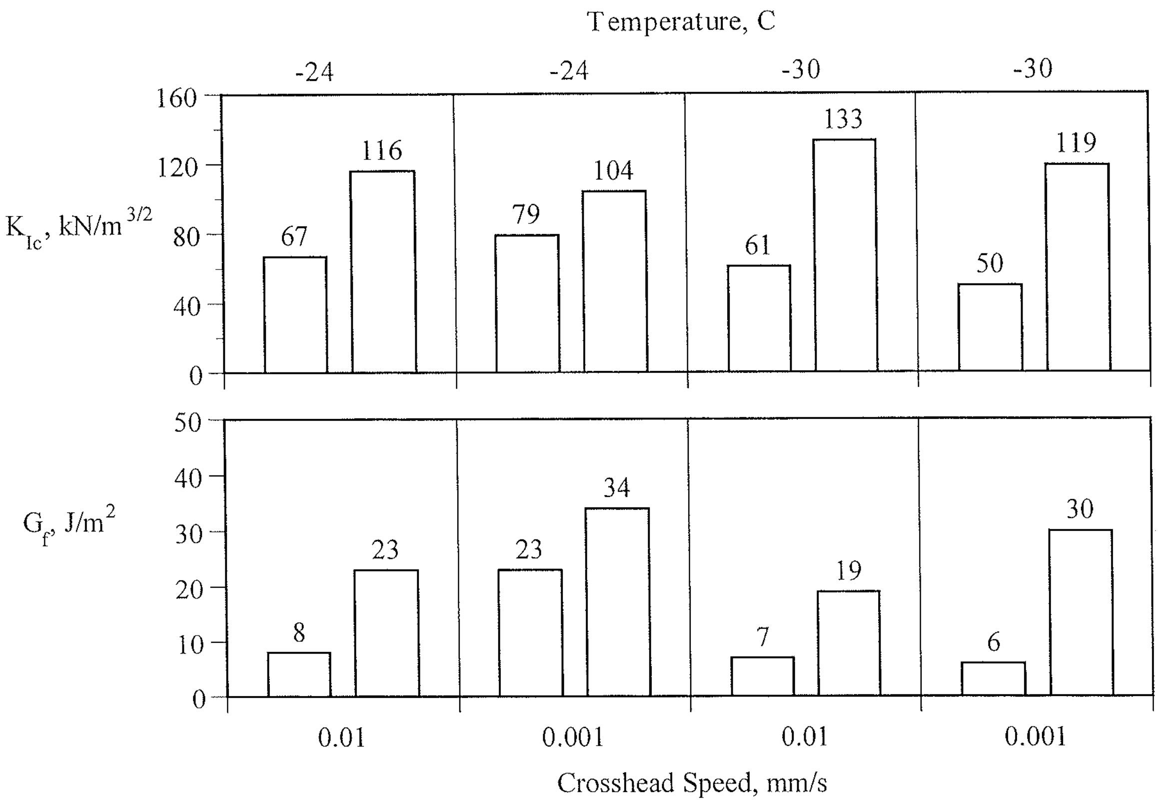

Figure 4.20 Comparison of binder fracture data for sections 118-1 and 118-6, respectively.

PAV-Aged Binders

The PAV residues were tested in more detail to compare the fracture mechanics-based rankings determined with the SHRP AASHTO M320 and MP1a temperatures and eventually with field data. The fracture properties K_{Ic} and G_{Ic} (or G_f) were determined at two strain rates and various temperatures to determine the ductile-to-brittle transition temperatures for each binder and the properties in their brittle state.

Samples were stored for three days at their grading temperature before being tested in the three-point bend test. The mold design that was used is shown in Figure 4.19, with a sample span, S, of 100 mm, a sample depth, W, of 25.4 mm, a sample width, B, of 12.7 mm, a notch width of 25 μm, and a notch depth, a, of 5.0 mm (a/W = 0.197). Due to the high degree of reproducibility for the new specimen design, the testing of duplicates was sufficient for most samples.

The fracture energy data and limiting fracture energy temperatures are given in Table 4.20. The results show that the fracture energy in the brittle state varies less between different binders when compared to the RTFO and unaged data (Table 4.19). However, the ductile-to-brittle transition temperatures as defined by a 100 J/m^2 limit in fracture energy vary by as much as 18°C (ranging from -1.5°C for section 118-1 to -19.5°C for 118-4).

A comparison of the results for section 118-1 and 118-6 shows that the binder used in section 118-6 has a 3.5°C edge over the binder used in 118-1. Furthermore, the fracture energy of binder 118-6 in its brittle state is also higher than that of binder 118-1. These trends are in accordance with those found for the RTFO and unaged materials.

Table 4.20 Average Fracture Energies and Limiting Fracture Energy Grading Temperatures for PAV-Aged Highway 118 Binders

Section	T, °C	G_f or G_{Ic} @ 0.001 mm/s, J/m²	G_f or G_{Ic} @ 0.01 mm/s, J/m²
118-1	-15	21	14
	-12	20	21
	-9	28	23
	-6	53	46
	-3	117	52
	0	-	157
	3	-	345
T at which G_{Ic} = 100 J/m², °C		**-3.5**	**-1.5**
118-3	-21	20	15
	-18	31	30
	-15	26	-
	-12	165	142
	-9	679	381
	-6	-	1218
T at which G_{Ic} = 100 J/m², °C		**-12.0**	**-13.0**
118-4	-24	25	27
	-21	46	81
	-18	140	82
	-15	287	442
	-12	327	1760
T at which G_{Ic} = 100 J/m², °C		**-19.5**	**-18.0**
118-5	-24	12	10
	-18	20	17
	-15	30	30
	-12	154	87
	-9	319	162
	-6	758	-
T at which G_{Ic} = 100 J/m², °C		**-13.0**	**-11.5**
118-6	-15	30	19
	-12	32	20
	-9	57	47
	-6	126	62
	-3	228	228
	0	-	564
T at which G_{Ic} = 100 J/m², °C		**-7.0**	**-5.0**

Data are averages of a minimum of duplicates. Estimated errors are ~20%. Binders were tested after three-day conditioning at their AASHTO M320 grade temperature +10°C. Fracture energies were determined from the area under the force displacement curve according to equation 4-9.

The ranking of the Highway 118 binders as given in Table 4.20 will be compared with the respective AASHTO M320 grade temperatures from section 4.2 and with the field transverse cracking data from section 4.6 in section 4.7.

4.5.3.2 Fracture Properties of Recovered Highway 118 Asphalt Binders

A small number of binders from Highway 118 were recovered after eight years of in-service aging according to the protocol as described in section 3.1.3.1. The results for the fracture tests on these samples are provided in Figures 4.21 and 4.22.

The data on the recovered binders are interesting from several points of view. First, as with the SHRP limiting temperatures (Figure 4.3), the ductile-to-brittle transition temperature does not appear to be very sensitive to the effect of aging. Figure 4.21 provides the data for the limiting 100 J/m^2 fracture energy temperatures for both PAV-aged and field-aged materials. These results show that the transition temperatures for the PAV materials agree to within a few degrees with the transition temperatures of the field-aged materials.

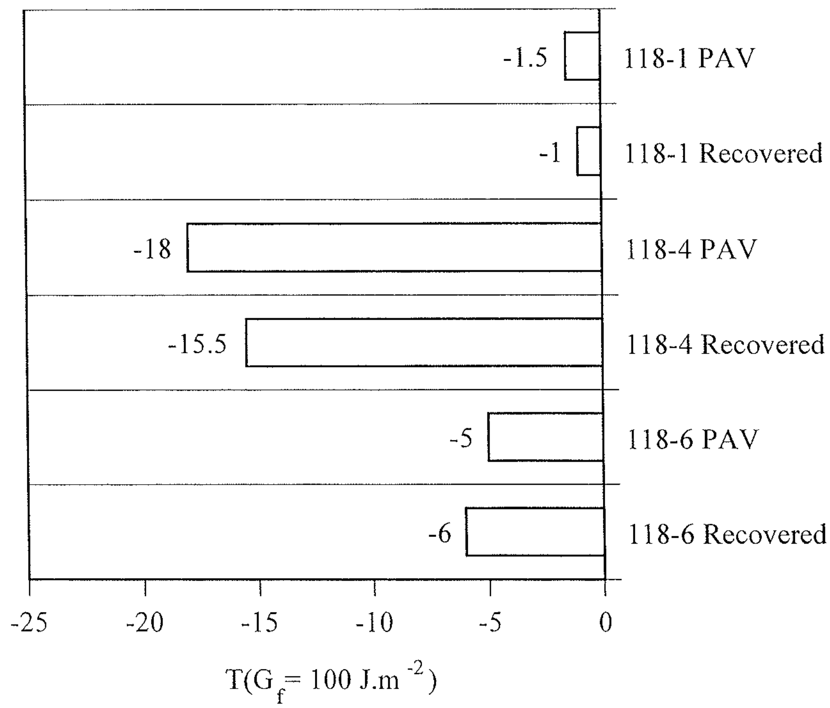

Figure 4.21 Comparisons of limiting fracture energy temperatures for 118-1, 118-4, and 118-6 section binders (not shifted).

In contrast, Figure 4.22 provides a comparison of the fracture energies in the brittle regime. These data show that there are very significant differences between the fracture properties of the binders aged in the PAV and those aged under in-service conditions. (Note that the error in many of the measurements is much less than the estimated 20 percent.) The fracture energy in the brittle regime is much lower for the field-aged materials than it is for the PAV-aged materials for both sections 118-4 and 118-6 whereas for 118-1 there is no big difference. These findings agree well with the spectroscopic results of section 4.1, which revealed that the styrene-butadiene polymers in sections 118-4 and 118-6 had degraded well beyond what was predicted by the RTFO and PAV protocols (Figure 4.1).

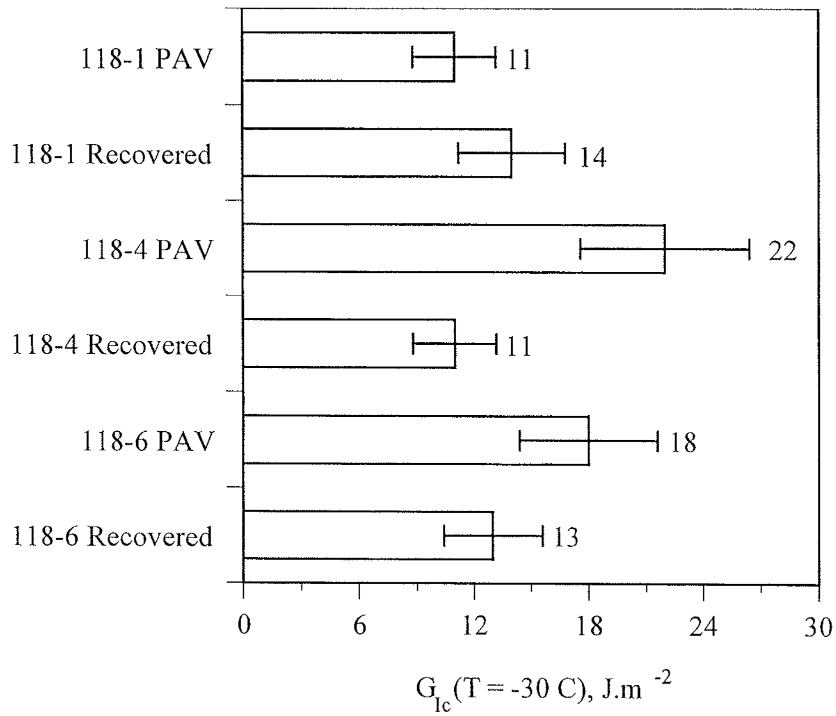

Figure 4.22 Comparisons of fracture energies in the brittle regime for 118-1, 118-4, and 118-6 section binders (estimated error bars of ± 20 percent).

This finding is interesting since it suggests that some of the high toughness values as reported on *unaged* and *RTFO* materials in previous papers (Hoare and Hesp (2000), Champion et al. (1999, 2000), Anderson (2000, 2001)) may not be very relevant to what actually happens in the field. However, the least brittle binder in this study, used in section 118-4, is not impressive to start. Hence, it would not be prudent to extrapolate this single observation to all other polymer-modified binders.

In addition to the fracture energy at low temperatures in the brittle regime, the fracture energies in the ductile state must also be considered. Section 4.9 gives some preliminary results on unaged materials that show significant differences between binders. Furthermore, test results on the recovered mixture shows that section 118-4 does possess superior fracture properties in the ductile state, even after eigth years in service (see section 4.8). It is not clear at this moment how and to what extent the aging process affects the ductile fracture properties, but this is an area of active investigation. Since transverse cracking is a complex form of distress, only well-designed field trials will eventually lead us to a better understanding of the entire process.

4.5.3.3 Fracture Properties of Highway 17 Asphalt Binders

Due to material and time constraints, only the PAV-aged binders from Highway 17 were tested to determine their limiting G_{Ic} temperatures (i.e., their performance-grading temperatures according to a limiting 100 J/m^2 fracture energy criterion).

The fracture properties K_{Ic} and G_{Ic} were again determined at two strain rates and various temperatures to determine the ductile-to-brittle transition temperatures for each binder and the fracture properties in their brittle state. Samples were stored for three days at their grading temperature before testing in three-point bending. The mold design and testing conditions were identical to those used for the Highway 118 PAV-aged binders.

The fracture energy results and limiting fracture energy temperatures are given in Table 4.21. If and how the data can be reconciled with field data will be discussed in section 4.7 of this report.

Table 4.21 Average Fracture Energies and Limiting Fracture Energy Grading Temperatures for PAV-Aged Highway 17 Binders

Section	T, °C	G_{Ic} @ 0.001 mm/s, J/m^2	G_{Ic} @ 0.01 mm/s J/m^2
17-2 (870902)	-27	21	21
	-24	50	37
	-21	186	105
	-18	750	1198
	-15	-	12615
T at which G_{Ic} = 100 J/m^2, °C		**-23.0**	**-21.0**
17-3 (870903)	-24	11	8
	-21	22	18
	-18	24	25
	-15	74	50
	-12	426	1265
T at which G_{Ic} = 100 J/m^2, °C		**-15.0**	**-15.0**
17-4 (870960)	-12	10	6
	-9	26	17
	-6	112	29
	-3	237	204
	0	-	774
T at which G_{Ic} = 100 J/m^2, °C		**-6.5**	**-5.0**
17-5 (870961)	-24	11	10
	-18	30	22
	-15	58	36
	-12	94	158
	-9	167	224
T at which G_{Ic} = 100 J/m^2, °C		**-12.0**	**-13.0**

Data are averages of a minimum of duplicates. Estimated errors are ~20%. Binders were tested after three days of conditioning at their AASHTO M320 grading temperature + 10°C. Fracture energies were determined from the area under the force displacement curve according to equation 4-9.

4.5.4 Development of a Crack Opening Displacement Test Method

4.5.4.1 Calculated Crack Tip Opening Displacement Method

It was initially planned to calculate the crack tip opening displacement for the binder rather than to measure it directly, which is reported to be inaccurate in brittle failure (Anderson, 1995). Accepting the Dugdale model for the plastic zone, the CTOD can be calculated from the fracture energy in three-point bending and the yield stress in *tension*. This approach was taken earlier by a number of (highly reputable) researchers studying the failure properties of epoxy resins close to their ductile-to-brittle transition (Young and Beaumont, 1977; Gledhill et al., 1978; Spanoudakis and Young, 1984). However, in these studies the authors used the *compressive* yield stress as a substitute for the tensile yield stress, since the latter is inaccessible in the brittle state. (Samples fail in a catastrophic fashion before they yield.) As discussed in section 4.5.1, the Dugdale model provides the following relationship between CTOD, G_{Ic} and σ_y:

$$CTOD = \frac{G_{Ic}}{2\sigma_y} = \frac{K_{Ic}^2}{2E\sigma_y} \quad \text{(plane-strain)} \quad (4\text{-}11)$$

This equation is similar to the one for the size of the plastic zone in the Irwin model, r_y, ahead of the crack tip (Anderson, 1995):

$$r_y = \frac{1}{6\pi}\left(\frac{K_{Ic}^2}{\sigma_y}\right) \quad \text{(plane-strain)} \quad (4\text{-}13)$$

Hence, the K_{Ic} and σ_y properties can be used to obtain an estimate of the plastic zone size, which then provides us with an estimate of the level of plane-strain. If the plastic zone size is much smaller than the ligament thickness, i.e. r_p<<W-a, then the measured properties, K_{Ic} and G_{Ic}, should be independent of specimen size and as such should be very useful for performance grading (Cayard (1999)).

By using the typical *compressive* yield stresses and fracture energies as found for the binders in Tables 4.13 and 4.14, plastic zone sizes in the μm rather than the mm range are obtained. This suggests that the failure should be plane-strain for ligaments, W-a, of a few mm in dimension. However, the data in Table 4.18 suggest that this is not the case and that the plastic zone size approaches the ligament length for the samples with a 25.4-mm depth (W), a 50 percent notch depth and a 12.7-mm width (B). These facts can only be reconciled with the Irwin theory if the actual tensile yield stress is much *lower* than the substituted compressive yield stress. This has indeed been observed in studies on the compressive and tensile yield properties of certain plastics (e.g., Bucknall (1977), p. 232). It can therefore be concluded that it is incorrect to substitute the compressive yield stress for the tensile yield stress. This leaves us only with a direct measurement of the Crack Mouth Opening Displacement (CMOD) to obtain a measure of the CTOD. This approach is discussed next.

4.3.4.2 Direct Measurement of Crack Mouth Opening Displacement

The ultimate objective of this research is to develop a test method that can measure the crack opening displacement in a simple and reproducible manner. This would need to be done for several temperatures, after which a limiting COD temperature could then be determined for specification grading purposes.

In this project the measurement of COD properties was accomplished with a clip-on gage in the three-point bend geometry. The gage had a compressed force of only around 1 N; hence, it was considered to be negligible compared to the typical forces encountered towards the end of each fracture test. The fracture energies (area under the force-displacement curves) and crack opening displacements (CMOD) that were measured were compared for a limited set of binders. Figure 4.23 provides the results of such comparison for the PAV-aged binders of sections 118-1 and 118-4 and the recovered binder from 118-4.

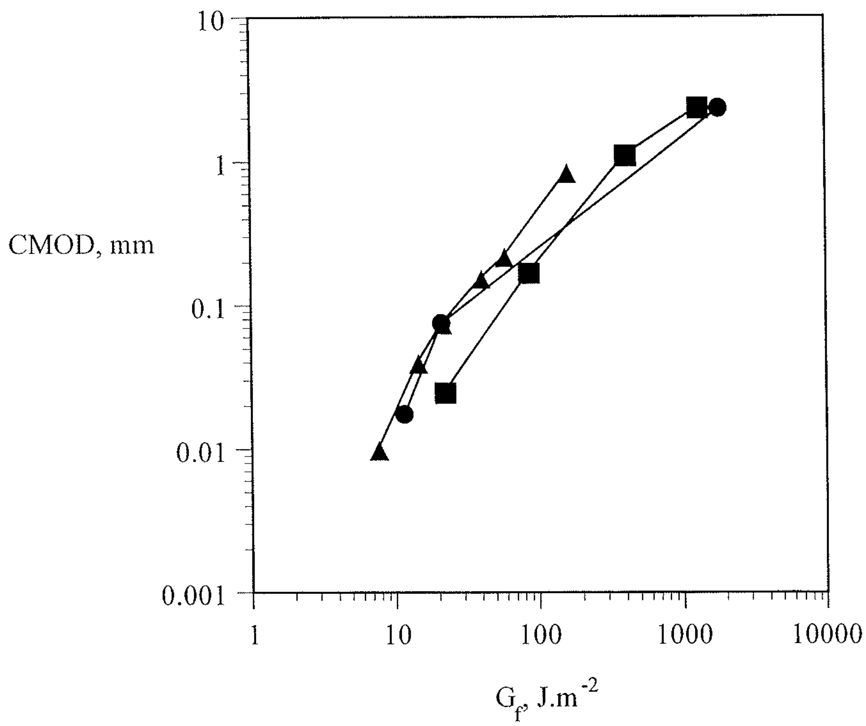

Figure 4.23 Comparisons of G_f and CMOD in the brittle and ductile regimes for 118-1 (PAV (▲)) and 118-4 (PAV (■) and recovered (●)) section binders.

The data show that the two fracture properties are somewhat related but that the relationship is probably different for different binders. For instance, the 118-4 PAV-aged binder data is shifted to higher energies compared to the 118-1 PAV-aged binder data. This suggests that in the end only one of the two properties is going to give better performance prediction. From a mechanistic perspective, this should be the CMOD. However, due to a shortage of material, a suitable test frame, and time, only fracture energy is considered in the remainder of this report since it was somewhat easier to determine.

In future work, fracture energy and crack opening properties should be determined simultaneously for other binders, and a field validation may possibly show more significant differences between the two grading approaches. This comparison is easier with the compact tension geometry, but this methodology was not yet perfected in this project.

4.6 Temperature Data and Crack Surveys for 1992-2003

4.6.1 Temperature Data

Minimum and maximum daily air temperatures were obtained from Environment Canada for weather stations located at the Kapuskasing and Muskoka airports as well as the station located within the confines of the Canadian Forces Base (CFB) in Petawawa. The Kapuskasing and Muskoka airports are located within 160 km and 16 km of the test sites, respectively. Although the temperatures for the Muskoka airport are probably very close to those at the actual Highway 118 site, it is likely that the temperatures for Highway 631 were a few degrees colder than those obtained for Kapuskasing. The weather station at CFB Petawawa is located within close proximity of the test site since that part of Highway 17 is bordered on both sides by the base.

Minimum surface temperatures were calculated according to the algorithm used in the LTPPBIND™ software (Mohseni (1998)) and were considered accurate within one or two degrees for both Highway 118 and 17, with a somewhat lower accuracy for Highway 631 due to its distance from the station.

The first period of sustained cold weather in the Kapuskasing/Hearst area occurred in 1994 when the pavement surface temperature went down to -31.8°C, -33.0°C and -32.3°C, on three separate occasions. In early 1996 the surface temperature went down to -32.5°C on a single occasion. Other notable events occurred in 1997 (-30.1°C), 1999 (-30.6°C), 2002 (-28.4°C), and three times more in early 2003 (-29.4°C, -28.8°C and -27.5°C). Additional information is provided in Figure 4.24.

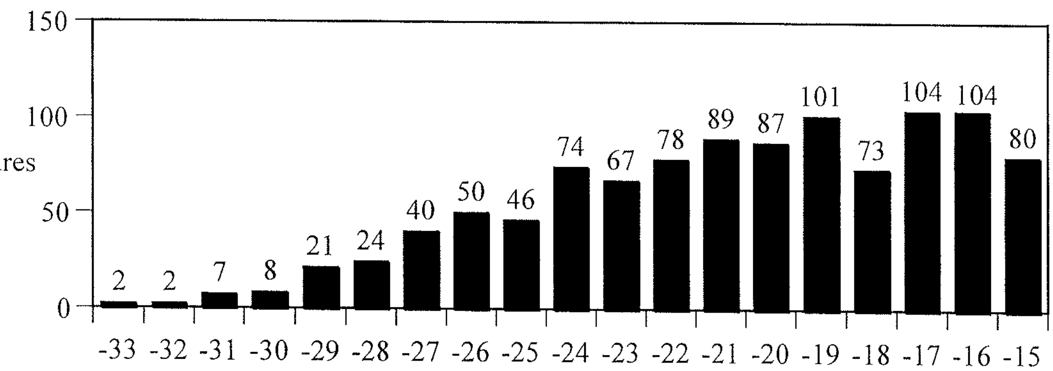

Figure 4.24 Minimum pavement surface temperatures for Highway 631 test sections as calculated from air temperatures recorded at the nearest weather station in Kapuskasing.

The first significant cold weather in the Bracebridge area occurred in 1996 when the pavement surface temperature went down to a low of -26.6°C. The following year, the surface temperature fell to -27.5°C, while the lowest temperature came in early 2003, at which point it fell to -27.8°C, followed shortly thereafter by -26.5°C. Figure 4.25 provides additional details for the Highway 118 site.

The SPS-9A sections on Highway 17 were exposed to significant distress in their first winter when the pavement surface temperature dropped to -25.0°C, -26.5°C and -26.8°C on separate occasions. Two years later, in early 1999, there was another cold day during which it dropped to -24.7°C. The lowest temperature was reached in 2003 when the temperature fluctuated between -26.5°C and -27.2°C for about a week. A complete account of all exposures is provided in Figure 4.26. It should be noted that in the first seven years of service, at no time did the pavement surface temperature fall below -31.0°C, the continuous AASHTO M320 temperature for the PG 58-28 section.

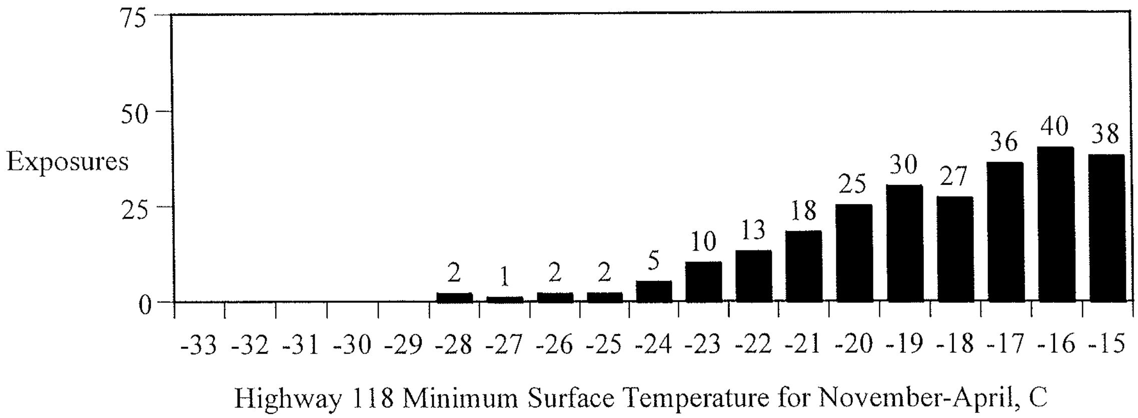

Figure 4.25 Minimum pavement surface temperatures for Highway 118 test sections as calculated from air temperatures recorded at the nearest weather station in Muskoka.

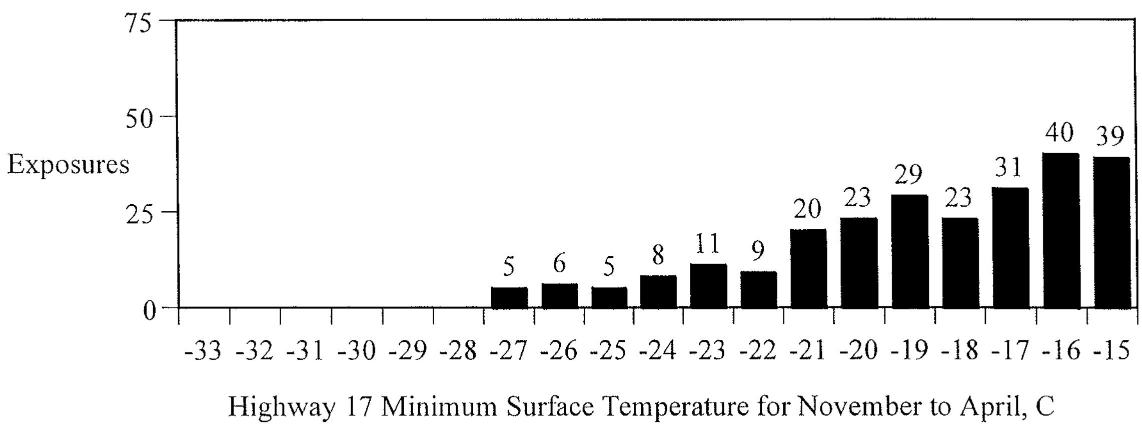

Figure 4.26 Minimum pavement surface temperatures for Highway 17 test sections as calculated from air temperatures recorded at the nearest weather station at CFB Petawawa.

4.6.2 Crack Surveys

Crack surveys for the Highway 631 test sections were taken at irregular intervals until 1996, after which the site was not visited until 2003. The early cracking numbers, some of which are discussed in section 4.7, are reported in C-SHRP Technical Brief 19 (C-SHRP (2000)). The transverse and longitudinal crack maps obtained during the two visits in 2003 are provided in Figures 4.27-4.30 and Figures 4.31-4.34, respectively.

For the transverse stress crack maps, a single line reaching across the graph indicates a full width crack, while a line with a fractional height indicates a crack that spans a fraction of the width at the indicated distance from the south end of the contract. Actual locations within the lane are not given in this set of figures. For the longitudinal maps the thickness of the line indicates the approximate severity. For the thickest lines the cracks cover some 40-60 percent of the pavement width while for the thinnest lines there could be just one single crack in the center of the lane.

The data show significant differences between the sections in both transverse and longitudinal cracking. A discussion of this is provided in section 4.7.

Crack surveys for Highway 118 were taken on a yearly basis from 1995 (just after construction) to 1998, after which there was a gap of a little over three years because of staff reassignments within the Ministry of Transportation. In the fall of 2001, the monitoring program was resumed under the contract that covers this project. It is planned to follow this road for a few more years.

The mapping results are given in Figures 4.35 to 4.39, with a summary of the cracking numbers in Figure 4.40. No maps are provided for sections 2 and 2A since no binder was tested in this project.

The data for all the test sections show a gradual increase in the number of transverse cracks. What is not included in the figures, however, is the significant amount of longitudinal cracking that was present starting early in the monitoring program in 1997, indicating that there are significant fatigue and perhaps subgrade problems for this road. Also, the severity of the individual cracks is not evident from these drawings. It is interesting to note that section 118-1, with the most transverse cracks in numbers, also showed the most severe cracking patterns, with some cracks reaching over several meters wide across the entire width of the pavement. This is clearly caused by fatigue and low-temperature distress mechanisms aggravating each other. However, the fatigue component is difficult to assess because of varying traffic levels within this test site. A number of photographs of actual cracks in Highway 118 are given in Figures 4.41 to 4.43.

Before the surveys from 2001 and 2002, no records were taken for cracks in the east-bound lane; hence, no significance should be placed on the fact that in 1997 and 1998 there are no cracks that progress into the opposing lanes. This is one issue we hope will be avoided with the new test sections on Highway 655, in that both lanes were constructed with the same asphalt binder.

Cracks were randomly distributed except in section 118-3, which had a disproportionate number between 180 and 240 m located at an intersection. This is another indication of how fatigue damage caused by slow-moving traffic could show up after cold winter weather as transverse stress cracking. The numbers of Figure 4.40 do not include the large number of cracks right within the intersection.

Detailed crack surveys for Highway 17 were taken in both 2002 and 2003. Earlier data for section 17-1 (PG 58-28) were collected under the Long Term Pavement Performance Program (LTPP). The reader is referred to information available from LTPP for a detailed description of the early performance data. The 2002 and 2003 transverse crack mapping results are provided in Figures 4.44 to 4.46, with a summary of the cracking numbers in Figure 4.47. So far no cracks have been observed in the two PG 58-40 sections on Highway 17, so no maps are provided. Since the 85-100 penetration graded binder was also unavailable for testing, it is omitted from further analysis.

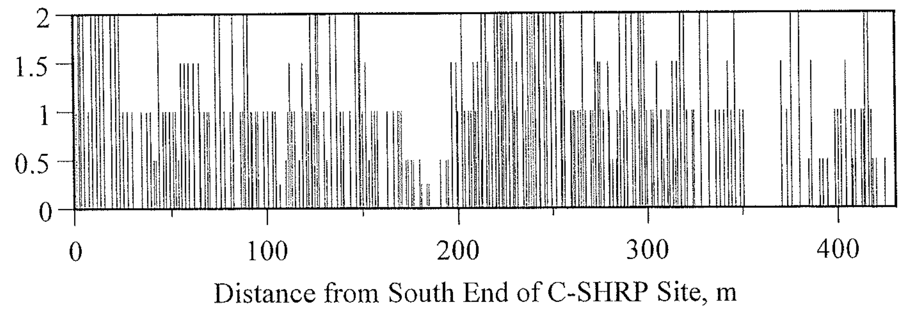

Figure 4.27 Transverse crack map for section B (PG 52-28) on Highway 631.

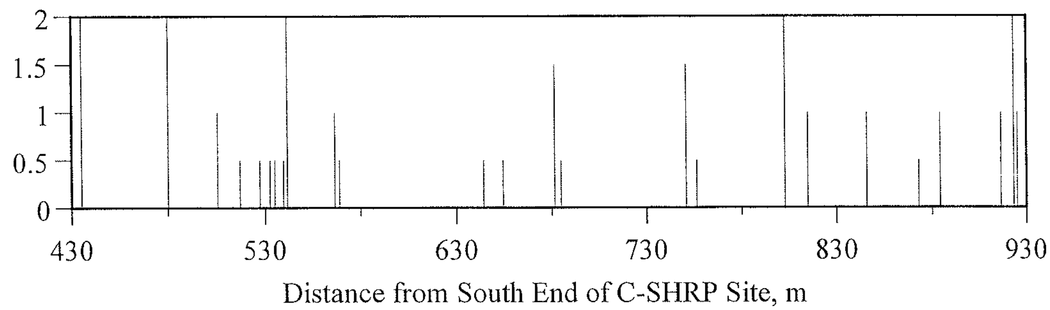

Figure 4.28 Transverse crack map for section A (PG 52-28) on Highway 631.

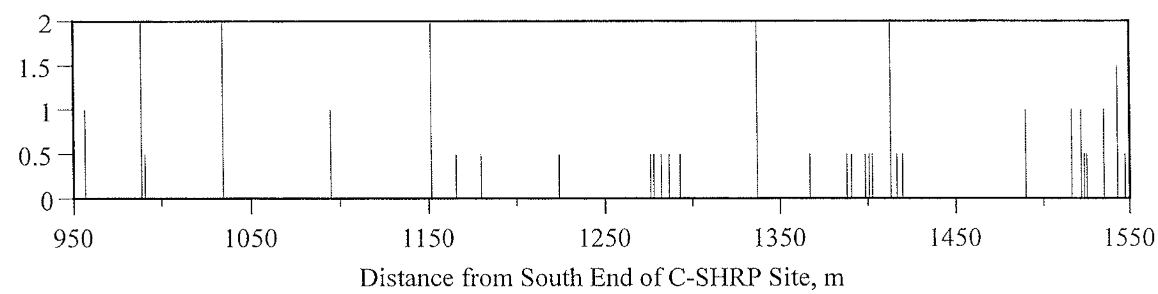

Figure 4.29 Transverse crack map for section AA (PG 46-34) on Highway 631.

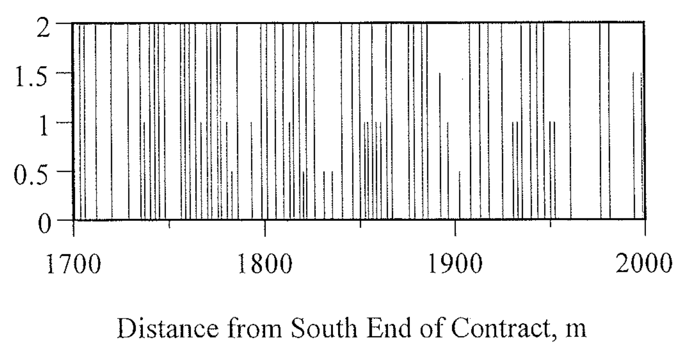

Figure 4.30 Transverse crack map for section BB (PG 52-28) on Highway 631.

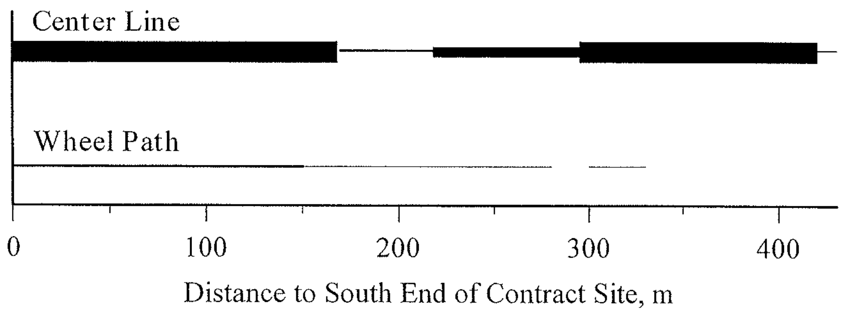

Figure 4.31 Longitudinal crack map for section B (PG 52-28) on Highway 631.

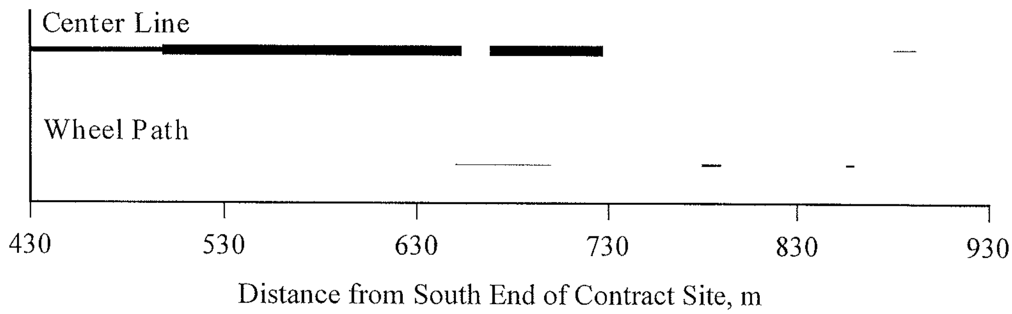

Figure 4.32 Longitudinal crack map for section A (PG 52-28) on Highway 631.

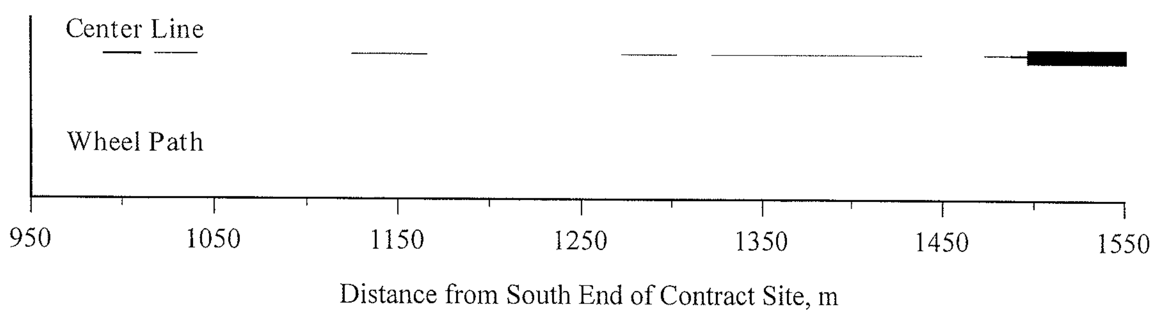

Figure 4.33 Longitudinal crack map for section AA (PG 46-34) on Highway 631.

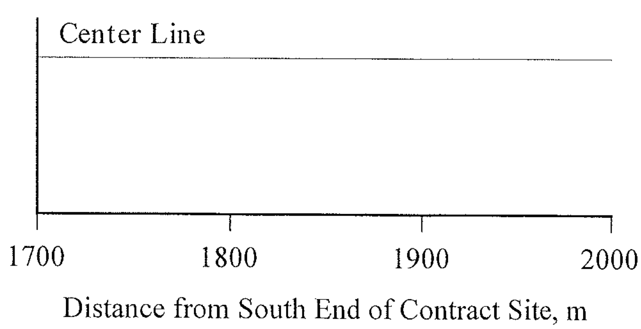

Figure 4.34 Longitudinal crack map for section BB (PG 52-28) on Highway 631.

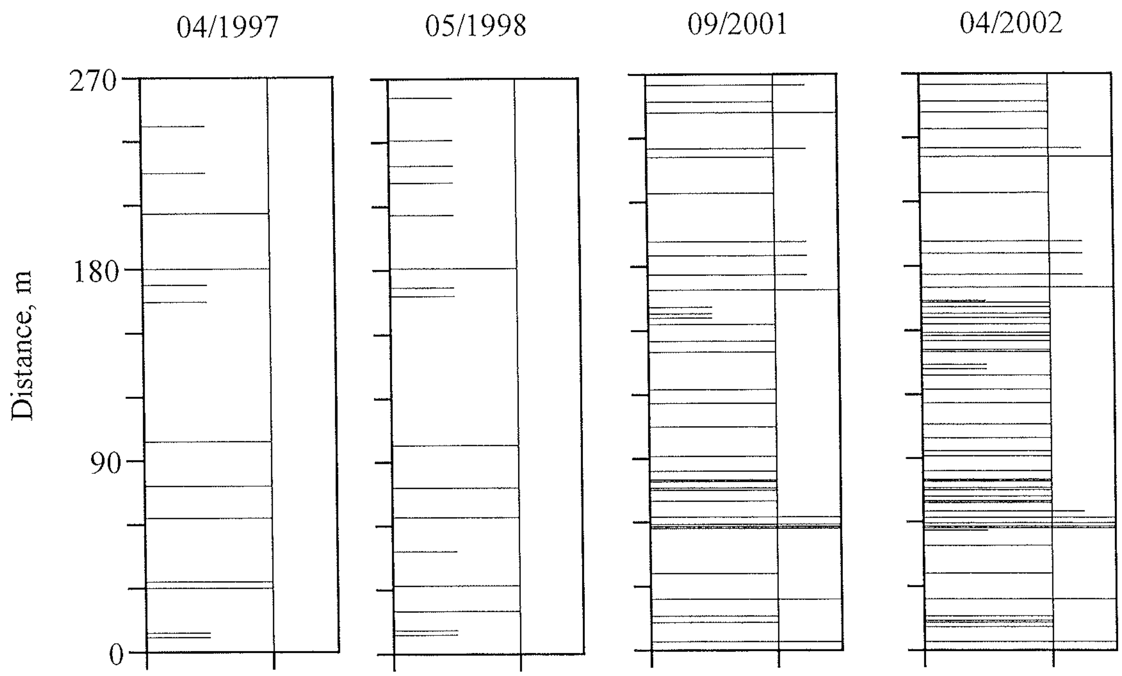

Figure 4.35 Crack maps for section 118-1.

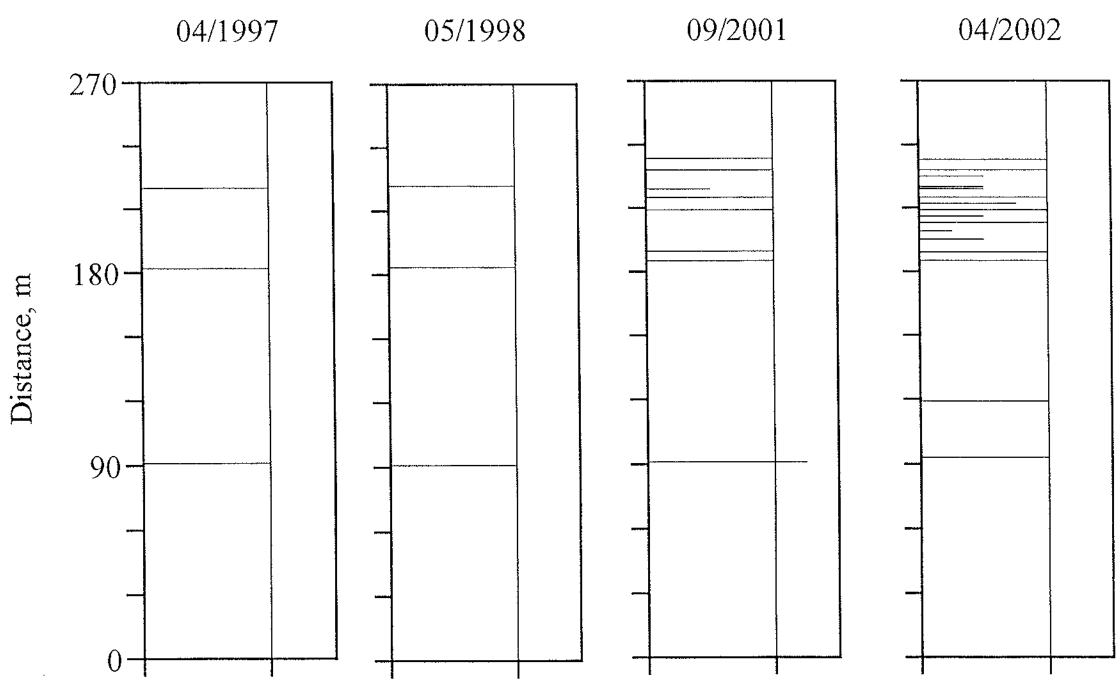

Figure 4.36 Crack maps for section 118-3.

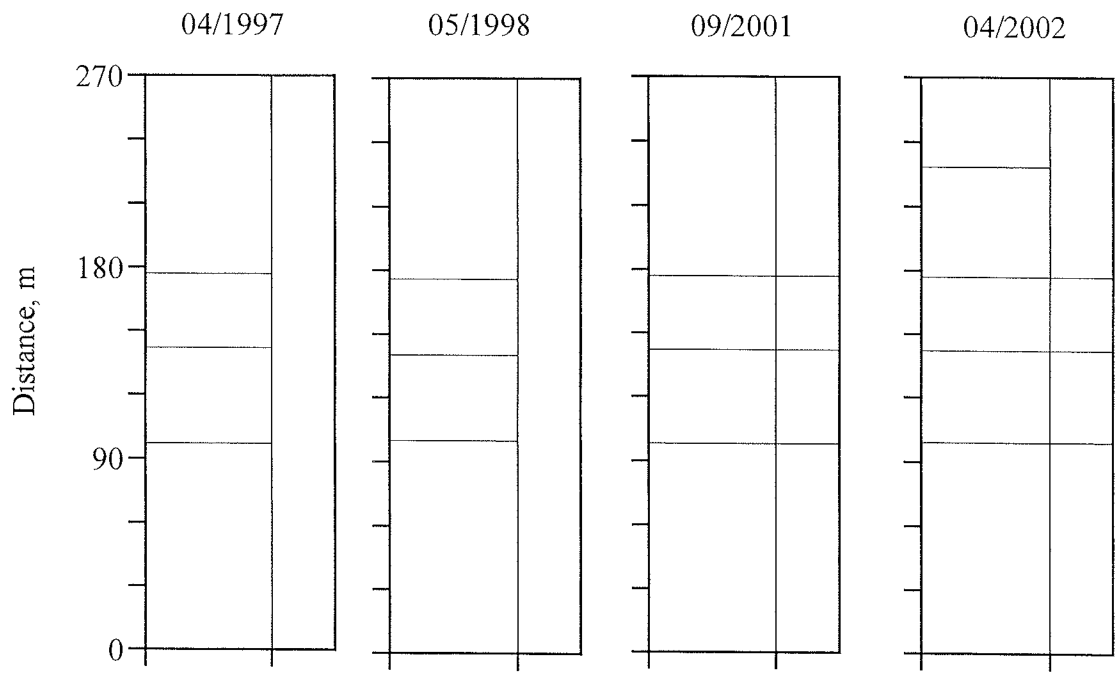

Figure 4.37 Crack maps for section 118-4.

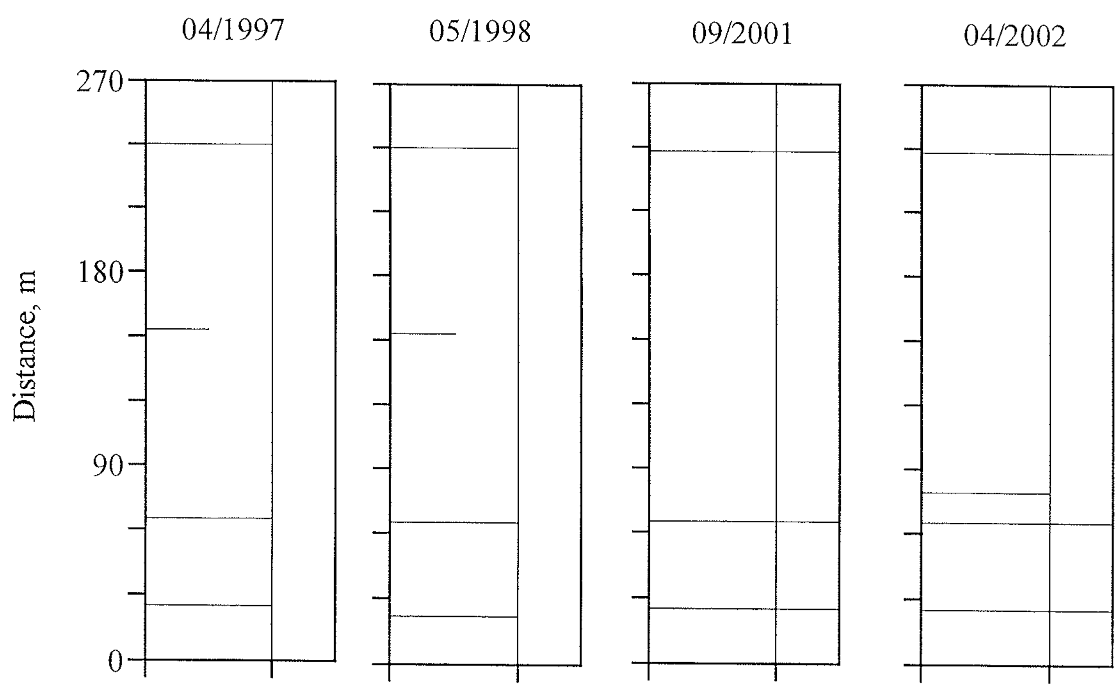

Figure 4.38 Crack maps for section 118-5.

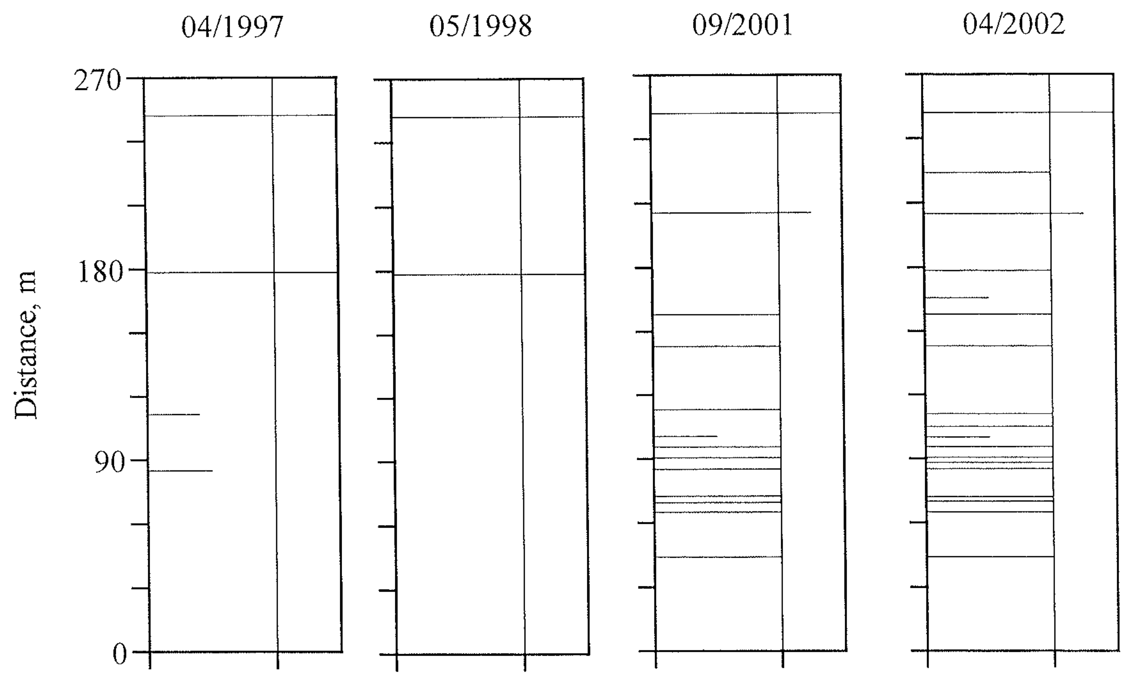

Figure 4.39 Crack maps for section 118-6.

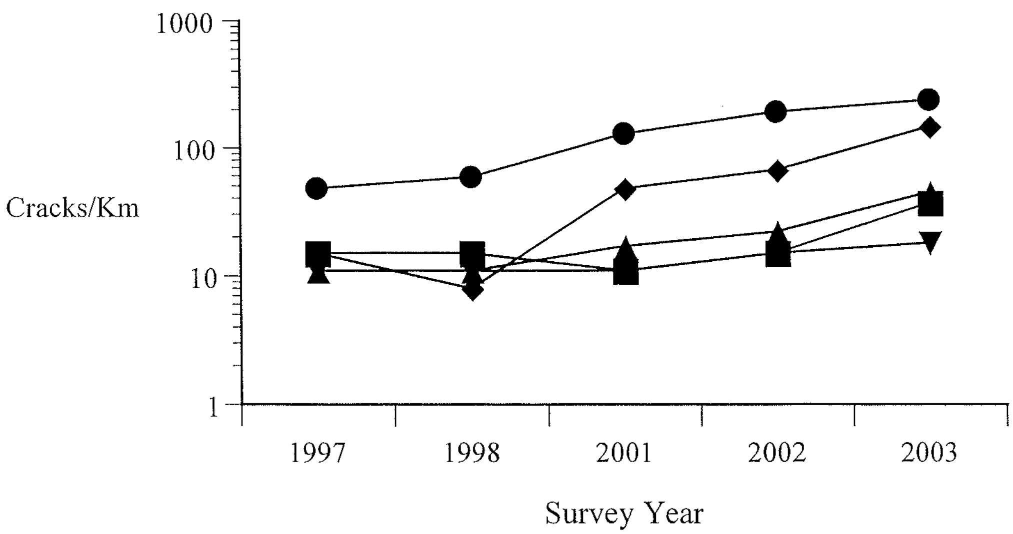

Figure 4.40 Historical crack data for Highway 118 sections 1 (●), 3 (▲), 4 (▼), 5 (■) and 6 (♦).

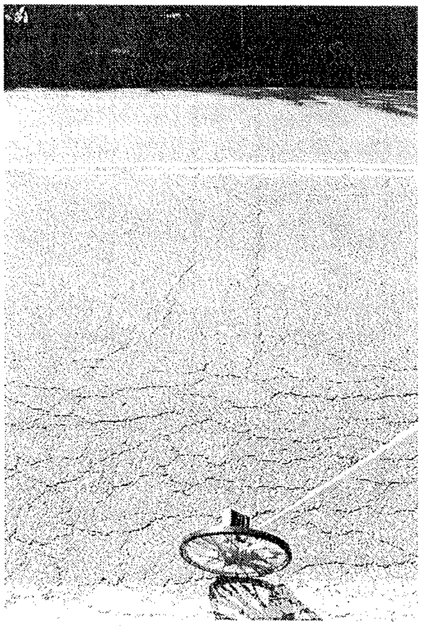

Section 1 @ 5 m

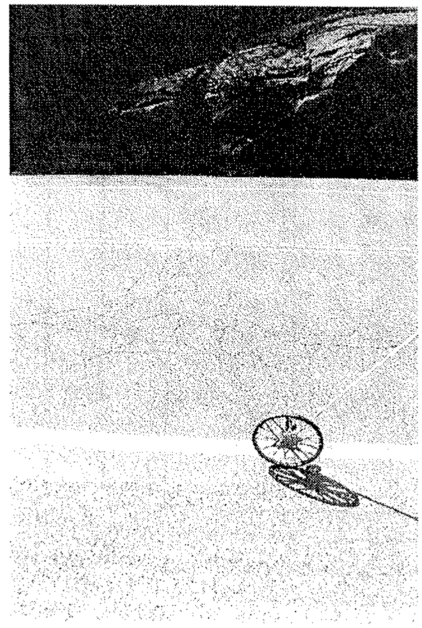

Section 1 @ 170 m

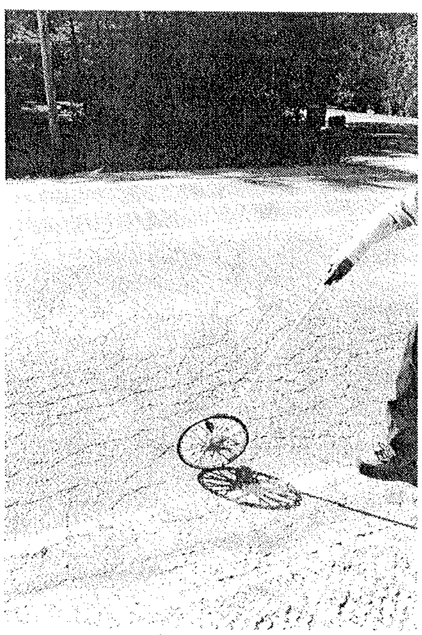

Section 1 @ 35 m

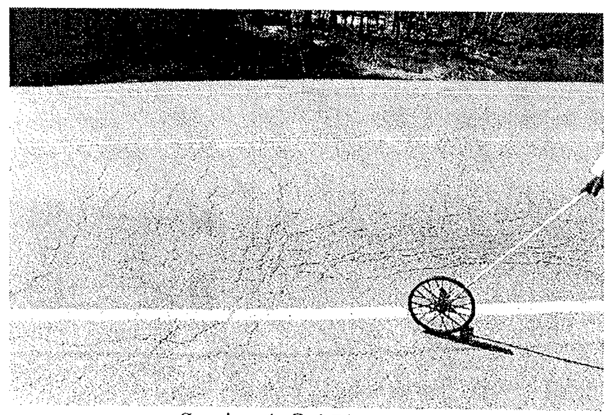

Section 1 @ 270 m

Figure 4.41 Photographs of selected cracks in section 118-1 (wheel diameter is 32 cm).

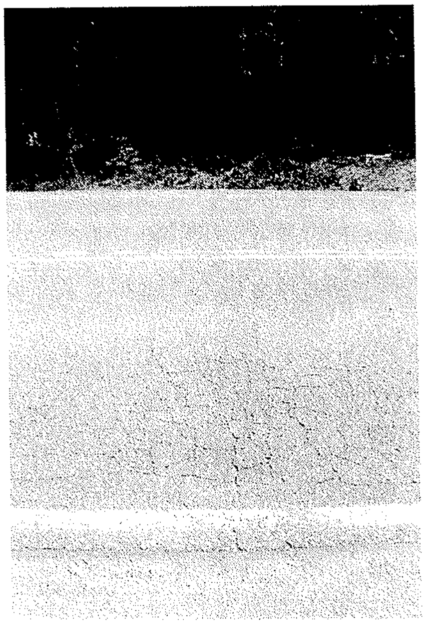

Section 6 @ 1 m

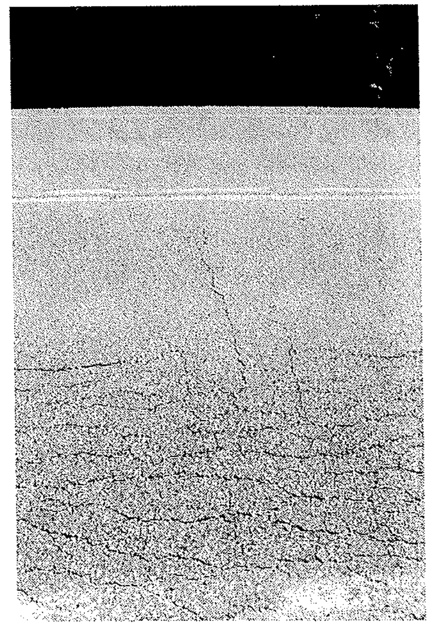

Section 6 @ 65 m

Section 6 @ 43 m

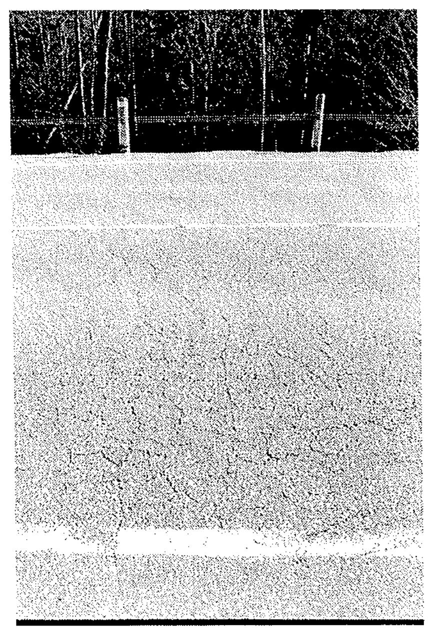

Section 6 @ 144 m

Figure 4.42 Photographs of selected cracks in section 118-6 (wheel diameter is 32 cm).

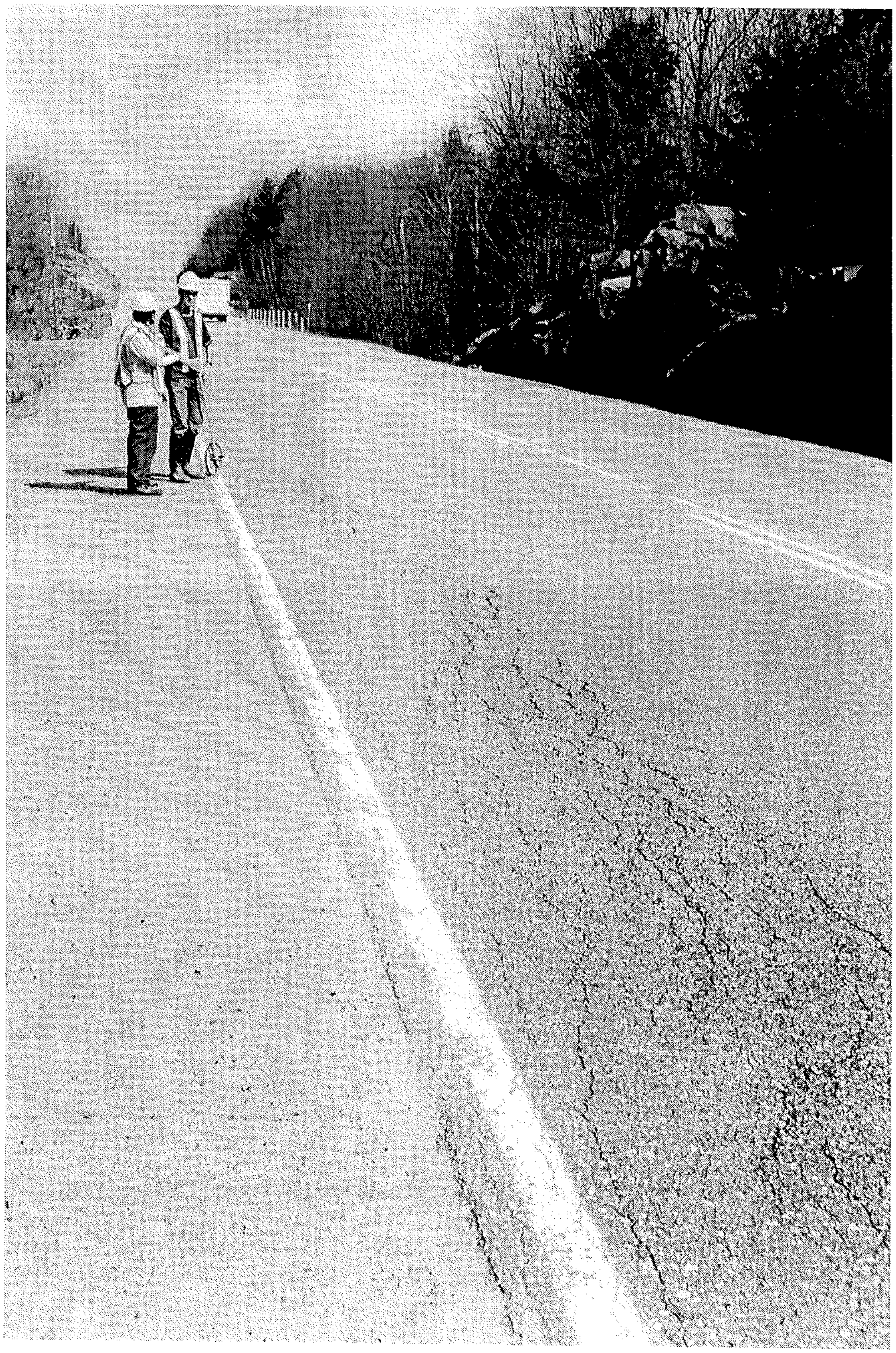

Figure 4.43 Illustrative picture for longitudinal cracking in section 118-5.

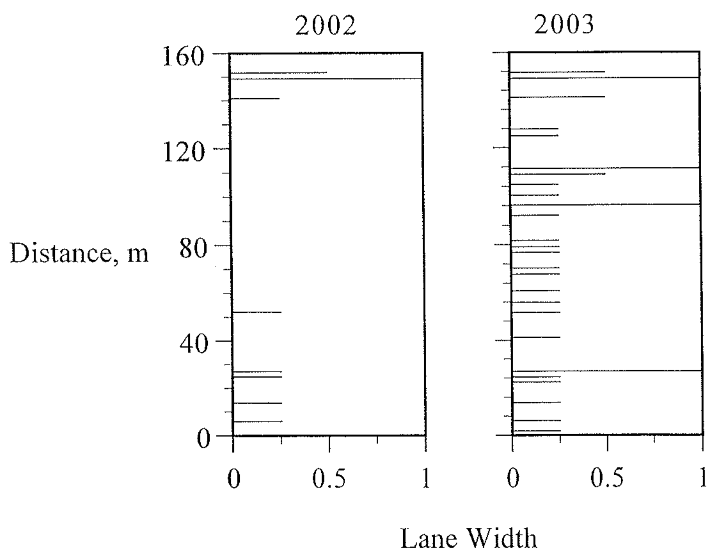

Figure 4.44 Crack maps for section 17-1 (PG 58-28).

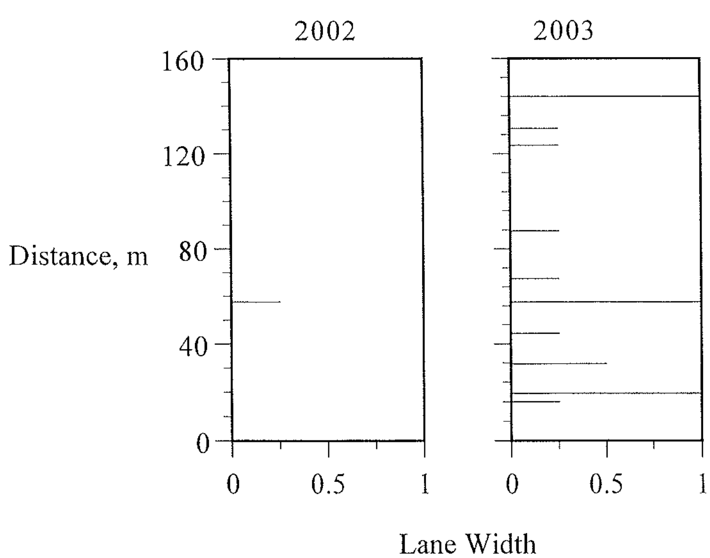

Figure 4.45 Crack maps for section 17-2 (PG 58-34 P).

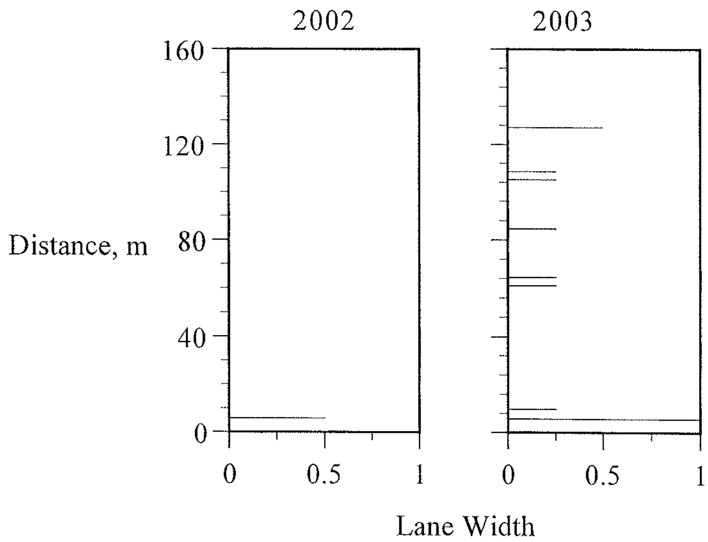

Figure 4.46 Crack maps for section 17-3 (PG 58-34 NP).

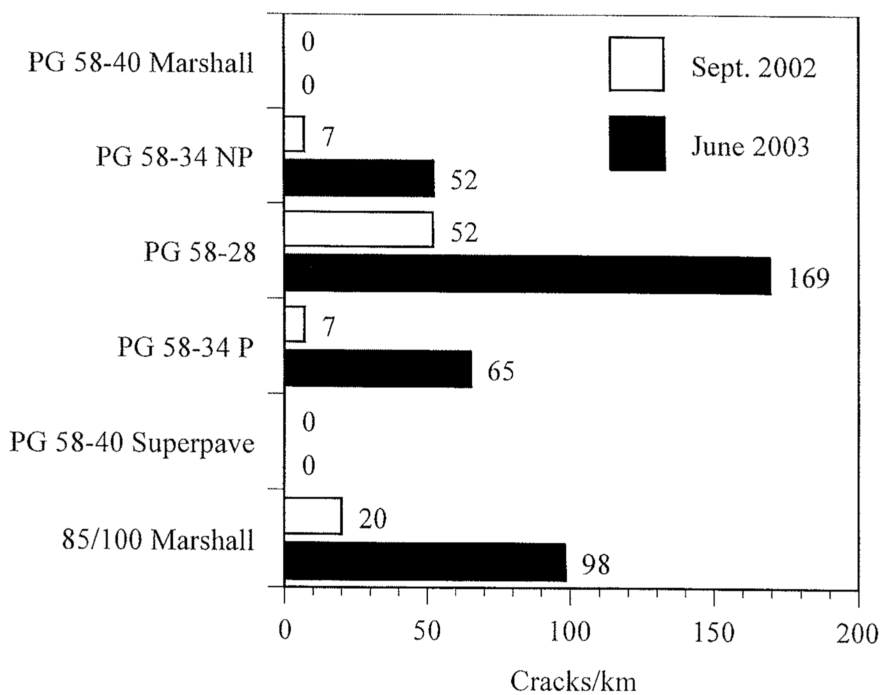

Figure 4.47 Summarized crack data for Highway 17 test sections.

4.7 Correlation between Binder Properties and Field Cracking Onset and Severity

4.7.1 Comparison of Asphalt Binder Grading Methods

Before the binder grading methods are validated or invalidated with field cracking onset and severity, it is instructive to compare the various methods among each other. Figure 4.48 provides a comparison of limiting temperatures determined according to: (1) AASHTO M320 after one-hour and three day conditioning (Figures 4.2 and 4.4); (2) AASHTO MP1a after one-hour and three-day conditioning (Figures 4.2 and 4.4); and (3) the fracture energy-based approach after three days conditioning at two different rates of loading (Tables 4.20 and 4.21). The x-axis provides the 300 MPa limiting stiffness temperatures whereas the y-axis provides all the other limiting temperatures.

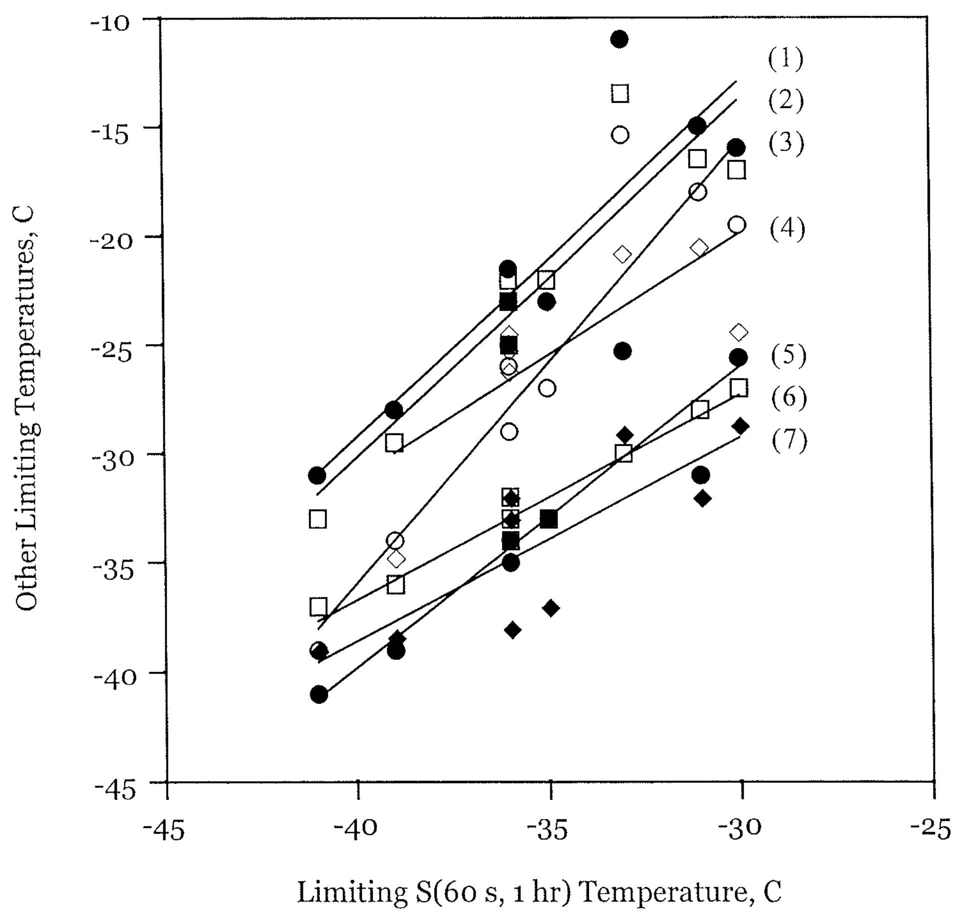

Figure 4.48 Comparisons of limiting temperatures: (1) • – G_{Ic} = 100 J/m^2 @ 0.01 mm/s; (2) □ – G_{Ic} = 100 J/m^2 @ 0.001 mm/s; (3) ○ – m(60 s) = 0.3 after three-day soak; (4) ◊ – MP1a after three-day soak; (5) • – m(60 s) = 0.3 after one-hour soak; (6) □ – S(60 s) = 300 MPa after three-day soak; and (7) ♦ – MP1a after one-hour soak.

The data is interesting from several perspectives. First, the general trend for all the grading temperatures is the same. This is not surprising since many rheological and fracture properties of asphalt binders respond strongly to changes in temperature. The results are also reassuring for users of current methods, since it means that no method is completely off.

However, close examination reveals a significant degree of scatter. There are in fact significant differences between different grading temperatures for some binders. The most striking difference is between the one-hour and three-day data. It appears that after three days anywhere from 3°C to 13°C is lost in the low-temperature grade. In the context of typical weather statistics such as those provided in Figure 2.3, this is an enormous amount. The implications become clear in discussion of the crack surveys for Highways 118 and 17 in the next section.

4.7.2 Field Validation and Invalidation of Binder Grading Methods

4.7.2.1 Highway 631 C-SHRP Trial near Hearst, Ontario

Robertson (1995) has discussed the inability of the BBR specification test to predict the onset of cracking for all C-SHRP trials. In Hearst, cracking in the 50-mm thick sections started as much as 11.8°C warmer than the critical temperature as determined with the BBR, which is most likely related to the effects of fatigue, differences in the susceptibility to physical aging (see Figure 4.48), or perhaps a combination of these and other less recognized factors. In contrast, for the Lamont, Alberta, C-SHRP site, the onset of cracking occurred at lower temperatures than the BBR predicted (Robertson (1995)).

The main differences between Hearst and Lamont are the pavement thickness (50 mm in Hearst vs. 100 mm in Lamont) and the traffic levels (300 vehicles/day with 25 percent truck traffic in Hearst versus 260 vehicles/day or 9 ESALS/day for Lamont) (Robertson (1995)). It is the pavement structure, traffic levels as well as the performance-based properties of the binder that determine whether cracks appear or remain as micro-damage without any negative consequences. Traffic exposure during spring-thaw and summer will naturally aggravate the situation in subsequent winters, so the fracture resistance at 0°C and typical summer temperatures may also need to be measured in order to obtain a comprehensive performance assessment for an asphalt binder.

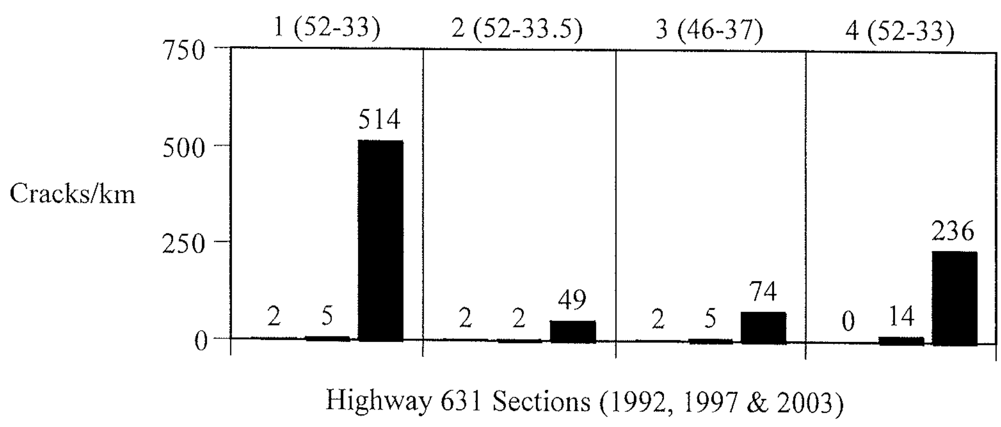

Figure 4.49 Historical cracking data for Highway 631 C-SHRP sections.

As the oldest of the three sites, Highway 631 has probably the most severe transverse cracking. Figure 4.49 provides a comparison of the severity in time with the SHRP grade temperatures for all four sections. The early numbers are taken from C-SHRP Technical Brief 19, which compiles data from others (C-SHRP (2000)). It should be noted that the site was not monitored between 1997 and 2002.

The most striking observation is that the difference in cracking for the apparently identically graded 631-1 and 631-2 is more than a factor ten (or twenty if length is used to measure severity). These are graded at -33°C and -33.5°C, respectively and therefore one would expect them to show approximately the same cracking. Obviously the current method is of questionable validity for predicting the relative performance for these two sections.

The second noteworthy observation relates to the performance of section 631-2 with respect to the minimum temperatures that have occurred over the life of the road (Figure 4.24). This shows that while the section graded at -33.5°C should have been cracked severely, having reached below -30°C on about 19 days since its construction in 1991, it is in fact in reasonably good shape with 49 cracks/km. Only 20 percent of these span the width of the road after twelve years in service. For some reason, the section shows only moderate cracking in spite of repeated excursions close to the grade temperature.

The third noteworthy observation relates to the difference in cracking severity due to the pavement thickness. The 100 mm section has only about 58 percent of the cracking severity of the 50 mm section that was constructed with the same asphalt binder, which suggests that fatigue is a major contributing factor to the occurrence of transverse cracks. Deme and Young (1987) reported the same effect the St. Anne test road.

A final observation relates to the fact that section 631-3 on Highway 631, which is made with a binder that is graded at -37°C and hence should not have cracked at all, shows a transverse cracking severity that is approximately 50 percent greater than that of section 631-2, which is made with a binder graded at only -33.5°C. At the low levels of cracking in these two sections it may not be a very significant difference but tests with longer sections may be more conclusive.

Since no binder samples were kept from this trial it is difficult to determine the exact reason(s) for the observed anomalies. Physical aging could perhaps explain the higher cracking in some instances since Figure 4.24 shows that the frequency of exposure to damaging temperatures increases rapidly with only a minor loss in grade temperature.

It should be noted that Roque and Hiltunen (C-SHRP (2000)) were able to show a difference in performance between the two sections with the identical grade from tests on samples from the pavement in the early 1990s. They found differences in mixture creep stiffness at 1800 s loading times at -20°C and limited results on the recovered binders revealed that there was a significant difference in binder stiffness at -18°C (see Table 3.2).

Currently efforts are underway to recover the Highway 631 binders and to test these under the various grading protocols. This may better explain if the differences are due to chemical or physical aging, the shortcomings of the BBR, or a combination of these and perhaps other unknown factors.

4.7.2.2 Highway 118 Trial

It is difficult to say much about the ability of the grading methods to predict the onset of cracking since early data were not obtained for the Highway 118 test sections. However, Figure 4.50 compares historical cracking data with the grade temperatures from Figure 4.2. There are a number of observations that can be made with respect to the data. First of all, in general, the BBR appears to do a reasonable job for these sections at predicting the relative ranking in terms of cracking in 2003. Binders used in sections 118-1 and 118-6 were both graded at approximately -25°C but show a 40 percent difference in cracking. This may perhaps be explained by the difference in traffic volumes (see section 3.2.2). However, three-day conditioned materials also possess limiting temperatures that are considerably warmer than one-hour conditioned materials. In fact, the binder used in section 118-1 loses the most at 9.9°C while the 118-6 material loses 6.1°C. To what extent this difference has caused the higher cracking in 118-1 is hard to determine since it also had the highest traffic.

Furthermore, the mixed-mode fracture energies of the RTFO-aged binders, G_f, are also different by up to a factor of five for these two binders (see Figure 4.20).

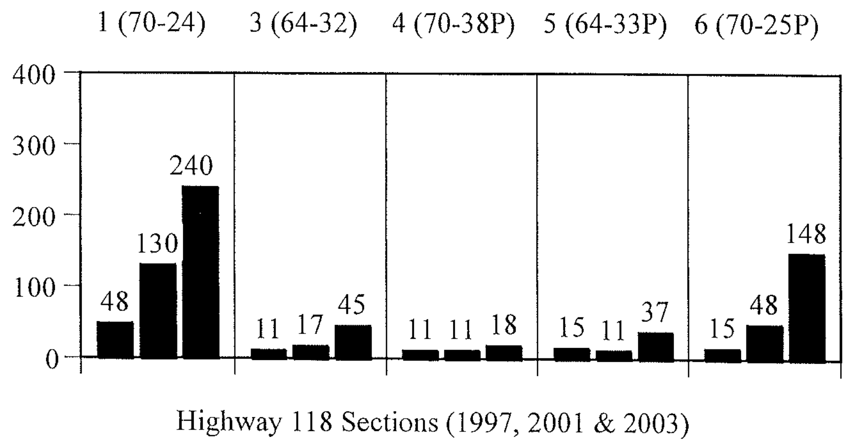

Figure 4.50 Historical cracking data for Highway 118 sections.

It is difficult to find out to what extent physical- and chemical-aging and differences in fracture properties have individually contributed to the cracking in this site since the early temperature and crack monitoring efforts were not as intensive as desirable. However, the effects of these factors could explain most if not all of the cracking in sections 118-3, 118-4 and 118-5. None of these have been exposed below their regular AASHTO M320 grade temperatures; hence, they should show no cracks. The reality is different in that section 118-3, with a continuous BBR grade of -31.7°C, already has 45 cracks/km; section 118-4, with a lower grade of -37.6°C, has less distress at 18 cracks/km; and section 118-5, with a grade of -33.3°C, has a similar number at 37 cracks/km. If the limiting BBR temperatures after three days of conditioning, -27.0°C (118-3), -34.0°C (118-4) and -26.0°C (118-5), are compared with the lowest recorded surface temperatures, -26.6, -27.5, -27.8 and -26.5°C, then it may be concluded that physical aging is a factor that can explain a significant part of the observed cracking. It would not be unreasonable to infer that a significant part of the observed cracking is due to physical aging and the rest may be due to chemical aging (above and beyond the PAV), notch sensitivity around voids and flaws in the asphalt concrete, brittleness in the brittle and/or ductile temperature regimes, or other factors such as base instability.

4.7.2.3 Highway 17 SPS-9A Trial

Perhaps the most useful yet disconcerting results were obtained from the sections on Highway 17. At an AADT of 6000 it is the busiest of the three test roads. The SPS-9A sections on Highway 17 were exposed to significant low-temperature distress in their first winter when the pavement surface temperature dropped below -25.0°C on three occasions. It should be noted that the binder course for this site was constructed in late 1996 while the surface course was constructed in June 1997. In early 1999, on another cold day the temperature dropped to -24.7°C. The lowest pavement surface temperature was reached in 2003 when the temperature fluctuated between lows of -26.5 and -27.2°C for about a week. A complete account of all exposures is provided in Figure 4.26. It should be noted that in the first seven years of service, at no time did the pavement surface temperature fall below -31.0°C, the continuous AASHTO M320 temperature for the PG 58-28 section (see Figure 4.4).

Figure 4.51 shows that the AASHTO M320 method here also fails to predict the cracking onset for the PG 58-28, 58-34 and 58-34P sections. These cracked at temperatures well above what was predicted by the BBR limits. The PG 58-28 section started to crack after the first winter but since no direct measurements were made it is impossible to determine exactly when it started. The continuous grade temperature after three days of conditioning shows an astonishing loss of 13°C compared to the regular AASHTO M320 temperature determined after one hour, rising from -31.0°C to -18°C. Hence, cracking likely started anywhere above -27°C but below -18°C. Although, the limiting fracture energy criterion for this section predicts a slightly warmer cracking onset temperature of -15°C, using a limit of 100 J/m^2, loading rate of 0.01 mm/s and temperature shift of 10°C.

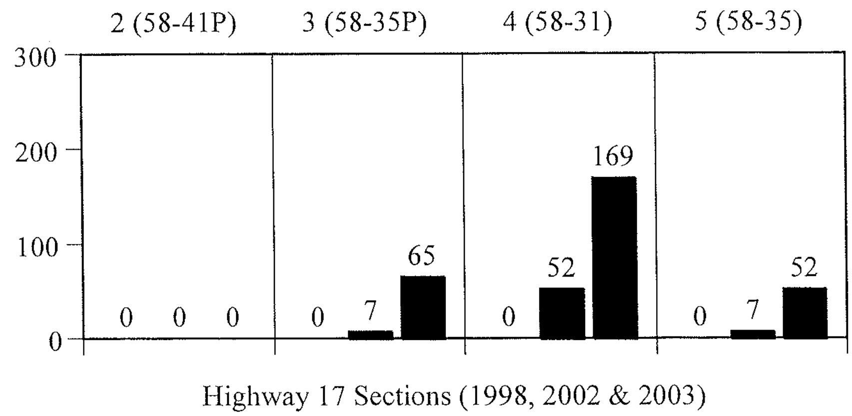

Figure 4.51 Historical cracking data for Highway 17 SPS-9A sections.

It is perhaps more revealing to consider the two PG 58-34 sections. These should not have failed until the temperature dropped to at least -34°C, which is more than six degrees colder recorded thus far. However, Figure 4.51 shows that this is clearly not what happened since a significant 52 and 65 transverse cracks/km have occurred, at a relatively early stage in the design life for this pavement.

Reviewing the grading temperatures for both binders reveals that the limiting m-value predicts a cracking onset at -35°C after one-hour conditioning and -29°C after three-day conditioning (see Figure 4.4). The limiting fracture energy temperatures as determined after three-day conditioning predict the onset of cracking at -23°C and -25°C (see Table 4.21), which are obviously more discriminating temperatures. The AASHTO MP1a critical temperatures for these sections were determined to be -38.0 and -33.0°C after one-hour conditioning and -26.3 and -25.3°C after three days at the grading temperature, using a pavement constant of 18 (see Figure 4.4). It should be added that the error in all these temperatures is probably a few degrees hence the differences may not be significant.

Figure 4.52 provides a comparison of observed with predicted cracking temperatures for the sections for which it was possible to determine the actual temperature for the onset of transverse cracking with some accuracy.

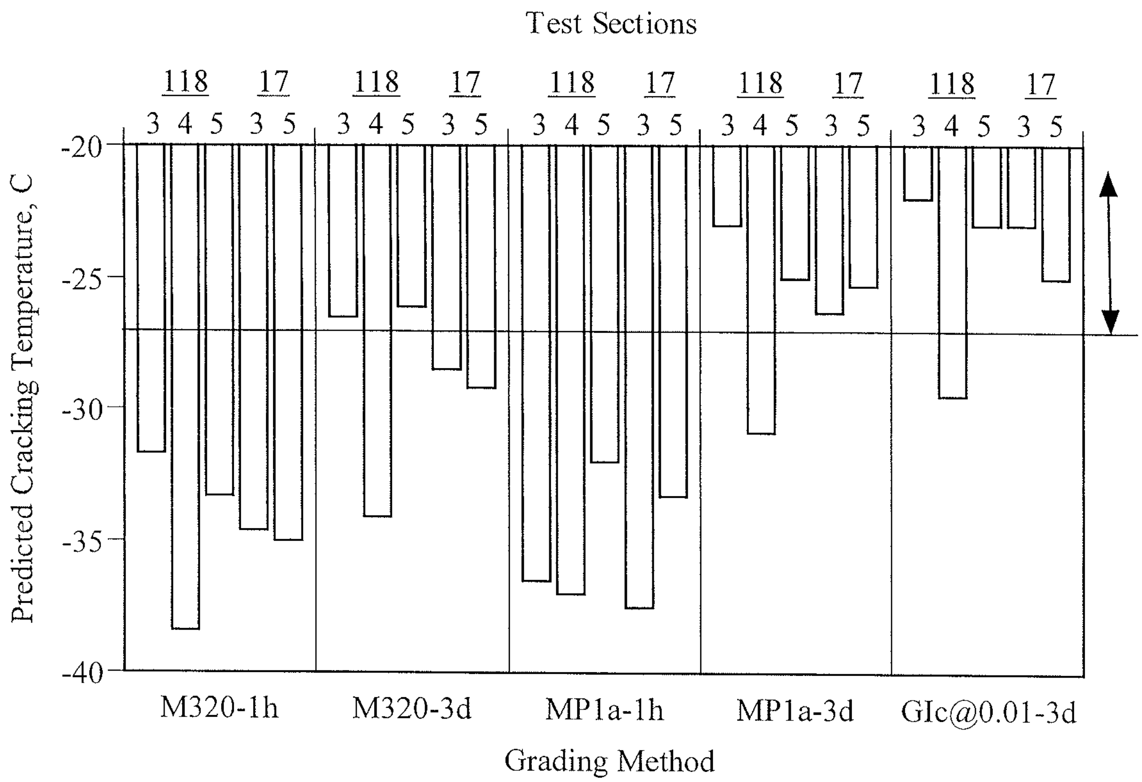

Figure 4.52 Lowest observed pavement surface temperatures compared to predicted cracking temperatures for sections 118-3, 118-4, 118-5, 17-3 and 17-5: M320-1h – AAHTO M320 after one-hour soak; M320-3d – AASHTO M320 after three-day soak; MP1a-1h – MP1a after one-hour soak; MP1a-3d – MP1a after three-day soak; and GIc@0.01-3d – limiting G_{Ic} = 100 J/m^2 @ 0.01 mm/s temperature after three-day soak.

The horizontal line at -27°C indicates the approximate lowest surface temperature observed for both sites while the arrow on the right of the graph indicates the likely temperature range over which cracking occurred. The other four sections for which binder was available either did not crack (17-2 & 17-6) or were under designed by so much that it became difficult to determine the actual temperatures at which cracking had started (118-1 & 118-6). The comparison in Figure 4.52 does not include a limiting S(60 s)=100 MPa temperature, but it was also found to over-predict the performance for four of the five binders by a couple of degrees.

It should be noted that the comparisons in Figure 4.52 omit a number of important factors. Variations in the cracking severity, pavement thickness, brittle fracture toughness, and traffic levels are not considered. For instance, section 118-4 had on average a 20 percent lower thickness than the other sections in Highway 118 (see Table 3.7). This small difference translates into nearly a 50 percent reduction in stiffness, which is very significant in terms of fatigue cracking. The recovered 118-4 binder also had the lowest fracture energy in the brittle state at -30°C (see Figure 4.22). In spite of the above facts, it had only 18 cracks/km as compared to the 37 (118-5), 45 (118-3), 52 (17-5) and 65 (17-3) detected in the other four sections. Probable reasons for this superior performance include the lower grading temperature as well as a higher toughness in the ductile state. More on these factors will be presented in the next sections.

However, first it is worthwhile to consider Figure 4.52 in some more detail. Several observations can be made regarding the data presented. First, the limiting temperatures as determined after one-hour conditioning consistently over-predict performance compared to the observed lowest possible cracking temperatures in the pavement. Second, the three-day conditioned tests all appear to predict temperatures that come much closer to the observed lowest possible cracking temperatures for four of the test sections. The only anomaly is section 118-4 for reasons given above, and still it is not missed by much. Finally, the limiting fracture energy temperature appears to be the most *critical* in that it consistently predicts the warmest cracking temperatures for all five binders.

Although the literature on physical aging is inconclusive on whether it actually does influence low-temperature performance (e.g., see the thermal stress restrained specimen test (TSRST) studies by Romero et al. (1999), Dongré (2000), Lu et al. (2003)) the data in Figure 4.52 suggests that the phenomenon, together with the effect of the notch in the fracture test, would be able to explain to a large degree the unpredicted distress found in these five test sections. The problem with laboratory studies on unnotched samples, such as those documented in the above references, is that they often fail to accurately replicate the entire distress process in a failing pavement.

A recent study by Hesp et al. (2000) was able to show that the regular TSRST is in fact ambiguous but that TSRST tests with deep notches are more discriminating. Brittle samples often failed in a catastrophic fashion while the toughest samples were able to withstand thermal cycling to much lower temperatures without any signs of gross failure regardless of the presence of sharp notches.

Since the above comparison between different grading temperatures only includes results for five binders, it would be unwise to draw any final conclusions. Only well designed pavement trials such as the one recently constructed on Highway 655 with seven sections of nearly the same AASHTO M320 grade will allow us to determine the optimum conditioning time and the effect of the notch on the grading temperatures. For instance, Figure 4.52 suggests that the AASHTO MP1a method after three days of conditioning provide an equally good prediction compared to the fracture energy approach. However, it should be noted that there are binders that may not show the same behaviour in both tests. Some binders such as the EVA-modified system presented in Figure 2.2 could show significant notch sensitivity, which is best assessed in a fracture mechanics-based test in the presence of a sharp notch. In this context it is worthwhile to mention that an effort was made to get one of the new trial sections on Highway 655 constructed with an EVA-modified binder but that the only answer obtained from various suppliers is that the modifier is no longer used.

The data in Figure 4.52 suggest that the conditioning time can probably be somewhat less than three days, which would bring the predicted temperatures closer to the actual failure temperatures. For that reason, the draft laboratory test method as presented in the appendix contains a number of options which allow the determination of the limiting fracture temperature after two conditioning times to be specified by the user agency in order to asses the effect of physical aging. Using the pioneering investigations of Struik (1978) as a guide, the most rapid physical aging would probably occur around 6°C above the ductile-to-brittle temperature. Hence, a 24-hour conditioning period at $T_{design} + 6$ probably comes close enough to a representative degree of aging as it would occur in service.

In conclusion, asphalt binders should be graded after sufficient physical aging in the presence of a sharp notch to replicate the absolute worst possible conditions as they may materialise at some point in the life of the pavement. Once the proposed grading system is implemented it is expected that the predicted performance will more closely match the observed performance and that unnecessary failures can be avoided.

4.8 Fracture Testing of Recovered Field Core Samples

Significant time and resources were expended to test the fracture properties of the asphalt mixtures as recovered from Highways

118 and 17 after eight and six years in service, respectively. The eight remaining cores for each section were cut with a diamond-tipped masonry saw to yield specimens of approximately 150 mm (length) x 40 mm (height) x 15 mm (depth). These specimen were notched to yield samples all having a ratio of crack depth to specimen height, a_o/W, of between 0.45 and 0.55 as required by the various ASTM methods. Tests were conducted at 3°C intervals around the brittle-to-ductile transition temperature at a constant rate of loading of 0.001 mm/s in three-point bending.

The main purpose of these experiments was to investigate the fracture behavior of the mixtures as they existed in the pavement. This eliminated from the analysis possible spurious effects caused by solvent extraction (when recovered binders were tested) and it also dealt with the problem that various sections were either over- or under-designed and hence were not challenged to the same degree in the field.

Figure 4.53 to 4.58 present the fracture toughness, K_{Ic}, fracture energy, G_f, and crack opening displacement (CMOD) properties determined for the Highway 118 and 17 mix specimens. The error bars give plus or minus one pooled standard deviation from the entire set of data, which included well over two hundred specimens tested.

The data are instructive in several respects. First, for Highway 118 materials the fracture energies of the mixtures appear to go through a brittle-to-ductile transition for all sections except for section 118-1. The latter material appears to remain brittle even at relatively high temperatures. Second, the G_f and the CMOD of the 118-4 specimens is highest under ductile conditions but not under brittle conditions. This suggests that the radial SBS polymer used in section 118-4 lost significant toughness in its brittle state but that it had retained some toughness (i.e., strength in the presence of flaws) in the ductile state. These results are in agreement with those presented in Figure 4.23 which compares PAV-aged with field-aged binders for these sections.

The results presented in Figures 4.56 to 4.58 show that the PG 58-34 grade with the polymer modifier is no tougher than the one without the polymer modifier in the brittle state but that this is changed in the ductile state. This may explain the similar number of cracks in the two PG 58-34 sections. However, the scatter in the data is large and at this moment it is better to use caution when drawing such conclusions.

For the new pavement trial that was recently constructed on Highway 655, a significant amount of material was retained for future laboratory testing purposes. The binder for each section was sampled at 75 gallons while three tons of aggregates were retained. This material will be used for a more extensive mixture test program, which will include the brittle as well as ductile fracture properties. It is anticipated that we will find similar differences in fracture properties as the ones found in this study and that these will eventually show up as differences in fatigue and thermal fracture performance.

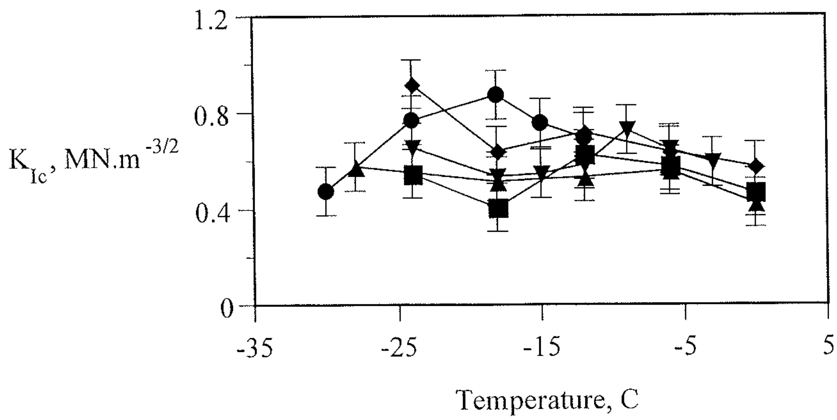

Figure 4.53 Mixture Fracture Toughness Data for Highway 118 Materials.
(■ – 118-1, ♦ – 118-3, ● – 118-4, ▲ – 118-5, and ▼ – 118-6)

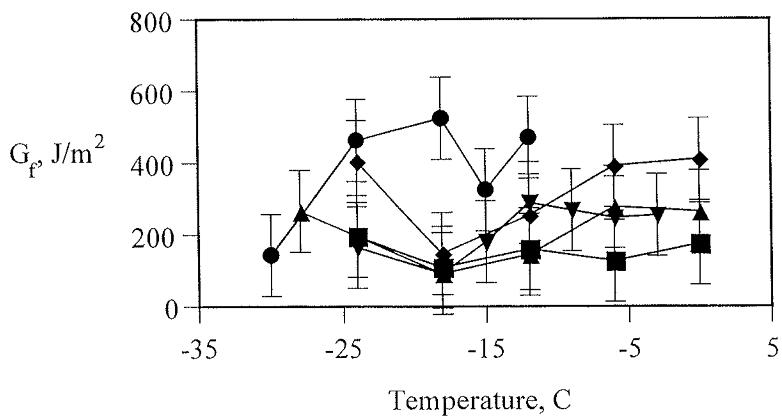

Figure 4.54 Mixture Fracture Energy Data for Highway 118 Materials.
(■ – 118-1, ♦ – 118-3, ● – 118-4, ▲ – 118-5, and ▼ – 118-6)

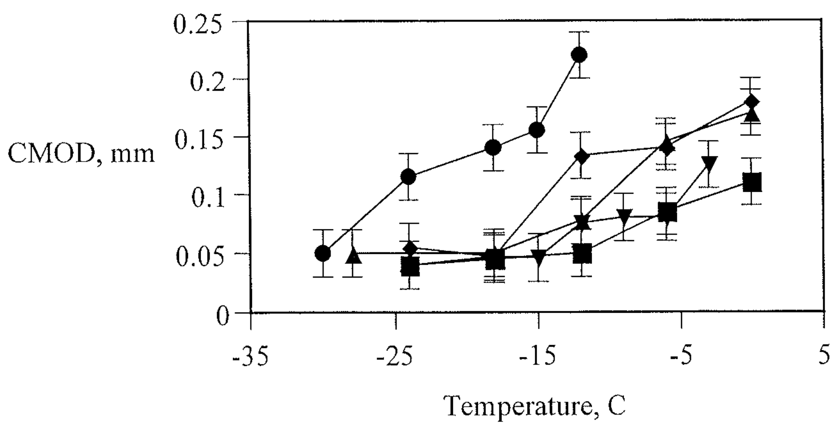

Figure 4.55 Mixture Crack Mouth Opening Displacement Data for Highway 118 Materials.
(■ – 118-1, ♦ – 118-3, ● – 118-4, ▲ – 118-5, and ▼ – 118-6)

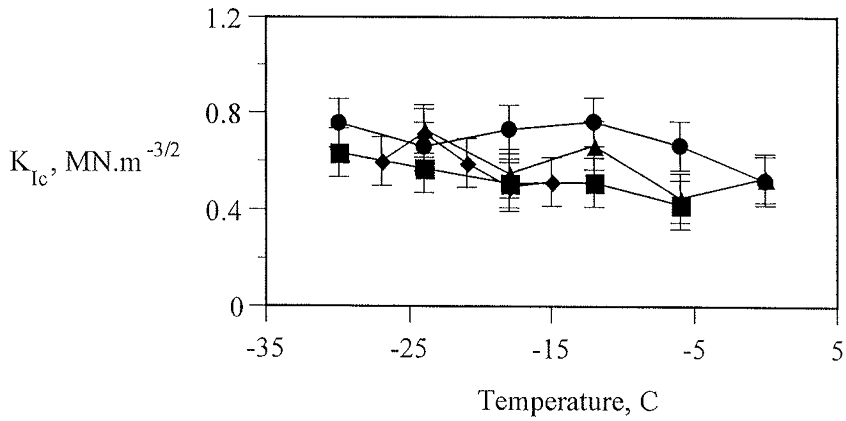

Figure 4.56 Mixture Fracture Toughness Data for Highway 17 Materials.
(▲ – 17-4 (PG 58-28), ■ – 17-5 (PG 58-34 NP), ● – 17-3 (PG 58-34 P), ♦ – 17-2 (PG 58-40))

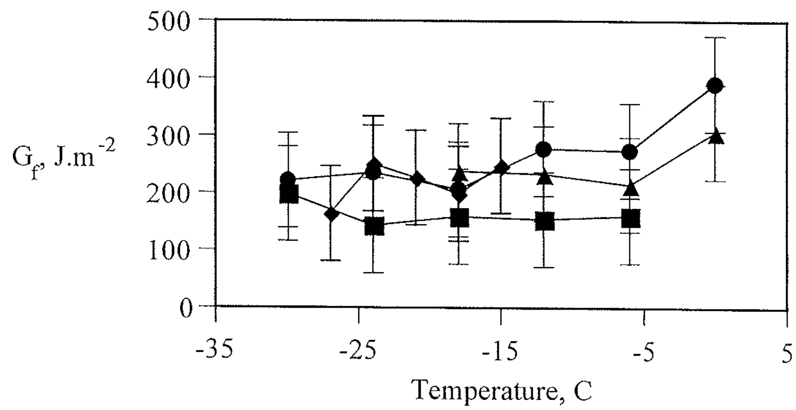

Figure 4.57 Mixture Fracture Energy Data for Highway 17 Materials.
(▲ – 17-4 (PG 58-28), ■ – 17-5 (PG 58-34 NP), ● – 17-3 (PG 58-34 P), ♦ – 17-2 (PG 58-40))

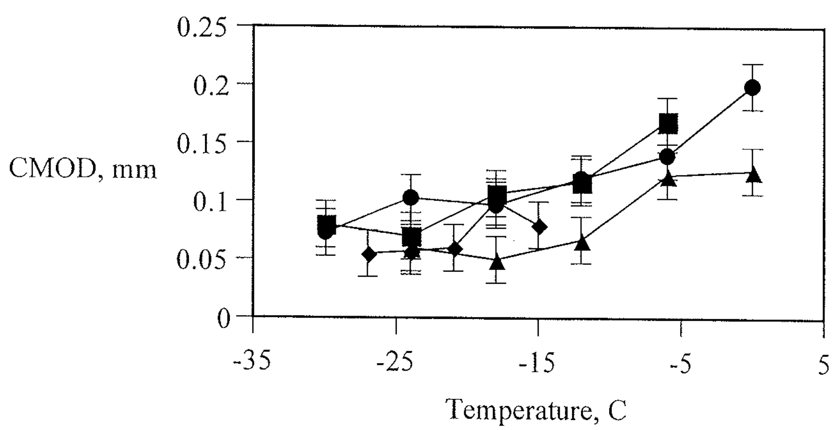

Figure 4.58 Mixture Crack Opening Displacement Data for Highway 17 Materials.
(▲ – 17-4 (PG 58-28), ■ – 17-5 (PG 58-34 NP), ● – 17-3 (PG 58-34 P), ♦ – 17-2 (PG 58-40))

4.9 Ductile Failure in Unaged Highway 118 Asphalt Binders

A comparison of the surveys from sections B and BB on Highway 631 near Hearst (see Figures 4.27 and 4.30) and from the area around the intersection in section 118-3 on Highway 118 near Bracebridge (see Figure 4.36) suggested that fatigue failure at higher temperatures could play an important role in low-temperature cracking. These are similar observations as those reported by Deme and Young (1987) on truck lanes and truck hill-climbing lanes and by others. In addition, mixture test results as presented in Figure 4.53 to 4.58 suggested that there are significant differences in toughness in the ductile state for samples that have been in service for six to eight years. These observations motivated a short investigation into the binder fracture properties in the ductile state.

A limited number of tests were conducted on unaged binders from sections 118-1, 118-4, 118-5, and 118-6 to determine the fracture properties in the ductile regime. Time and material constraints precluded us from testing other materials. The tests were performed according to a recently developed protocol that employs the essential and plastic works of fracture test method as first developed for plastics by Cotterel, Mai and coworkers at the University of Sydney, Australia (see Andriescu et al. (2003), Mai et al. (2000) and references therein). Since the plane-strain essential work of fracture is a fundamental material property, it should be particularly useful for the performance grading of asphalt binders for fatigue.

For a detailed description of the test method refer to Andriescu et al. (2003) or section 8.2.11 of Ministry of Transportation Ontario *Draft Laboratory Standard 296 – Laboratory Standard for Fracture Performance Grading of Asphalt Binders* as attached as an appendix to this report.

In brief, double-edge notched samples of 40 mm (length (L)) x 30 mm (width (W)) x 6.5 mm (thickness (t)) were tested with sharp, 45° notches on two sides in direct tension. The areas under the force-displacement curves were integrated to yield the total work of fracture, W_f. The specific total work of fracture, w_f or W_f/lt, was plotted versus the ligament length, l. The straight line plot gives an intercept equal to the specific essential work of fracture, w_e, and a slope equal to a geometry constant times the plastic work of fracture, βw_p. The essential work is the energy needed to create the new fracture surfaces, and under the correct circumstances provides a material property, while the plastic work is the energy dissipated in areas of the sample away from the fracture surface. The plastic work is dependent on geometry but may still play an important role in fatigue specification development. For further details see Andriescu et al. (2003).

Only unaged binders were tested at 0°C and a single rate of 30 mm/min to reveal the significant differences that exist between four materials used on Highway 118. Figure 4.59 shows a typical DENT specimen after failure. Figure 4.60 shows typical raw data for the binder from section 118-4. And Figure 4.61 shows the works of fracture as determined for the four unaged binders that were investigated.

Eventually it would be useful to do tests on appropriately aged materials at different temperatures and rates of loading to obtain a complete picture of the fracture resistance of these binders under various conditions. However, the data as presented in Figure 4.61 show that there are very significant differences for the ductile fracture properties of just four binders. The w_e values varied from 3.9 $kJ.m^{-2}$ to 23.3 $kJ.m^{-2}$ while the βw_p values varied from 0.5 $MJ.m^{-3}$ to 2.7 $MJ.m^{-3}$. Whether such large differences exist for appropriately aged materials remains to be further investigated. However, a more comprehensive study of this issue is better left for the investigation of the binders and mixtures from the new Highway 655 trial sections since for these materials shortage is not an issue. A generous 75 gallons of binder per section is set aside for future research and development purposes.

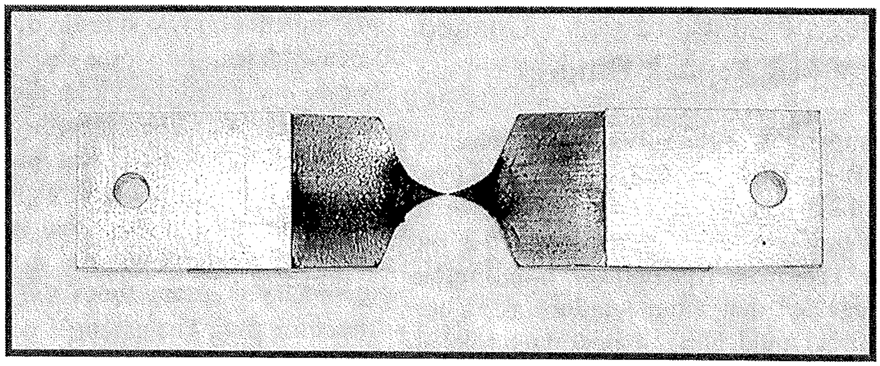

Figure 4.59 Typical DENT specimen after testing in the essential work of fracture method.

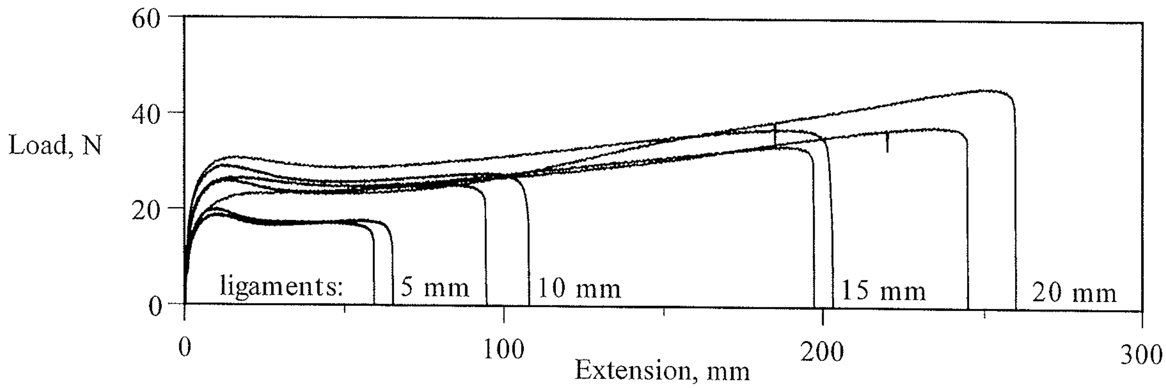

Figure 4.60 Typical duplicate measurements for essential and plastic work of fracture tests on 118-4 binder.

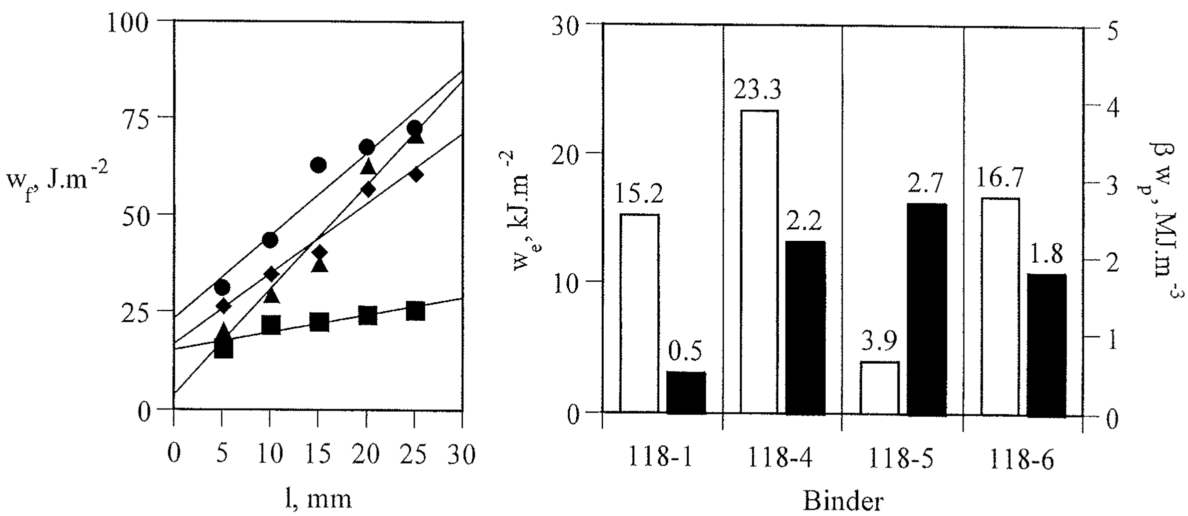

Figure 4.61 Essential works of fracture and plastic works of fracture terms at 0°C and 30 mm/min for (■) 118-1, (●) 118-4, (▲) 118-5, and (♦) 118-6 binders.

Chapter 5
CONCLUSIONS AND RECOMMENDATIONS

Given the results presented in this report, we may come to the following conclusions and recommendations:

- The AASHTO M320 and MP1a low-temperature asphalt binder specification methods are unable to provide an accurate indication for the onset or severity of transverse stress cracking. Efforts should continue until a satisfactory specification test protocol is validated and accepted by both users and producers of asphalt binders. The appendix to this report outlines a proposed specification test protocol with many improvements over current methods.
- Fracture energy in the ductile-to-brittle regime, G_f, appears to be a discriminating indicator of when a binder becomes brittle, and as such it should be particularly suitable for performance grading at low temperatures.
- Crack opening properties of asphalt binders are somewhat correlated with their fracture energies. However, the two properties will likely provide different rankings. From a mechanistic viewpoint the most sensible property for specification grading is the crack opening displacement since it provides a measure of strain tolerance in the presence of sharp cracks close to the ductile-to-brittle regime. Careful field validation studies will have to determine which property is best suited for specification grading. The proposed test method provides options to set limits on both fracture energy and/or crack opening properties.
- Crack surveys from 17 Ontario test sections indicate that fatigue distress can be a significant aggravating factor for low-temperature transverse stress cracking. This is especially problematic in thin pavements, nearby intersections, and perhaps in other areas of slow moving traffic such as in truck lanes or truck hill-climbing lanes. It is recommended that an improved low-temperature binder specification method assess a binder's resistance to fatigue cracking through the use of the essential and plastic work of fracture test method. The proposed specification test method provides the user agency with an option to set lower limits on both the essential and plastic works of fracture at different temperatures and rates of loading.
- Freeze-thaw cycles can be another serious aggravating factor for generalized deterioration of northern roads through fracture. It is therefore recommended that asphalt binders be graded according to the essential and plastic works of fracture at 0°C at an appropriate rate of loading for pavements where freeze-thaw distress is likely. The proposed specification test method provides the user agency with an option to set a lower limit on both the essential and plastic works of fracture at 0°C and an appropriate rate of loading.
- The essential and plastic works of fracture as determined with a double-edge notched tensile (DENT) geometry were found to vary a great deal between different binders. It is recommended that the DENT test be evaluated for specification grading of binders in respect to their fatigue performance.
- The brittle-to-ductile temperature as measured in the various grading test methods does not change much due to long-term field aging. However, fracture energy in the brittle temperature regime, G_{Ic}, is more sensitive, especially for SBS-modified binders.
- The combined effects of physical aging, excessive chemical aging (above and beyond what is induced by the pressure aging vessel), and notch sensitivity can, in large part, explain the

differences between predicted and observed cracking onset and severity in several Ontario test sections that showed early distress.

- The current rolling thin film oven (RTFO) and pressure aging vessel (PAV) procedures do not age asphalt binders for more than the equivalent of approximately two to three years of field exposure. Hence, it is recommended to double the PAV aging time to 40 hours as a stop-gap measure. Eventually a new and innovative method would have to be developed to overcome the deficiencies of the current binder aging approach.
- Oxidative aging of the base asphalt occurs at a faster rate than the aging of modifiers in the RTFO/PAV procedure. Consequently, a simple doubling of the PAV aging time may not completely solve the problem associated with the inadequate binder aging in this method.

REFERENCES

Abd El Halim, A.O., Razaqpur, A.G., Humar, J., Carrick, J.J., and Davidson, K. (1999) Laboratory evaluation of asphalt mixes using engineered binders under static and cyclic thermal stresses. *Proceedings, Canadian Technical Asphalt Association,* 44, pp. 49-66.

Abd El Halim, A.O., Hassan, Y., Kandil, K., Bhutta, S.A., and Davidson, K. (2001) Comparison of mechanical properties of asphalt concrete mixes with aged asphalt cements. *Proceedings, Canadian Technical Asphalt Association,* 46, pp. 33-50.

Abdulshafi, A.A. and Majidzadeh, K. (1986) J-integral and cyclic plasticity approach to fatigue and fracture of asphaltic mixtures. *Transportation Research Record,* 1034, pp. 112-123.

Aglan, H., Shehata, I., Figueroa, L., and Othman, A. (1992) Structure-fracture toughness relationships of asphalt concrete mixtures. *Transportation Research Record,* 1353, pp. 24-30.

American Society for Testing and Materials (1993) E 1290-93: Standard test method for crack tip opening displacement (CTOD) fracture toughness measurement. Annual Book of ASTM Standards, 03.01, ASTM, Philadelphia, Pennsylvania, pp. 814-823.

American Society for Testing and Materials (1996) D 5045-96: Standard test method for plane-strain fracture toughness and strain energy release rate of plastics. Annual Book of ASTM Standards, 08.03, ASTM, Philadelphia, Pennsylvania, pp. 314-322.

American Society for Testing and Materials (1990) E 399-90: Standard test method for plane-strain fracture toughness of metallic materials. Annual Book of ASTM Standards, 03.01, ASTM, Philadelphia, Pennsylvania, pp. 413-443.

Anderson, D.A., Christensen, D.W., Bahia, H.U., Dongré, R., Sharma, M.G., Antle, C.E. and Button, J. (1994) Binder Characterization and Evaluation. Volume 3: Physical Characterization. SHRP-A-369 Final Report, Strategic Highway Research Program, National Research Council, Washington DC.

Anderson, T.L. (1995) <u>Fracture Mechanics. Fundamentals and Applications</u>. Second Edition, CRC Press, Boca Raton, Florida.

Anderson, D.A. and Dongré R. (1995) The SHRP direct tension specification test-its development and use. In: Physical Properties of Asphalt Cement Binders. John C. Hardin (Ed.), ASTM STP 1241, American Society for Testing and Materials, Philadelphia, pp. 51-66.

Anderson, K.O., Christison, J., Bai, B., Johnston, C.D., Quinn, T. and McCullough, D. (1998) Temperature and thermal contraction measurements as related to the development of low temperature cracking on the Lamont test road. *Proc., Canadian Technical Asphalt Association,* 43, pp. 16-47.

Anderson, D.A. Superpave binder tests and specification (1999a) In *Workshop Briefing, Performance Related Properties for Bituminous Binders,* May 1999, Eurobitume Workshop, Luxembourg.

Anderson, M.R., Walker, D. and Turner, P. (1999b) Low temperature evaluation of Kentucky PG 70-22 asphalt binders. *Transportation Research Record,* 1661, pp. 69-74.

Anderson, D.A., Marasteanu, M., Champion-Lapalu, L., Yan, L.H., Didier, M., and Planche, J.-P. (2000) Low temperature thermal cracking of asphalt binders as ranked by strength and fracture properties. *Proceedings, 2nd Eurasphalt and Eurobitume Congress,* Barcelona, Book I, pp. 7-15.

Anderson, D.A., Champion-Lapalu, L., Marasteanu, M.O., LeHir, Y.M., Planche, J.P., and Martin, D. (2001) Low-temperature thermal cracking of asphalt binders as ranked by strength and fracture properties. *Transportation Research Record: Journal of the Transportation Research Board,* 1766, pp. 1-6.

Andriescu, A., Hesp, S.A.M, and Youtcheff, J.S. (2003) On the essential and plastic works of ductile failure in asphalt binders. Accepted for Publication, *Transportation Research Record: Journal of the Transportation Research Board*, 2004.

Bahia, H.U., Anderson D.A. and Christensen D.W. (1992) The bending beam rheometer; A simple device for measuring low-temperature rheology of asphalt binders. *Journal of the Association of Asphalt Paving Technologists,* 61, pp. 117-153.

Bardesi, A., Brule, B., Corte, J-F., Diani, E., Gerritsen, A., Lefevre, G., Planche, J-P., Sybilski, D., Stawiarski, A., Verhee, F. and Watkins, S. (1999) Use of modified bituminous binders, special bitumens and bitumens with additives in pavement applications, Technical Committee Flexible Roads (C8), World Road Association (PIARC).

Basu, A. (2002) An Evaluation of the Time-Temperature Equivalence Factor and of the Physical Hardening Effects on Low-Temperature Asphalt Binder Specifications. M.S. thesis, Department of Civil Engineering, University of Minnesota.

Basu, A., Marasteanu, M.O. and Hesp, S.A.M. (2003) Time-temperature superposition and physical hardening effects in low-temperature asphalt binder grading. *Transportation Research Records: Journal of the Transportation Research Board,* TRB, National Research Council, Washington, D.C., in press.

Bhurke A., E. Shin, and L. Drzal. (1997) Fracture morphology and fracture toughness measurement of polymer-modified asphalt concrete. In *Transportation Research Record, No. 1590,* TRB, National Research Council, Washington, D.C., pp. 23-33.

Bouldin, M.G., Dongré, R., Rowe, G.M., Sharrock, M.J. and Anderson, D.A. (2000) Predicting thermal cracking of pavements from binder properties. *Journal of the Association of Asphalt Paving Technologists,* 69, pp. 455-496.

Bouldin, M.G. and Dongré, R. (2000) Implications of the new low temperature specification on PG grading and testing of asphalt binders. *Proceedings, 2nd Eurasphalt and Eurobitume Congress,* Barcelona, Spain, September 2000, Book I, pp. 212-219.

Broek, D. (1998) Elemental Engineering Fracture Mechanics. Fourth Revised Edition, Kluwer Academic Publishers, The Netherlands.

Bucknall, C.B. (1977) Toughened Plastics. Applied Science Publishers, London.

Button, J.W. and Hastings, C.P. (1998) How well can new binder tests predict cracking? *Proc., Canadian Technical Asphalt Association,* 43, pp. 48-72.

C-SHRP (2000) Technical Brief #19 SUPERPAVE VS. THE CANADIAN WINTER: Low-Temperature Performance at C-SHRP Test Roads. Canadian Strategic Highway Research Program, June 2000.

Cayard, M.S. Fracture Toughness Characterization of Polymers. Ph.D. Dissertation, Texas A&M University, Austin, Texas.

Champion, L., Gerard, J.-F., Planche, J.-P., Martin, D. and Anderson, D.A. (1999) Evaluation of the low-temperature fracture properties of modified binders. *Workshop Briefing, Performance Related Properties for Bituminous Binders.* Eurobitume Workshop, Luxembourg.

Champion-Lapalu, L., Planche, J.-P., Martin, D., Anderson, D.A. and Gerard, J.-F. (2000)

Low-temperature rheological and fracture properties of polymer-modified bitumens. *Proceedings, 2nd Eurasphalt and Eurobitume Congress,* Barcelona, Book I, pp. 122-130.

Deme, I. (2000) Transverse cracking of Hwy. #118 (Bracebridge) pavements. Report prepared for the October 11, 2000, Canadian Users Producers Group Meeting in Winnipeg, Manitoba.

Deme, I. (1996) Prevention of pavement cracking and rutting with Multigrade-type bitumens. Proceedings, 31st Annual Congress of the Association Québécoise du Transport et des Routes, March 1996, Québec.

Deme, I.J. and Young, F.D. (1987) Ste. Anne test road revisited twenty years later. *Proceedings, Canadian Technical Asphalt Association,* Vol. 32, pp. 254-283.

Dongré R., Sharma, M.G and Anderson, D.A. (1989) Development of a fracture criterion for asphalt mixes at low temperatures. *Transportation Research Record,* 1228, pp. 94-105.

Dongré R., Button J.W., Kluttz R.Q., and Anderson D.A. (1997) Evaluation of Superpave binder specification with performance of polymer-modified asphalt pavements. In: Jester RN (Ed) Progress of Superpave (Superior Performing Asphalt Pavement) Evaluation and Implementation. ASTM STP 1322, American Society for Testing and Materials, pp. 80-100.

Dongré, R. (2000) Effect of physical hardening on stress relaxation behavior of asphalt binders. *Proceedings, 2nd Eurasphalt and Eurobitume Congress*, Barcelona, Book I, pp. 220-228.

El Hussein, H.M., Kim, K.W., and Ponniah, J. (1998) Asphalt concrete damage associated with extreme low temperatures. *Journal of Materials in Civil Engineering,* Vol. 10, No. 4, pp. 269-274.

Evans, A.G. (1972) The strength of brittle materials with a second-phase dispersion. *Philosophical Magazine,* 26, pp. 1327-1344.

Ewalds, H.L. and Wanhill, R.J.H. (1985) Fracture Mechanics. Second Edition. Ewald Arnold (Australia) Pty., Victoria, Australia.

Fabb, T. (1974) The influence of mix composition, binder properties and cooling rate on asphalt cracking. Journal of the Association of Asphalt Paving Technologists, 43, pp. 285-331.

Fortier, R. and Vinson, T.S. (1998) Low-temperature cracking and aging performance of modified asphalt concrete specimens. *Transportation Research Record,* 1630, pp. 77-86.

Frechette, L. and Shalaby, A. (1997) Reflective cracking trends in C-SHRP LTPP sites. Long-Term Pavement Performance Project, Canadian Strategic Highway Research Program (C-SHRP LTPP), Transportation Association of Canada (TAC), pp. 30-31, Site # 870505.

Fromm, H.J. and Phang W.A. (1970) Temperature susceptibility control in asphalt cement specifications. Department of Highways, Ontario, Report IR 35, November 1970.

Garcés Rodríguez, M., Morrison, G.R., vanLoon, J. and Hesp, S.A.M. (1996) Low temperature failure in particulate-filled asphalt binders and mixes. *Journal of the Association of Asphalt Paving Technologists,* 65, pp. 159-192.

Gledhill, R.A., Kinloch A.J., Yamini, S. and Young, R.J. (1978) Relationship between mechanical properties of and crack propagation in epoxy resin adhesives. *Polymer,* 19, pp. 574-582.

Green, D.J., Nicholson, P.S. and Embury, J.D. (1979) Fracture of a brittle particulate composite. *Journal of Materials Science,* 14, pp. 1657-1661.

Griffith AA. (1921) The phenomena of rupture and flow in solids. Philosophical Transactions of the Royal Society of London A 221, pp. 163-197.

Ha Anh, T. and Vu-Khanh, T. (2001) Fracture and yielding behaviors of polystyrene/ethylene-propylene rubber blends: Effect of interfacial agents. *Polymer Engineering and Science,* 41(12), pp. 2073-2081.

Harder, N.A. (1992) Brittleness, fracture energy and size effect in theory and reality. *Materials and Structures,* Vol. 25, pp. 102-106.

Herrin, M. and Jones, G.E. (1963) The behavior of bituminous materials from the viewpoint of the absolute rate theory. *Proc., Association of Asphalt Paving Technologists,* 32, pp. 82-105.

Herrin, M., Marek, C.R. and Strauss, R. (1966) The application of the absolute rate theory in explaining the behavior of bituminous materials. *Proc. Association of Asphalt Paving Technologists,* 35, pp. 1-18.

Hesp, S.A.M., Terlouw, T. and Vonk, W.C. (2000) Low temperature performance of SBS-modified asphalt mixes. *Journal of the Association of Asphalt Paving Technologists,* 69, pp. 540-573.

Hesp, S.A.M., Smith, B.J. and T.R. Hoare (2001) The effect of filler particle size on low and high temperature performance of asphalt mastics and mixtures. *Journal of the Association of Asphalt Paving Technologists,* Vol. 70, pp. 492-508.

Hesp, S.A.M, and Roy, S.D. (2004) How temperature and strain rate affect the yield behavior in polymer-modified asphalt systems. *International Journal of Pavement Engineering* (in press).

Hesp, S.A.M., Iliuta, S., Marasteanu, M.O., Masliwec, T., and Tam, K.K. (2003) Field validation study of low-temperature performance grading tests for asphalt binders. *Transportation Research Record: Journal of the Transportation Research Board,* Accepted for Publication, 2004.

Heukelom, W. (1966) Observations on the rheology and fracture of bitumens and asphalt mixes. *Journal of the Association of Asphalt Paving Technologists,* 35, pp. 3-48.

Heukelom, W. (1969) A bitumen test data chart for showing the effect of temperature on the mechanical behavior of asphaltic bitumens. *Journal of the Institute of Petroleum,* Vol. 55, No. 546, pp. 404-417.

Hills J.F. (1974) "Predicting the fracture of asphalt mixes by thermal stresses." *Journal of the Institute of Petroleum*, pp. 1-11.

Hoare, T.R. and Hesp, S.A.M. (2000) Low-temperature fracture testing of asphalt binders. *Transportation Research Record: Journal of the Transportation Research Board,* 1728, pp. 36-42.

Ioannides, A.M. (1997) Fracture mechanics in pavement engineering. *Transportation Research Record: Journal of the Transportation Research Board,* 1568, pp. 10-16.

Irwin GR in Fracturing of Metals. American Society of Metals, Cleveland 147-166 (1948).

Irwin LH (1977) Use of fracture energy as a fatigue failure criterion. *Proceedings, Association of Asphalt Paving Technologists,* 46, pp. 41-63.

Isacsson, U. and Zeng, H. (1998) Low-temperature cracking of polymer-modified asphalt. *Materials and Structures,* 31, pp. 58-63.

Jacobs, M.M.J. (1995) Crack Growth in Asphaltic Mixes. Ph.D. Thesis, Delft University of Technology, Delft, The Netherlands.

Jacobs, M.M.J., Hopman, P.C. and Molenaar, A.A.A. (1996) Application of fracture mechanics principles to analyze cracking in asphalt concrete. *Journal of the Association of Asphalt Paving Technologists,* 65, pp. 1-39.

Jennings P.W., Pribanic, J.A., Desando, M.A., Raub, M.F., Stewart, F., Hoberg, J., Moats, R., Fanconi, B., Vanderhart, D.L., Manders, W.F. (1993) Binder Characterization and Evaluation by Nuclear Magnetic Resonance Spectroscopy. SHRP-A-335 Final Report, Strategic Highway Research Program, National Research Council, Washington DC.

Jenq, Y.-S., and Perng, J.-D. (1991) Analysis of crack resistance of asphalt concrete using cohesive crack model. *Transportation Research Record,* 1317, pp. 90-99.

Jenq, Y.-S., Liaw, C.-J. and Liu, P. (1993) Analysis of crack resistance of asphalt concrete overlays – a fracture mechanics approach. *Transportation Research Record,* 1388, pp. 160-166.

Jew, P. and Woodhams, R.T. (1986) Polyethylene-modified bitumens for paving applications. *Journal of the Association of Asphalt Paving Technologists,* 55, pp. 541-563.

Jung, D.H. and Vinson T.S. (1994) Low-temperature cracking: test selection. SHRP-A-400 Final Report, Strategic Highway Research Program, National Research Council, Washington DC.

Kandhal, P.S., Dongré, R. and Malone, M.S. (1996) Prediction of low-temperature cracking of pennsylvania project using Superpave specifications. *Journal of the Association of Asphalt Paving Technologists,* 65, pp. 491-531.

Kim K.W. and El Hussein H.M. (1995) Effect of differential thermal contraction on fracture toughness of asphalt materials at low temperatures. *Journal of the Association of Asphalt Paving Technologists,* 64, pp. 474-499.

Kim, Y.R., Lee, H.-Y., Kim, Y., and Little, D.N. (1997) Mechanistic evaluation of fatigue damage growth and healing of asphalt concrete: Laboratory and field experiments. Proceedings, Eight International Conference on Asphalt Pavements, Seattle, Washington, Vol. 2, pp. 1089-1107.

King, G.N., King, H.W., Harders, O., Arand W. and Planche, J.-P. (1993) Influence of asphalt grade and polymer concentration on the low temperature performance of polymer modified asphalt. *Journal of the Association of Asphalt Paving Technologists,* 62, pp. 1-22.

Kinloch, A.J., Shaw, S.J. and Hunston, D.L. (1983) Deformation and fracture behavior of a rubber toughened epoxy: *Polymer,* 24, pp. 1355-1363.

Kluttz, R.Q. and Dongré, R. (1997) Effect of SBS polymer modification on the low-temperature cracking of asphalt pavements. In Usmani A.M. (Ed) Asphalt Science and Technology, Marcel Dekker, New York, pp. 217-233.

Lange, F.F. (1970) The interaction of a crack front with a second-phase dispersion. *Philosophical Magazine,* 22, pp. 983-992.

Latzko, D.G.H., Turner, C.E., Landes, J.D., McCabe, D.E. and Hellen, T.K. (1984) Post-yield Fracture Mechanics. Second Edition, Elsevier Applied Science Publishers Ltd.

Lee, N. and Hesp, S.A.M. (1994) Low temperature fracture toughness of polyethylene-modified asphalt binders. *Transportation Research Record,* 1436, pp. 54-59.

Lee, N.K., Morrison, G.R. and Hesp, S.A.M. (1995) Low temperature fracture of polyethylene-modified asphalt binders and concrete mixes. *Journal of the Association of Asphalt Paving Technologists,* 64, pp. 534-574.

Little, D.N. and Mahboub, K. (1986) Engineering properties of first generation plasticized asphalt binders and low temperature fracture evaluation of plasticized sulfur paving mixtures. *Transportation Research Record,* No. 1034, pp. 103-111.

Lu, X., Isacsson, U., and Ekblad, J. (2003) Influence of polymer modification on low-temperature behavior of bituminous binders and mixtures. *Proceedings, 6th International RILEM Symposium,* Zurich, Switzerland, M.N. Partl, Ed., RILEM Publications, 2003, 435-441.

Mahboub, K. (1990) Elasto-plastic fracture characterization of paving materials at low temperatures. *Journal of Testing and Evaluation,* Vol. 18, No. 3, May 1990, pp. 210-218.

Mai, Y.-W., Wong, S.-C. and Chen, X.-H. (2000) Application of fracture mechanics for characterization of toughness of polymer blends. In: *Polymer Blends, Volume 2: Performance.* D.R. Paul and C.B. Bucknall (Eds.), John Wiley and Sons, Inc.

Marasteanu, M.O., Dai, S., Labuz, J.F., and Li X. (2002) Determining the low-temperature fracture toughness of asphalt mixtures. Transportation Research Record: Journal of the Transportation Research Board, No. 1789, pp. 191-199.

Marasteanu, M.O., Basu, A., Hesp, S.A.M., and Voller V. (2003) Time-temperature superposition and AASHTO MP1a critical cracking temperature for low-temperature cracking. Submitted for publication, International Journal of Pavement Engineering, May 2003.

McCrum, N.G., Buckley, C.P. and Bucknall C.B. (1997) Principles of Polymer Engineering. Second Edition, Oxford Science Publishers, pp. 189-194.

McLeod, N.W. (1968) Transverse pavement cracking related to hardness of the asphalt cement. *Proceedings, 13th Conference Canadian Technical Asphalt Association,* November 4-6.

Mobasher, B., Mamlouk, M.S. and Lin, H.-M. (1997) Evaluation of crack propagation properties of asphalt mixtures. *Journal of Transportation Engineering,* Vol. 123, No. 5, September 1997, pp. 405-413.

Mohseni, A. (1998) *LTPP Seasonal Asphalt Concrete (AC) Pavement Temperature Models.* Publication No. FHWA-RD-97-103, Federal Highway Administration, Washington D.C.

Monismith, C.L., Secor, G.A. and Secor, K.E. (1965) Temperature induced stresses and deformations in asphalt. *Journal of the Association of Asphalt Paving Technologists,* Vol. 34, pp. 248.

Morrison, G.R., J.K. Lee, and S.A.M. Hesp (1994) Chlorinated polyolefins for asphalt binder modification. *Journal of Applied Polymer Science*, Vol. 54, pp. 231-240.

Planche, J.-P., Lesueur, D., Hines, M.L. and King, G.N. (1996) Evaluation of elastomer modified bitumens using SHRP binder specification. *Proc., Eurasphalt & Eurobitume Congress,* Paper E&E 5.121.

Orowan, E. (1952) In Fatigue and Fracture of Metals. MIT Symposium, June 1950, Murray WM (Ed), Wiley, New York, 139-167.

Pearson, R.M. (1994) The application of small Nuclear Magnetic Resonance Spectrometers to Quality Control measurements of asphalt and asphalt-aggregate mixes. SHRP Final Report, SHRP-A-382, Strategic Highway Research Program, National Research Council, Washington, DC.

Petersen, J.C. (1986) Quantitative functional group analysis using differential infrared spectrometry and selective chemical reactions-theory and application. *Transportation Research Record,* No. 1096, pp. 1-11.

Phillips, M.C. (1999) The pseudo-Black diagram: A new technique using the BBR for diagnosing phase changes and rheological simplicity in binders. *Proceedings, Eurobitume Workshop 99 – Performance Related Properties for Bituminous Binders,* Paper 114.

Ponniah, J.E. and Hesp, S.A.M. (1996) Use of facture energy in performance-based specifications of asphalt binders. *Proceedings, Canadian Technical Asphalt Association,* 41, pp.127-144.

Ponniah, J.E. and Kennepohl, G. (1998) Comparison of laboratory test results with field performance of polymer-modified asphalt. *Proc., Canadian Technical Asphalt Association,* 43, pp. 337-355.

Raad, L., Saboundjian, S., Sebaaly, P. and Epps, J. (1998) Thermal cracking models for AC and modified AC mixes in Alaska. *Transportation Research Record,* 1629, pp. 117-126.

Radovskiy, B. (2000) Discussion. *Journal of the Association of Asphalt Paving Technologists,* 69, pp. 488-489.

Ramsamooj, D.V. (1991) Prediction of fatigue life of asphalt concrete beams from fracture tests. *Journal of Testing and Evaluation,* Vol. 19, No. 3, May 1991, pp. 231-239.

Readshaw, E.E. (1974) Asphalt specifications in British Columbia for low temperature performance. *Journal of the Association of Asphalt Paving Technologists,* 42, pp. 562-581.

Reinke, G. and Dai S. (2001) Performance properties of three mixes constructed at the MnRoad test site. *Proceedings, Canadian Technical Asphalt Association,* Vol. 46, pp. 213-248.

Robertson, W.D. (1995) Using the SHRP specification to select asphalt binders for low temperature service. *Proceedings, Canadian Technical Asphalt Association,* Vol. 40, pp. 170-195.

Romero, P., Youtcheff, J., and Stuart, K. (1999) Low-temperature physical hardening of hot-mix asphalt. *Transportation Research Record: Journal of the Transportation Research Board,* 1661, 22-26.

Roy, S.D. and Hesp, S.A.M. (2001a) Fracture energy and critical crack tip opening displacement. *Proc., Canadian Technical Asphalt Association,* 46, pp. 187-214.

Roy, S.D. and Hesp S.A.M. (2001b) Low-temperature binder specification development. *Transportation Research Record: Journal of the Transportation Research Board,* 1766, pp. 7-14.

Sabbagh, A. and Lesser, A. (1998) Effect of particle morphology on the emulsion stability and mechanical performance of polyolefin modified asphalt. *Polymer Engineering and Science,* 38, pp. 707-15.

Schmidt, R.J. (1966) Discussion. *Proc. Association of Asphalt Paving Technologists,* 35, pp. 17.

Shenoy, A. (2002) Single-event cracking temperature of asphalt pavements directly from the bending beam rheometer data. *Journal of Transportation Engineering*, Vol. 128, No. 5, pp. 465-471.

Shin, E., A. Bhurke, E. Scott, S. Rozeveld, and L. Drzal. Microstructure, morphology, and failure modes of polymer-modified asphalts. *Transportation Research Record 1535,* TRB, National Research Council, Washington, D.C., pp. 61-73, 1996.

Spanoudakis, J. and Young, R.J. (1984) Crack propagation in a glass particle-filled rpoxy tesin. *Journal of Materials Science,* 19, pp. 473-486.

Stock, A.F. and Arand, W. (1993) Low-temperature cracking in polymer-modified binders. *Journal of the Association of Asphalt Paving Technologists,* 62, pp. 23-53.

Strategic Highway Research Program, Materials Reference Library (1994) Information Sheet.

Struik, L.C.E. (1978) Physical Ageing in Amorphous Polymers and Other Materials. Elsevier, Amsterdam, The Netherlands.

Sulaiman, S.J. and Stock, A.F. (1995) The use of fracture mechanics for the evaluation of asphalt mixes. *Journal of the Association of Asphalt Paving Technologists,* 64, pp. 500-533.

Tobolsky, A. and Eyring, H. (1943) Mechanical properties of polymeric materials. *Journal of Chemical Physics,* 11, p. 14.

Van der Poel, C. (1954) A general system Describing the viscoelastic properties of bitumens and their relation to routine test data. *Journal of Applied Chemistry,* 4, p. 221-236.

Van der Poel, C. (1955) Time and temperature effects on the deformation of asphaltic bitumens and bitumen-mineral mixtures. *Society of Plastics Engineering Journal,* September, 1955, pp. 47-53.

Wells, A.A. (1962) Unstable crack propagation in metals. *Proc., Crack Propagation Symposium Cranfield.* College of Aeronautics, Cranfield, England 1, pp. 210-230.

Williams JG (1984) Fracture Mechanics of Polymers. Ellis Horwood Series in Engineering Science, Ellis Horwood Publishers Ltd., Chichester, West Sussex, England.

Xing, H.S. (2003) Chemical and Physical Hardening of Asphalt Binders. Master of Science Thesis, Queen's University, Kingston, Ontario, Canada.

Young, R.J. and Beaumont, P.W.R. (1977) Failure of brittle polymers by slow crack growth. *Journal of Materials Science,* 12, pp. 684-692.

APPENDIX

DRAFT LABORATORY STANDARD FOR FRACTURE PERFORMANCE GRADING OF ASPHALT BINDERS

The attached laboratory standard for fracture performance grading of asphalt binders is a draft specification test method. It needs an actual binder specification alongside it, which can only be developed through careful testing of asphalt binders from new pavements and trial sections. Performance monitoring of these contracts will provide appropriate grading temperatures as well as limiting fracture energies in the brittle and ductile regimes, for different geographical areas and traffic levels. Such effort will eventually result in a solidification of the method and hopefully a broad acceptance by the paving industry.

The method is prepared in the format of the Laboratory Testing Manual of the Ministry of Transportation Ontario, however, it can easily be changed to AASHTO or ASTM formats if these agencies desire to adopt it.

REFERENCE:

Laboratory Standard for Fracture Performance Grading of Asphalt Binders. Test Method LS-296, Laboratory Testing Manual, Ministry of Transportation Ontario, Downsview, Ontario, Canada, August 2003.

LABORATORY STANDARD FOR FRACTURE PERFORMANCE GRADING OF ASPHALT BINDERS (DRAFT)

1. SCOPE

1.1 This standard covers the performance grading of conventional as well as modified asphalt binders at various temperatures by means of fracture mechanics-based test methods. These methods are intended to rank the onset as well as the severity of transverse stress cracking in asphalt pavements due to the combined effects of low-temperature and traffic exposure.

1.2 The determination of the binder fracture toughness (K_{Ic}) and fracture energy (G_{Ic}) properties is based in large part on ASTM method D 5045-96 *Plane-Strain Fracture Toughness and Strain Energy Release Rate of Plastic Materials,* which in turn is based on ASTM method E 399-90 *Standard Test Method for Plane-Strain Fracture Toughness of Metallic Materials.* The determinations of the critical crack opening displacement properties, COD and COD_p, is based on ASTM method E 1290 *Standard Test Method for Crack Tip Opening Displacement (CTOD) Fracture Toughness Measurement.* The determination of the specific essential work of fracture for the binder, w_e, and the specific plastic work of fracture, w_p, are based on publications in the open literature. Hence, conditions of testing and specimen configuration are similar to those found in the ASTM methods and various publications cited throughout this document. However, a number of important simplifications and modifications are made for the purpose of grading of asphalt binder materials.

1.3 Preparation and thermal conditioning requirements prior to fracture testing are specific for asphalt binders and may significantly affect performance prediction for in-service conditions.

1.4 The onset and severity of transverse and traffic related stress cracking at low temperatures are dependent on design variables such as binder content, aggregate type and gradation, pavement thickness, quality of base course, traffic levels, and probably other factors. This method is intended to rank the performance of binders but cannot fully account for mixture and pavement design variables.

1.5 The severity of transverse and traffic-related stress cracking is dependent on the aging characteristics of the asphalt binder. This method recommends a 40-hour pressure aging vessel procedure to simulate field aging so it cannot account for actual differences in aging behavior of samples exposed to in-service conditions. When a more realistic aging method becomes available it should be substituted for the pressure aging vessel procedure.

1.6 *This standard involves the handling of hot asphalt materials, hazardous solvents and the operation of potentially dangerous equipment. This standard does not address any safety problems associated with its use. The user of this standard is responsible for establishing appropriate safety practices and determining the applicability of regulatory limitations prior to use.*

2. RELEVANT DOCUMENTS

2.1 *AASHTO Standards:*

T 240 Effect of Heat and Air on Rolling Film of Asphalt (Rolling Thin-Film Oven Test).

PP 1 Standard Practice for Accelerated Aging of Asphalt Binder Using a Pressurized Aging Vessel (PAV).

2.2 *ASTM Standards:*

D 8 Standard Definitions of Terms Relating to Materials for Roads and Pavements. Annual Book of ASTM Standards, Vol. 04.03.

D 113 Standard Test Method for Ductility of Bituminous Materials. Annual Book of ASTM Standards, Vol. 04.03.

D 5045 Plane-Strain Fracture Toughness and Strain Energy Release Rate of Plastic Materials. Annual Book of ASTM Standards, Vol. 08.03.

E 399 Standard Test Method for Plane-Strain Fracture Toughness of Metallic Materials. Annual Book of ASTM Standards, Vol. 03.01.

E 616 Terminology Relating to Fracture Testing. Annual Book of ASTM Standards, Vol. 03.01.

E 1290 Standard Test Method for Crack-Tip Opening Displacement (CTOD) Fracture Toughness Measurement. Annual Book of ASTM Standards, Vol. 03.01.

3. TERMINOLOGY

3.1 *Symbols and Abbreviations*

3.1.1 Symbols:

a	Crack length, m
a'	Crack length in spacers, m

B	Specimen width in SENB or CT, m
b	Specimen thickness in DENT, m
E	Young's modulus, $N.m^{-2}$
G_{Ic}	Plane-strain fracture energy, $J.m^{-2}$
K_{Ic}	Plane-strain fracture toughness, $N.m^{-3/2}$
l	Ligament length in DENT, m
P	Load, N
P_f	Failure load, N
S	Span in three-point bending, m
T	Temperature, °C
t	Time, s
U	Energy under load versus load-line displacement diagram, J
v	Load-line displacement, m
v_p	Plastic component of load-line displacement, m
W	Specimen height in SENB or CT, m
W-a	Ligament length, m
W-a'	Ligament length in spacers, m
W_e	Essential work of fracture, J
w_e	Specific essential work of fracture, $J.m^{-2}$
W_f	Total work of fracture, J
w_f	Specific total work of fracture, $J.m^{-2}$
w_{Ie}	Plane-strain specific essential work of fracture, $J.m^{-2}$
W_p	Plastic work of fracture, J
w_p	Specific plastic work of fracture, $J.m^{-2}$
β	Plastic zone shape factor
ϕ	Calibration factor for calculating G_{Ic} from U
σ_{ty}	Tensile yield stress, $N.m^{-2}$

3.1.2 Abbreviations:

AASHTO	American Association of State Transportation Highway Officials
ASTM	American Society for Testing and Materials
COD	Crack opening displacement, m
COD_p	Plastic component of crack opening displacement, m
CT	Compact tension test geometry
CTOD	Crack tip opening displacement, m
$CTOD_p$:	Plastic component of crack tip opening displacement, m
DENT	Double edge notched tension test geometry

LTTPBIND	Long Term Pavement Performance Program binder software
PAV	Pressure aging vessel
PFA	Polyfluorinated alkoxyde
RTFO	Rolling thin film oven
SENB	Single edge notched bend specimen geometry

3.2 *Definitions:*

3.2.1 Definitions for terms related to asphalt materials are found in ASTM D 8.

3.2.2 Definitions for terms related to fracture testing are found in ASTM E 616.

3.2.3 *asphalt binder* – an asphalt-based cement that is produced from petroleum residue either with or without the addition of non-particulate organic or inorganic modifiers.

3.2.4 *asphalt modifiers* – include oils, elastomers, plastomers, reactive polymers, acids, resins, waxes, oxidation catalysts, and other additives commonly used to enhance or alter the performance of asphalt binders. This test method has not been validated for binders in which fibers or other solid particles larger than 5 μm in size are present.

3.2.5 *in-service* – refers to asphalt binder performance in the pavement as a result of the combined effects of thermal and traffic induced stresses, stress concentrations, physical aging, chemical aging, moisture, and the environment.

3.2.6 *physical aging* – refers to a process that involves the collapse of unoccupied or free volume, structure formation and possibly the crystallization of wax components and other phase transitions within the asphalt binder at low temperatures.

3.2.6.1 *Discussion* – Physical aging may affect stiffness and relaxation ability in a time-dependent manner and as such it is considered in this grading method. Some binders that are tested after only an hour of isothermal conditioning may give significantly better performance properties as compared to when they are tested after one or several days of conditioning close to the grade temperature. It is difficult to decide what an appropriate conditioning time would be for any given area but user agencies should consider the effect of isothermal conditioning on binder performance properties. For a more detailed discussion on this issue, refer to reference (1).

3.3 *Description of Terms Specific to This Standard:*

3.3.1 *crack opening displacement, COD* – refers to the distance by which the crack mouth of a sharply notched sample opens during loading. The COD relates directly to the CTOD through a geometric constant. (See ASTM method E 1290-93 for further details).

3.3.2 *crack tip opening displacement, CTOD* – the critical value refers to a measure of strain tolerance in the presence of a sharp crack close to the ductile-to-brittle transition for the asphalt binder. Critical crack tip opening displacement combines a measure of strength in the presence of a sharp crack, as given by K_{Ic}, with a measure of stiffness, as given by E, and a measure of relaxation ability, as given by the yield stress in tension, σ_{ty}. See 3.3.13 for additional definitions.

3.3.3 *essential work of fracture, w_e* – refers to the work required to fracture a unit surface area of asphalt binder under essentially ductile, plane-stress conditions. See references (2-3) and further references therein for additional discussions on the essential work of fracture method.

3.3.4 *ductile-to-brittle transition temperature*, $T_{ductile\text{-}to\text{-}brittle}$ – refers to the temperature at which a lower limit for a critical fracture property is reached.

3.3.5 *grade temperature, T_{grade}* – refers to the temperature that is 10°C below the ductile-to-brittle transition temperature as measured in the laboratory in either SENB or CT at a rate of 0.01 mm/s. The grade temperature is considered to be the minimum acceptable service temperature for the binder.

3.3.6 *test temperatures* – refers to the temperatures at which the critical fracture properties are measured and ranked.

3.3.7 *plane-strain fracture toughness, K_{Ic}* – refers to a measure of material strength in the brittle state in the presence of a sharp crack. See 3.3.13 for additional definitions.

3.3.8 *plane-strain essential work of fracture, w_{Ie}* – refers to the work required to fracture a unit surface area of asphalt binder under essentially ductile, plane-strain or "near plane-strain" conditions. See references (2-3) for further discussions on the essential work of fracture method.

3.3.9 *plane-strain fracture energy, G_{Ic}* – refers to a measure of material toughness in the brittle state in the presence of a sharp crack. Fracture energy is a toughness parameter based on the energy required to fracture. It combines a measure of strength, as given by K_{Ic}, with a measure of stiffness, as given by Young's modulus, E. See 3.3.13 for additional definitions, and see references (4-9) for additional discussions on the use of the plane-strain fracture energy as a grading property for low-temperature failure in asphalt binders.

3.3.10 *plastic work of fracture term, βw_p* – refers to the plastic work term for essentially ductile failure. The β factor is a geometry constant that depends on the shape of the ductile zone on either side of the notch, and w_p is the plastic work done during failure in areas away from the fracture surface. See references (2-3) and further references therein for additional discussions on the β factor and the plastic work term.

3.3.11 *specification temperature, T_{spec}* – refers to the design temperature of the pavement.

3.3.11.1 *Discussion*: At the specification temperature, the risk level as given by the LTPPBIND® software, available from the United States Federal Highway Administration, should be acceptable to avoid repeated exposure to temperatures that can lead to catastrophic pavement failures in terms of transverse and traffic-induced stress cracking. The LTPPBIND® software program provides statistical estimates for how often a pavement surface can be expected to reach a given temperature in a given geographical location. However, the software does not address in any way the effects of traffic-induced cracking, which is likely a significant factor in the onset of transverse cracking in thin pavements, in truck lanes, in truck hill-climbing lanes, or close to intersections, at temperatures warmer than those generally accepted as safe in terms of weather statistical data alone.

3.3.12 *time-temperature shift* – refers to the temperature shift that is used to translate laboratory grade temperatures, determined at relatively high speeds, to minimum service temperatures in the pavement, which are determined by slow rates of thermal contraction. In this standard a -10°C shift is used to convert grade temperatures to minimum service temperatures.

3.3.12.1 *Discussion*: The 10°C temperature shift accounts for a time shift of a factor 120 which means that tests done in one minute at the test temperature should give an equivalent result to tests done in two hours (120 minutes) at 10°C below the test temperature. For a more detailed discussion on this issue, refer to references (1,8).

3.3.13 See ASTM methods D 5045-96, E 399-90, E 616-89, and E 1290-93 for additional explanation of definitions.

4. SUMMARY OF LABORATORY STANDARD

4.1 The test standard allows for the determination of a simple grade temperature above which transverse cracking is largely prevented in pavements that are expected to fail from distress other than fracture (Method A). Or, as an alternative, it allows for a more comprehensive performance grading, involving a full set of fracture mechanics-based property evaluations below and above the brittle-to-ductile transition temperature (Method B).

4.2 Method A involves the loading of a sharply notched asphalt binder specimen in single edge notched three point bending (SENB) or in notched compact tension (CT), while monitoring the load, P, and load-line displacement, v. The load versus the load-line displacement data is used to determine the plastic component of the displacement, v_p. The temperature at which this plastic component nearly disappears (i.e., purely brittle failure is approached) is used to determine a simple grade temperature for asphalt binders that can be used in pavements which are primarily expected to fail through forms of distress other than fracture. Due to the high rate of loading employed in the grading test method as compared to the rate at which the pavement contracts during a typical cold winter night, the temperature at which the binder becomes brittle is shifted to colder temperatures by 10°C to obtain the grade temperature for the binder. Above this grade temperature the pavement is not expected to show gross low-temperature fracture. If the grade temperature falls below the minimum design temperature for the pavement, then the binder passes the grading test. Conversely, if the grade temperature falls above the minimum design temperature, then the binder fails the grading test. The low-temperature risk levels for the minimum design temperature are obtained from the LTTPBIND® temperature database as available from the United States Federal Highway Administration.

4.3 Method B involves the loading of sharply notched asphalt binder samples in either SENB or CT as well as the loading of samples in double edge notched tension (DENT). In the ductile-to-brittle temperature regime, the load-line displacement at failure, v, or the crack opening displacement at failure, COD, is used to calculate the plastic component of the load-line displacement, v_p, or the plastic component of the crack opening displacement, COD_p. The temperature at which either the v_p or the COD_p nearly disappears (i.e., purely brittle failure is approached) is used as the ductile-to-brittle transition temperature. In the same way as for Method A, due to the relatively high rate of loading employed, the ductile-to-brittle temperature in Method B is shifted to colder temperatures by 10°C to obtain the grade temperature. The low-temperature risk levels for the minimum design temperature are also obtained from the LTTPBIND® temperature database. If the grade temperature falls below the design temperature, then the binder passes the grading test. Conversely, if the grade temperature falls above the design temperature, then the binder fails the grading test. In addition, Method B also evaluates material properties in the brittle and ductile regimes. In the brittle temperature regime, the load at failure is used to calculate the fracture toughness, K_{Ic}, and the area under the load versus load-line displacement diagram is used to calculate the fracture energy, G_{Ic}. Finally, in the ductile regime, the total work of fracture, W_f, in a DENT test is used to determine the specific essential work of fracture, w_e, and the specific plastic work of fracture, w_p.

4.4 In both Methods A and B, testing is conducted before and after thermal conditioning (i.e., physical aging) to determine load versus load-line displacement data, crack tip opening displacements, fracture toughness, fracture energies, essential works of fracture, and plastic works of fracture, at specified temperatures and rates of loading. If significant losses occur in the grading properties after thermal conditioning, then the binder must be classified in a lower grade.

4.5 A lower limit on the fracture energy, G_{Ic}, in the brittle regime may be used to control thermal and traffic-induced fatigue cracking (Method B). It is believed that cracks initiated by this fatigue-type distress mechanism can add to the severity of transverse stress cracking at lower temperatures in subsequent winters.

4.6 Lower limits on the specific essential work of fracture, w_e, and the specific plastic work of fracture, w_p, at close to 0°C may be used to control load-induced cracking caused by spring-thaw related distress (Method B). It is likely that cracks initiated by this fatigue-type distress mechanism can also add to the severity of transverse stress cracking at lower temperatures in subsequent winters.

4.7 Lower limits on the specific essential work of fracture, w_e, and on the specific plastic work of fracture, w_p, at a temperature close to the expected average daily summer pavement temperature may be used to control load-induced cracking caused by traffic (Method B). It is likely that cracks initiated by this distress mechanism can also add to the severity of transverse stress cracking at lower temperatures in subsequent winters. This distress can be particularly severe for relatively thin pavements that take a significant amount of heavy traffic.

5. SIGNIFICANCE AND USE

The fracture properties of asphalt binders are strong functions of test temperature and rate, conditioning temperature and time, binder composition, and manufacturing method. A lower limit may be set on the plasticity as measured by the amount of plastic deformation at failure, v_p, or the plastic component of the crack opening displacement, COD_p, in a sharply notched asphalt binder specimen. Such a lower limit will accommodate shrinkage strain in the pavement in order to limit catastrophic failures due to cold temperature cracking. Lower limits may be set on fracture energies in the brittle and/or ductile states in order to control thermal and traffic-related fatigue cracking which may manifest itself at a later date in the form of transverse cracking. A limit may be set on the deterioration of these properties after a specified period of conditioning at the test temperature in order to control the effects of physical aging. Background information regarding the development of these specification tests for asphalt binders and how they differ from other low-temperature grading methods may be found in reference (9).

6. APPARATUS AND FIXTURES

6.1 *Testing Machine* – A constant rate of displacement device shall be used that is capable of generating rates of displacement varying from 0.001 mm/s to 100 mm/min. The set rate of displacement shall fluctuate by no more than ± one percent in time. The maximum stroke for the instrument(s) shall be 2 cm for SENB and CT tests and 20 cm for DENT tests. Commercial test frames specifically designed for the testing of asphalt binder samples in direct tension are suitable for the tasks described in this method provided that: (1) the low-temperature bath or environmental chamber can accommodate the test fixtures, (2) the maximum stroke requirement is met, and (3) the tolerances on strain rate and accuracy of displacement measurement fall within the specified limits.

6.2 *Fixtures* – The following sections specify the dimensions for the three-point bend (SENB), compact tension (CT), and double edge notched tension (DENT) fixtures. These specify dimensions only and not the actual design so that, provided that the tolerance and stiffness requirements are met, all three tests may be combined into one single fixture design. Such a design can do the individual tests with only minor changes in the positioning of the loading pins.

6.2.1 *SENB Fixtures* – For SENB specimen testing, a rigid three point bend fixture with a span, S, of 10.0 ± 0.1 cm is required. The fixture shall be similar in design to that depicted in Figure 1, for which the specified dimensions and tolerances are given in Table 1.

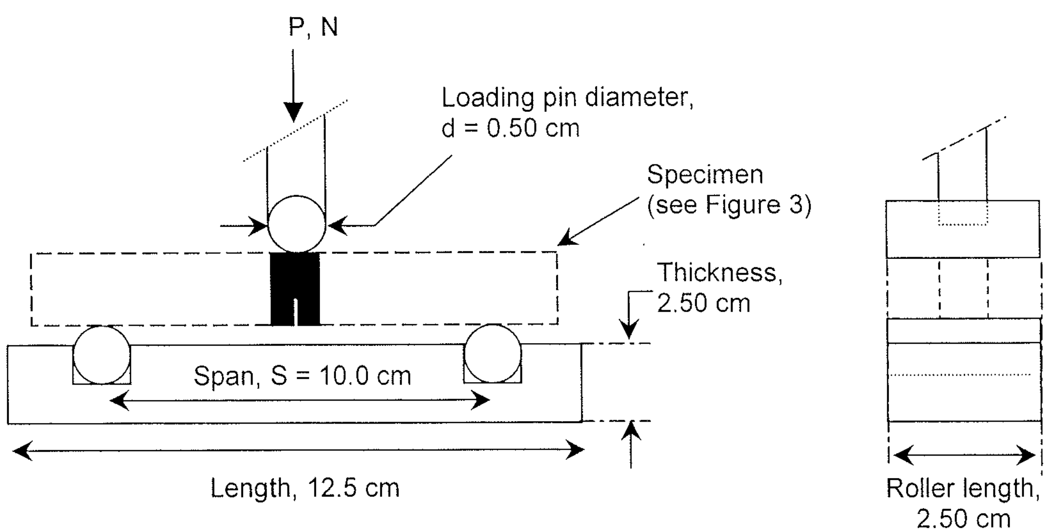

Figure 1 Bending rig for SENB test.

The rig shall be made from stainless steel or any other suitable metal that provides equivalent or better stiffness.

TABLE 1 SENB Rig Dimensions and Tolerances

Dimension	Size, cm	Tolerance, cm
Length	12.5	± 0.25
Thickness	2.50	± 0.05
Loading pin diameter, d	0.50	± 0.01
Loading pin length	2.50	± 0.05
Loading span, S	10.0	± 0.10

6.2.2 *CT Fixtures* – For tests employing the CT geometry, two identical clevises are used that load both sides of the sample through pins. The loading pins and clevises should allow for some rotation of the sample during testing. The fixtures shall be similar in design as that depicted in Figure 2, of which the specifications and tolerances are given in Table 2.

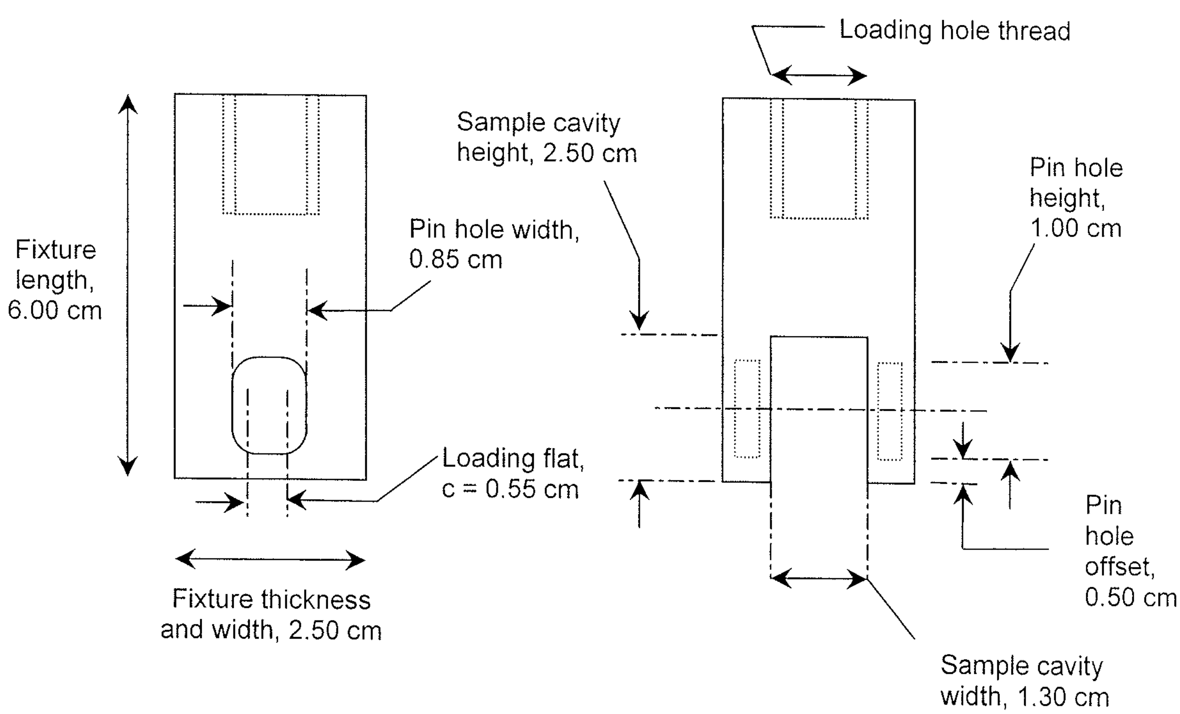

Figure 2 Clevis design for CT test.

The clevis design shall conform to the dimensions and tolerances as listed in Table 2. The loading hole thread shall be adapted to fit the load transfer rods of the testing machine. The fixture shall be made from stainless steel or any other suitable metal that provides equivalent or better stiffness.

TABLE 1 CT Clevis Dimensions and Tolerances

Dimension	Size, cm	Tolerance, cm
Fixture length	6.00	± 0.06
Fixture thickness and width	2.50	± 0.05
Loading flat, c	0.55	± 0.01
Pin hole width	0.85	± 0.01
Pin hole height	1.00	± 0.01
Pin hole offset	0.25	± 0.01
Sample cavity width	1.30	± 0.03
Sample cavity height	2.50	± 0.05

6.2.3 *DENT Fixtures* – For the essential work of fracture test (Method B), the sample is loaded in regular direct tension through a set of loading pins or hooks that assure precise alignment of the sample during the test. The fixtures for the CT test may be used to load the DENT specimen (see Figure 2 Clevis design for CT test).

6.3 *Displacement Measurement* – A load-line displacement measurement must be obtained to assure sufficient accuracy of the G_{Ic} and w_e properties and a crack mouth opening displacement must be obtained to assure sufficient accuracy of the *CMOD* and *CTOD* values. The displacement may either be measured through the crosshead movement of the test machine or from a separate displacement transducer positioned directly behind or under the loading fixtures. The accuracy of all displacement measurements shall be better than ± 0.5 μm.

6.4 *Load Measurement* – The sensitivity of the load sensor and recording electronics shall allow the load, P, to be measured at any point in time during the test within an accuracy of ± one percent. The load sensor shall have a nominal maximum force range of ± 500 N.

6.5 *Temperature Control* – The samples shall be conditioned at 6°C above the specification temperature prior to testing. The temperature of the samples shall fluctuate by no more than ± 0.5°C during this conditioning period. The samples are tested at the specified test temperatures which shall fluctuate by no more than ± 0.5°C.

7. SPECIMEN CONFIGURATIONS, SIZES AND PREPARATION

7.1 *Specimen Configurations and Sizes:*

7.1.1 The single edge notched bend (SENB) geometry shall be used with aluminum end pieces (inserts). Contact surfaces on the aluminum inserts shall be sand-blasted and free of any greasy substances in order to assure sufficient adhesion with the asphalt binder. The design of the SENB fracture specimen is given in Figure 3.

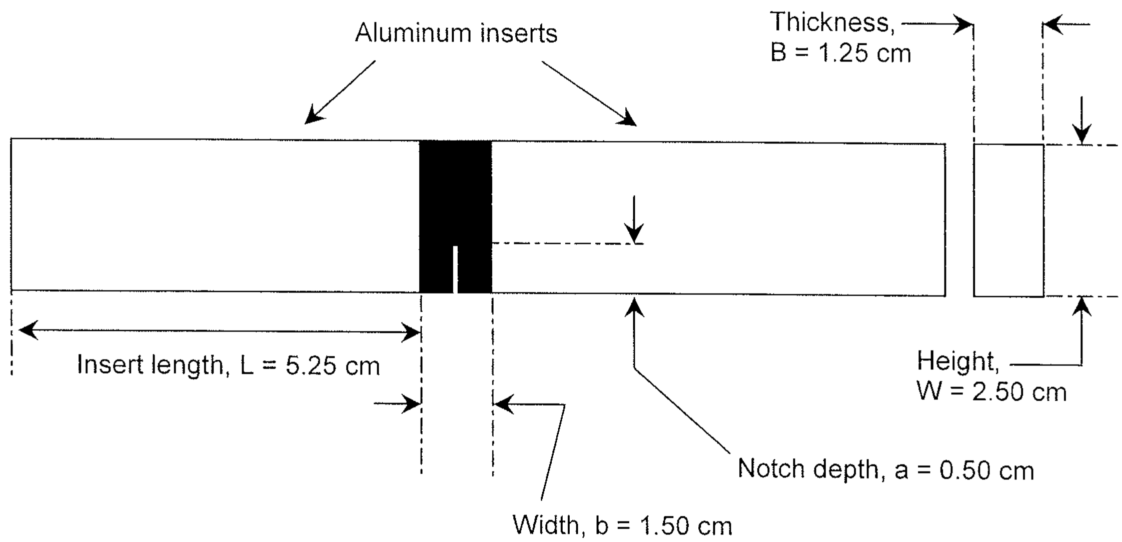

Figure 3 SENB specimen geometry.

The specimen dimensions shall conform to the dimensions and tolerances as listed in Table 3.

TABLE 3 SENB Specimen Dimensions and Tolerances

Dimension	Size, cm	Tolerance, cm
Specimen height, W	2.50	± 0.05
Specimen width, b	1.50	± 0.03
Specimen thickness, B	1.25	± 0.03
Notch depth, a	0.50	± 0.01
Insert length, L	5.25	± 0.05

7.1.2 The compact tension (CT) geometry shall be used with aluminum end pieces (inserts). Contact surfaces on the aluminum inserts shall be sand-blasted and free of any greasy substances in order to assure good adhesion with the asphalt binder. The design of the CT fracture specimen is given in Figure 4.

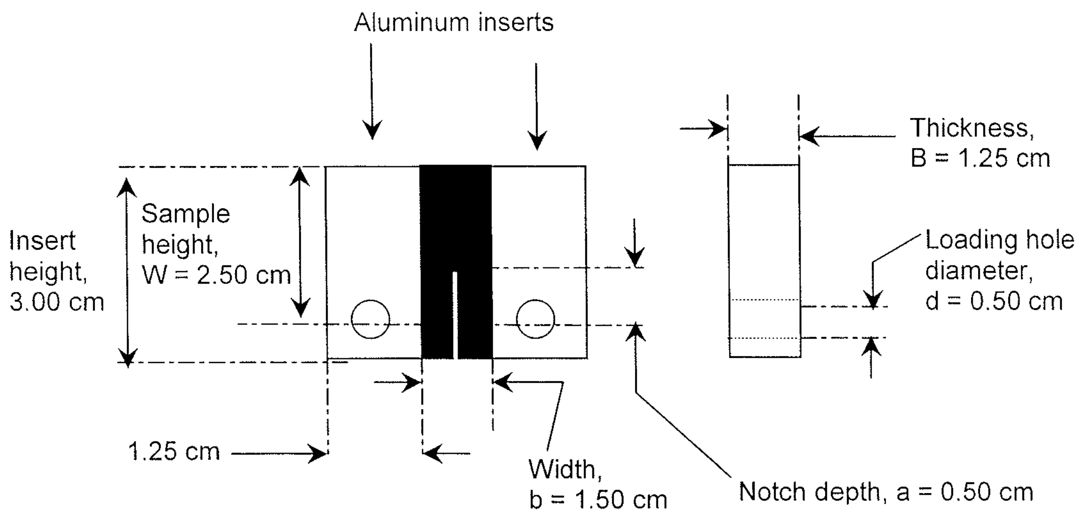

Figure 4 CT specimen geometry.

The specimen shall conform to the dimensions and tolerances as listed in Table 4.

TABLE 4 CT Specimen Dimensions and Tolerances

Dimension	Size, cm	Tolerance, cm
Specimen height, W	2.50	± 0.05
Specimen thickness, B	1.25	± 0.03
Specimen width, b	1.50	± 0.03
Notch depth, a	0.50	± 0.01
Insert width	1.25	± 0.03
Insert height	3.00	± 0.06
Loading hole diameter, d	0.50	± 0.01

The specimen height, W, shall be measured from the top of the specimen to the center point of the loading hole in the aluminum inserts. The notch depth, a, shall be measured upward from the center point of the loading hole in the aluminum inserts.

7.1.3 The double edge notched tension (DENT) geometry shall be used with aluminum end pieces (inserts) that attach to the test frame loading fixtures without causing excessive deformation or stress concentrations around the loading points in the asphalt binder. The design of the DENT fracture specimen shall be similar to that in Figure 5.

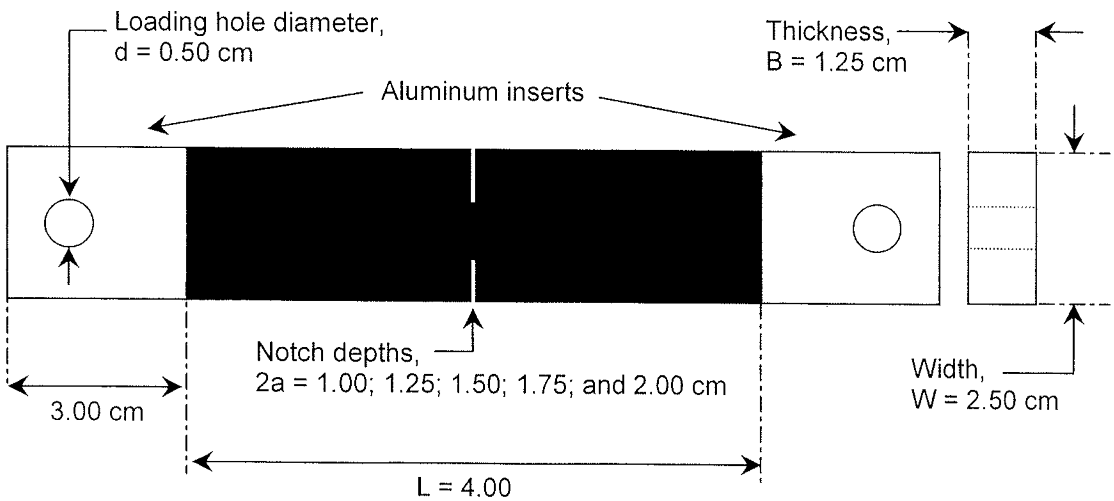

Figure 5 DENT specimen geometry.

The specimen dimensions shall conform to the dimensions and tolerances as listed in Table 5.

TABLE 5 DENT Specimen Dimensions and Tolerances

Dimension	Size, cm	Tolerance, cm
Specimen width, W	2.50	± 0.05
Specimen length, L	4.00	± 0.08
Total notch depths, 2a	1.00, 1.25, 1.50, 1.75, and 2.00	± 0.01
Aluminum insert thickness, B	1.25	± 0.03
Loading hole diameter, d	0.50	± 0.01

7.2 *Specimen Preparation:*

7.2.1 *Binder Aging* – Asphalt binders shall be aged by rolling thin film oven (RTFO) and successive pressure aging vessel (PAV) procedures (AASHTO T 240 and PP 1). The time and temperature for the RTFO procedure shall be as specified in AASHTO T 240. It is recommended that the asphalt be aged for 40 hours in the PAV at a temperature and pressure as specified in AASHTO PP 1. The binders obtained after aging shall be heated for a sufficient amount of time at 160 ± 5°C to ensure that they readily flow when dispensed from the container. The heating temperature may be raised to a maximum of 180°C to provide a low enough viscosity, but care should be taken to prevent overheating. The binder is homogenized by vigorous stirring after a minimum of one hour of heating, which is repeated just prior to use. Air entrapped during the PAV aging procedure or during stirring shall be removed in a vacuum oven.

7.2.2 *Mold Assembly* – The molds for making SENB, CT, and DENT specimens shall be assembled from aluminum inserts and spacers. The spacers and bottom of each mold shall be wrapped in a non stick PFA fluorocarbon release film to prevent sticking of the asphalt binder to the aluminum. The film is available under the Teflon® PFA trademark from DuPont. The preferred thickness of the non stick PFA film is 12.5 μm (LP 50 grade). Alternatively, the mold spacers can be made entirely from thick Teflon® PFA sheet, which may simplify the task of assembling the mold. The general configuration shall be similar to that shown in Figure 6 for one SENB specimen. A series of such assemblies may be clamped together in a suitable device to make more than one sample at once.

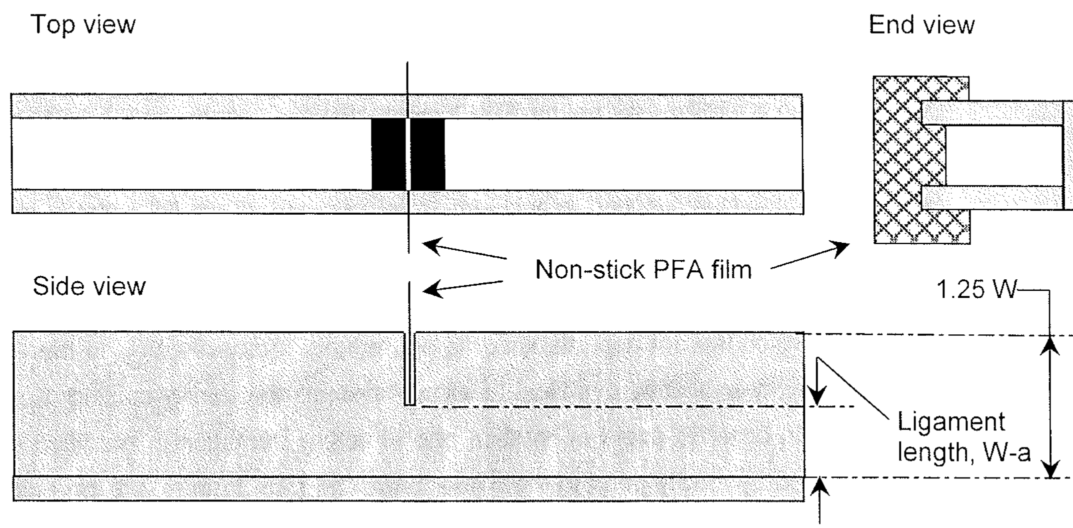

Figure 6 SENB mold assembly for specimen preparation.

The shaded parts represent the aluminum spacers and bottom, whereas the crosshatched part represents the 25 μm-thick Teflon® PFA film that shall produce the sharp notch. The film produces a thin slit notch, of depth a, in the asphalt binder after it is removed at low temperatures. The dimensions and permitted tolerances for the mold parts are specified in Table 6.

TABLE 6 SENB Mold Spacer Dimensions and Tolerances

Dimension	Size, cm	Tolerance, cm
Spacer height, 1.25 W	3.13	± 0.06
Spacer length	12.00	± 0.24
Spacer thickness, 0.5 B	6.25	± 0.15
Crack length in spacer, a'	1.13	± 0.02
Notch width	0.05	± 0.01
Spacer ligament length, 1.25 W – a'	2.00	± 0.04

The notch in the spacers shall be cut open with a sharp razor blade after which a piece of 25.0 ± 2.5 μm PFA release film (LP 100 grade) is inserted in a straight manner (the crosshatched part in Figure 6). If solid Teflon® spacers are used, then the film can be inserted directly without the need for cutting. The film is used to produce a sharp slit notch in the SENB asphalt specimen. Care shall be taken to make sure that the film reaches the bottom of the notch in both spacers and that it produces a straight demarcation at the desired depth within the cavity. The CT and DENT molds are assembled in a similar way as the SENB mold. However, for these the SENB inserts are replaced by CT and DENT inserts, while, simultaneously, for the DENT configuration an additional notch is introduced to accommodate a second 25 μm PFA film at the bottom of each spacer.

7.2.3 *Asphalt Pouring* – The assembled mold shall be heated on a hot surface to 160 ± 5°C, after which the hot asphalt binder is poured into the cavity around the PFA release film. The cavity is slightly overfilled to allow for shrinkage during cooling. For the DENT specimen, in order to avoid orientation and structure formation in modified binders, the cavity is filled by slowly pouring the binder back and forth from end to end until the mold is slightly overfilled. Once the mold is full, the assembly is left on the hot plate for at least 10 minutes after which the hot plate is turned off. It is then allowed to cool in a gradual manner to room temperature.

7.2.4 *Mold Disassembly* – Once the samples have reached room temperature, the mold is placed in a freezer or low-temperature bath at the conditioning temperature. The mold shall be disassembled and the PFA fluorocarbon film removed after at least half an hour at the conditioning temperature. Once the samples are removed from the mold, the fracture properties can be determined after the specified conditioning times have passed.

8. GENERAL PROCEDURES

8.1 *Method A – Simple Fracture Mechanics-Based Performance Grading.* The ductile-to-brittle transition for an appropriately aged, conditioned, and sharply notched sample shall be used as the only acceptance criterion for a given binder in a given climatic area.

8.1.1 *Number of Tests* – Fracture tests at a specified temperature and rate of loading shall be repeated a minimum of three times.

8.1.2 *Specimen Geometry* – The user agency shall specify either the single edge notched bend (SENB) or compact tension (CT) geometry for the determination of a simple grade temperature.

8.1.3 *Sample Conditioning* – Sample conditioning prior to testing can significantly alter the grading properties and shall therefore be specified by the user agency. It is recommended that the aged asphalt binders be tested after conditioning for 1 and 24 hours at a temperature that is 6°C warmer than the minimum pavement design temperature. Just prior to testing, the sample shall be equilibrated at the test temperatures for 30 minutes. The temperature of the samples shall fluctuate by no more than ± 1.0°C during conditioning periods, and the conditioning times shall be within ± 5 minutes of the specified times. After the ductile-to-brittle transition temperatures for the two conditioning times are compared, the user agency may accept the binder in the intended grade class or in a lower grade class. See references (8,9) for further details.

8.1.4 *Loading Rate and Test Temperatures* – The loading rate in the SENB and CT tests shall be kept at 0.01 mm/s and shall vary by no more than ± one percent during and in between tests. The test temperatures shall be specified by the user agency and shall vary by no more than ± 0.5°C. The temperatures shall cover a range so as to yield both purely brittle failure (i.e., complete linearity) as well as a limited degree of ductility followed by brittle failure (see Figure 7).

8.1.5 *Ductile-to-Brittle Transition* – The ductile-to-brittle transition is determined by fracturing binder specimens at several different temperatures that provide brittle failure both with and without a limited degree of ductility. Ductility in this context is defined as a non-linear load-displacement curve or load-crack opening displacement curve. Brittle failure is defined as a drop in load accompanied by a continuous increase in crack opening displacement. Figure 7 provides an example of the types of load-displacement curves that are to be obtained in SENB. Similar curves are obtained in CT, except that for these the CMOD-control provides a more stable crack growth and hence gradual decrease in load. If ductility is not observed at any of the specified test temperatures, then the binder is tested at progressively warmer temperatures until ductile failure is obtained in a minimum of three replicate tests.

8.1.6 *Plastic Component of Displacement* – A lower limit is set on the plastic component of the displacement, v_p, to determine the ductile-to-brittle transition temperature. The property v_p is determined by drawing a best straight line, tangent through the origin of the load-displacement curve, excluding any startup effects, and horizontally shifting this line to intercept the maximum load point. This generates an offset line which distance from the tangent line through the origin provides the plastic component of the displacement, v_p. The broken lines in Figure 7 provide an example of how this is accomplished. The property v_p shall be measured with an accuracy equal to or better than ± 0.01 mm.

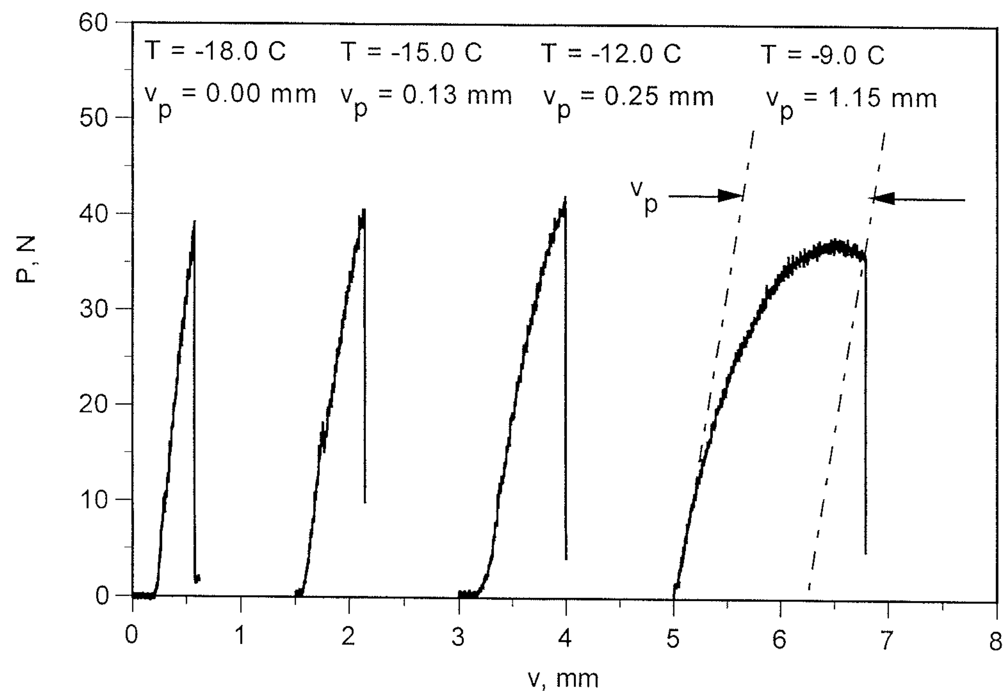

Figure 7 Typical load-displacement curves in SENB grading tests.

The user agency shall specify what limiting v_p constitutes a ductile or brittle failure. It is recommended that a v_p above 0.25 mm indicates ductile failure and that a v_p below 0.25 mm indicates brittle failure in both SENB and CT. The temperature at which the limiting v_p is either reached or exceeded in all three repeat samples to be tested is reported as the ductile-to-brittle transition temperature, $T_{ductile\text{-}to\text{-}brittle}$.

8.2 *Method B – Comprehensive Fracture Mechanics-Based Performance Grading.* The ductile-to-brittle transition temperature for an appropriately aged, conditioned, and sharply notched sample shall be used as the main acceptance criterion for a given binder in a given climatic area. In addition, lower limits are set on the fracture energy in the brittle regime, G_{Ic}, and on the essential and plastic works of fracture in the ductile regime, w_e and w_p, in order to control low-temperature and traffic-induced fatigue cracking in the pavement.

8.2.1 *Number of Tests* – Fracture tests in single edge notched bending (SENB) or compact tension (CT) at each specified temperature and rate of loading shall be repeated at least three times. Fracture tests in double edge notched tension (DENT) shall be repeated at least two times.

8.2.2 *Specimen Geometry* – The user agency shall specify either the SENB or CT geometry for the determination of the grade temperature. The same geometry shall be used to determine the fracture energy in the brittle state. The DENT geometry shall be used for the determination of the fracture energies in the ductile state.

8.2.3 *Critical Properties* – The user agency shall specify whether to use a lower limit on the plastic component of either the load-line displacement or the crack opening displacement for the determination of the grade temperature. For SENB these two properties are different, yet the grade temperatures may not differ by much. The bending geometry will require the use of an additional set of knife edges across the crack mouth as well as a crack opening gage, both meeting the specifications as set forth in ASTM E 399-90 and references therein, in order to measure the crack opening properties. Any commercial crack opening gage that is able to measure the crack opening displacement property with an accuracy of equal to or better than ± 0.01 mm would be acceptable. However, in CT both displacement properties are the same, since for this geometry the load-line displacement is equal to the crack opening displacement. Agencies that specify the CT geometry may use the crosshead displacement measurement of the test frame to monitor the crack opening displacement. The user agency shall specify lower limits on the fracture energy in the brittle state, G_{Ic}, and the specific essential and plastic works of fracture in the ductile state, w_e and w_p, respectively.

8.2.4 *Sample Conditioning* – Sample conditioning prior to testing can significantly alter the grading properties and shall therefore be specified by the user agency. It is recommended that for the determination of the ductile-to-brittle temperature, utilizing either the SENB or CT test, the aged asphalt binders are tested after conditioning for 1 and 24 hours at a temperature that is 6°C warmer than the specification temperature. Just prior to testing, the sample shall be equilibrated at the test temperature for 30 minutes. The temperature of the samples shall fluctuate by no more than ± 1.0°C during conditioning periods and the conditioning times shall be within ± 5 minutes of the specified times. After the ductile-to-brittle transition temperatures for the two conditioning times are compared, the user agency may accept the binder in the intended grade class or in a lower grade class. For the determination of the essential work of fracture, w_e, and plastic work of fracture, w_p, the appropriately aged binder specimens shall be conditioned at the actual test temperature for a minimum of 24 hours. The temperature of the samples shall fluctuate by no more than ± 1.0°C during the conditioning periods, and the conditioning times shall be within ± five minutes of the specified time.

8.2.5 *Loading Rate and Test Temperatures* – The loading rate in the SENB and CT tests shall be kept at 0.01 mm/s and shall vary by no more than ± one percent during and between tests. The test temperatures for the determination of the ductile-to-brittle transition in SENB or CT shall be specified by the user agency. The temperatures for the SENB and CT tests shall be chosen so as to yield both purely brittle failure (i.e., complete linearity) as well as a limited degree of ductility followed by brittle failure. The test temperatures shall vary by no more than ± 0.5°C from the specified temperatures during and between tests. The loading rates and test temperatures for the DENT test shall be specified by the user agency. The loading rates and temperatures for the DENT test shall be selected so as to yield completely ductile failure (see Figure 9).

8.2.6 *Ductile-to-Brittle Transition* – The ductile-to-brittle transition is determined by fracturing binder specimens at several different temperatures that need to show brittle failure both with and without a limited degree of ductility. Ductility in this context is defined as a non-linear load-displacement curve or load-crack opening displacement curve. Brittle failure is defined as a drop in load accompanied by a continuous increase in crack opening displacement. Figures 7 and 8 provide examples of the types of curves that are to be obtained in SENB for load versus load-line displacement and load versus crack opening displacement, respectively. Similar curves are obtained in CT, except that for these the COD-control provides a more stable crack growth and hence gradual decrease in load and increase in COD. If ductility is not observed at any of the specified test temperatures, then the binder is tested at the next warmer temperature until ductile failure is obtained in a minimum of three replicate tests. The user agency shall set a lower limit on either the plastic component of the load-line displacement, v_p, or on the plastic component of the crack opening displacement, COD_p, at peak load.

8.2.7 *Plastic Component of Load-Line Displacement, v_p* – The plastic component of the load-line displacement, v_p, is determined according to the procedure described in 8.1.6.

8.2.8 *Plastic Component of Crack Opening Displacement, COD_p* – The plastic component of the crack opening displacement, COD_p, is determined according to the procedure depicted in Figure 8. A best straight line is drawn tangent through the origin of the load-crack opening displacement curve, excluding any startup effects, and is horizontally shifted to intercept with the maximum load point. This generates an offset line, the distance of which from the tangent line through the origin provides the plastic component of the crack opening displacement, COD_p. The broken lines in Figure 8 provide an example of how this is accomplished. The property COD_p shall be measured with an accuracy that is equal to or better than ± 0.01 mm.

8.2.9 *Ductile-to-Brittle Transition Temperature,* $T_{ductile\text{-}to\text{-}brittle}$ – The user agency shall specify what limiting v_p or COD_p constitutes a ductile or brittle failure. It is recommended that a v_p or COD_p above 0.25 mm indicates ductile failure and that a v_p or COD_p below 0.25 mm indicates brittle failure in both SENB and CT. The temperature at which the limiting v_p or COD_p is either reached or exceeded in all three repeat samples to be tested is reported as the ductile-to-brittle transition temperature, $T_{ductile\text{-}to\text{-}brittle}$.

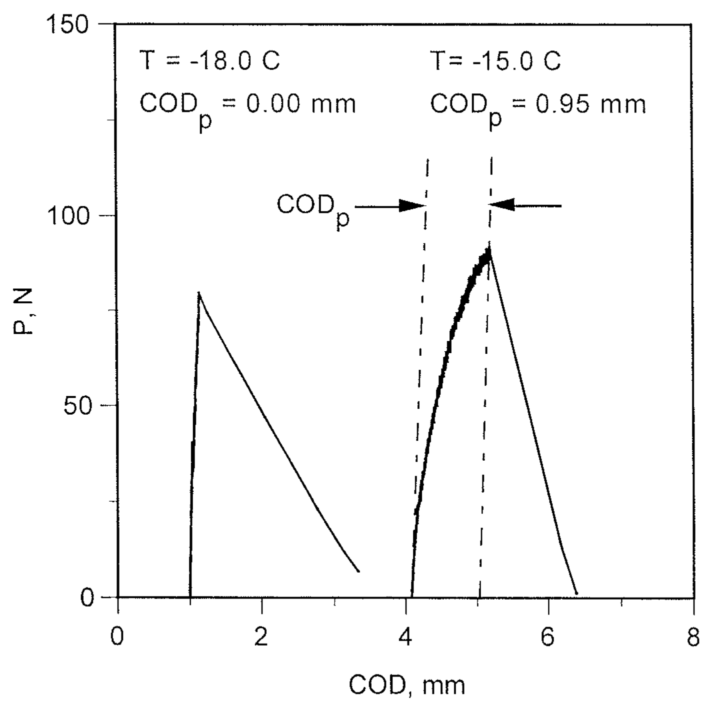

Figure 8 Typical load-crack opening displacement curves in SENB grading tests.

8.2.10 *Brittle Failure* – The fracture energy in the brittle temperature regime, G_{Ic}, is determined in order to control the severity of thermal and traffic-induced fatigue cracking. The user agency shall specify at which temperature(s) the fracture energy is to be determined. The test temperature shall be selected so as to yield complete linearity for the load versus load-line displacement record. It is recommended that the fracture energy is determined at 6°C above the minimum pavement design temperature. The fracture energy in the brittle state is determined from an accurate determination of the area under the load versus load-line displacement record. See Section 9.2.2 for further details on data analysis and interpretation.

8.2.11 *Ductile Failure* – The essential work of fracture, w_e, and plastic work of fracture, w_p, in the ductile temperature regime are determined in order to control the severity of thermal and traffic-induced fatigue cracking. The user agency shall specify the temperature and rate of loading for the double edge notched tension (DENT) test. It is recommended that tests are conducted at 0°C for pavements in areas where freeze-thaw conditions are prevalent. It is recommended that tests be conducted at the historical average daily pavement temperature in all areas where there is likely to be fatigue related distress. It is recommended that tests be conducted at a higher temperature in all areas where there is likely to be fatigue-related distress during short periods of extreme summer temperatures.

8.2.11.1 *Specimen Geometry* – The specimen geometry employed for the determination of the essential and plastic works of fracture shall be as depicted in Figure 5. The total notch depths, 2a, shall be 1.00, 1.25, 1.50, 1.75, and 2.00 cm, corresponding to ligament lengths, W-a, of 1.50, 1.25, 1.00, 0.75, and 0.50 cm, respectively.

8.2.11.2 *Load Versus Load-Line Displacement Data* – The load versus load-line displacement data shall be obtained at the specified temperatures and rates. The shapes of the curves, for all ligament lengths within one binder set must be similar in appearance, but the general appearance may be different between different sets. Figure 9 provides examples of two sets of data for different binders that individually show self-similar appearance but which are distinctly different for each. If the appearance of the load versus load-line displacement curve changes between samples with different ligament lengths, then the test shall be reported as invalid.

8.2.11.3 *Load Versus Load-Line Displacement Area* – The area under the load versus load-line displacement curve is determined for each ligament length and this value is reported as the total work of fracture, W_f, in Joules. The total works of fracture for all ligament lengths are used in 9.2.3 to determine the specific essential work of fracture, w_e, and the specific plastic work of fracture, w_p, for the binder being graded.

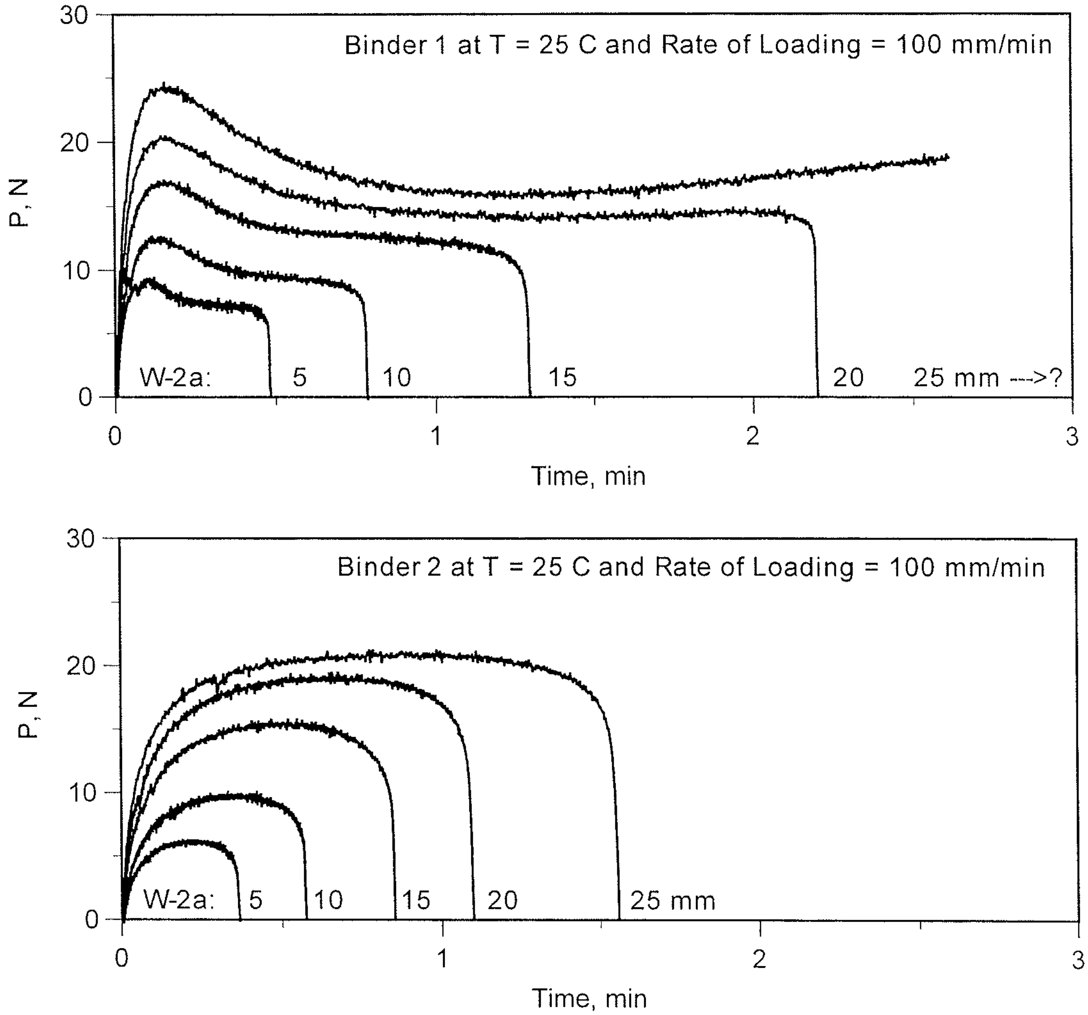

Figure 9 Typical load-displacement curves for essential work of fracture testing of two modified binders that individually show self-similar behavior yet differ between each.

9. CALCULATION AND INTERPRETATION OF RESULTS

9.1 *Method A – Simple Fracture Mechanics-Based Performance Grading.* To calculate the minimum permissible in-service temperature of a binder, T_{grade}, the ductile-to-brittle transition temperature, $T_{ductile\text{-}to\text{-}brittle}$, as determined in 8.1.6, is shifted lower by 10°C to account, more or less, for the difference in rate of loading between laboratory and field conditions:

$$T_{grade} = T_{ductile\text{-}to\text{-}brittle} - 10 \qquad (9.1)$$

The pavement is not likely to show severe transverse cracking provided that it remains above this limiting temperature for most of its life. The binder shall pass the grading test if T_{grade} is colder than the specified minimum design temperature for the pavement, T_{spec}. The binder shall fail the grading test if T_{grade} is warmer than the specified minimum design temperature for the pavement. The user agency shall specify what losses in grade temperature are acceptable for samples conditioned for 24 hours. It is recommended that binders that lose more than 3°C in their grade temperature after 24 hours of conditioning are only accepted with caution in a lower grade class. It has been shown that some poor quality binders can lose more than 10°C after three days of conditioning (9). The user agency shall use the LTPPBIND® software program for the selection of an acceptable degree of risk in the determination of the minimum pavement design temperature. See 3.3.10 for further details.

9.2 *Method B – Comprehensive Fracture Mechanics-Based Performance Grading.* The comprehensive performance grading involves the determination of a simple grade temperature as well as the fracture energies in both the brittle and ductile states.

9.2.1 *Grade Temperature* – For calculating the minimum permissible in-service temperature of a binder, T_{grade}, the ductile-to-brittle transition temperature, $T_{ductile\text{-}to\text{-}brittle}$, as determined in 8.2.9, is shifted lower by 10°C to account, more or less, for the difference in rate of loading between laboratory and field conditions:

$$T_{grade} = T_{ductile\text{-}to\text{-}brittle} - 10 \qquad (9.2)$$

The pavement is not likely to show severe transverse cracking provided that it remains above this limiting temperature for most of its life. The binder shall pass the test if T_{grade} is colder than the specified minimum design temperature for the pavement, T_{spec}. The binder shall fail the test if T_{grade} is warmer than T_{spec}. The user agency shall specify what losses in grade temperature are acceptable for samples conditioned for 24 hours. It is recommended that binders that lose more than 3°C of their minimum permissible in-service temperature after 24 hours of conditioning are only accepted with caution in a lower grade class. It has been shown that some poor quality binders can lose more than 10°C after three days of conditioning (9). The user agency shall use the LTPPBIND® software program for the selection of an acceptable degree of risk in the determination of the minimum pavement design temperature.

9.2.2 *Fracture Energy in Brittle Failure, G_{Ic}* – The fracture energy of the binder is determined at the temperature(s) specified by the user agency. The fracture energy in the brittle state, G_{Ic} in units of J/m^2, is determined from the area under the load versus load-line displacement curve, U in units of Joules, and the cross-sectional area of the fracture specimen, B x W in units of m^2, as follows:

$$G_{Ic} = U/(BW\phi) \qquad (9.3)$$

where ϕ is a calibration factor to account for the presence of the notch. The calibration factor is obtained for both SENB and CT geometries from ASTM method D 5045. The user agency shall specify a limiting value for the fracture energy in the brittle temperature regime. Fracture energies in the brittle state can vary over a wide range, with values from 10-300 J/m^2 not being uncommon (4-7). Hence, the user agency shall make a judicious choice of a limiting fracture energy for the particular load level experienced by the pavement.

9.2.3 *Works of Fracture in Ductile Failure* – The specific essential and plastic works of fracture, w_e and w_p, respectively, are determined from the area under the load versus load-line displacement curves. An accurate determination of this area provides the total work of fracture, W_f, in Joules. W_f is divided by the specimen thickness times the ligament length to obtain the specific total work of fracture, w_f, in J/m^2:

$$w_f = W_f/(l \times b) \qquad (9.4)$$

where l is the ligament length (W-2a) and b is the specimen thickness. The w_f property is plotted versus the ligament length, l, and the data is fitted to a straight line of the following form:

$$w_f = w_e + \beta w_p l \qquad (9.5)$$

where w_e is the specific essential work of fracture, β is a geometric constant that describes the shape of the plastic zone, and w_p is the plastic work of fracture. The method of least squares fitting is used to obtain values for the specific essential work of fracture, w_e, and the plastic work of fracture term, βw_p. For a detailed discussion regarding the basis of the essential work of fracture method, refer to references (2-3).

The user agency shall specify lower limits for the works of fracture at a number of different temperatures and rates of loading. Works of fracture in the ductile state can vary over a wide range, with values for w_e from 2-20 kJ/m^2 and values for βw_p from 0.2-2 MJ/m^3 not being unreasonable for binders tested at 25°C and 100 mm/min (see reference 2 for further details). Hence, the user agency shall make a judicious choice for the limiting works of fracture for the particular load levels experienced by the pavement.

10. REPORT

The user agency shall specify reporting requirements for both Methods A and B.

11. PRECISION AND BIAS

11.1 *Precision* – The precision of the test method has not been evaluated.

11.2 *Bias* – The grading method has not been evaluated for any possible bias with actual field cracking onset and severity. Field validation efforts are currently underway.

12. KEYWORDS

12.1 asphalt binder; polymer-modified asphalt binder; oxidized asphalt binder; low-temperature grading; fracture mechanics; brittle failure; plane-strain fracture toughness; plane-strain fracture energy; critical crack tip opening displacement; fatigue failure; ductile failure; essential work of fracture; plastic work of fracture; in-service performance; performance-based properties; material properties.

13. REFERENCES

(1) Basu, A., Marasteanu, M.O. and Hesp, S.A.M. (2003) Time-temperature superposition and physical hardening effects in low-temperature asphalt binder grading. *Transportation Research Records: Journal of the Transportation Research Board*, TRB, National Research Council, Washington, D.C., in press.

(2) Andriescu, A., Hesp, S.A.M, and Youtcheff, J.S. (2004) On the Essential and Plastic Works of Ductile Failure in Asphalt Binders. *Transportation Research Record: Journal of the Transportation Research Board*, in press.

(3) Mai, Y.-W., Wong, S.-C. and Chen, X.-H. (2000) Application of Fracture Mechanics for Characterization of Toughness of Polymer Blends. In: *Polymer Blends, Volume 2: Performance.* D.R. Paul and C.B. Bucknall (Eds.), John Wiley and Sons, Inc.

(4) Roy, S.D. and Hesp, S.A.M. (2001) Fracture Energy and Critical Crack Tip Opening Displacement: Fracture Mechanics-Based Failure Criteria for Low-Temperature Grading of Asphalt Binders. *Proceedings, Canadian Technical Asphalt Association*, pp. 185-212.

(5) Roy, S.D., and Hesp, S.A.M. (2001) Low-Temperature Binder Specification Development: Thermal Stress Restrained Specimen Testing of Asphalt Binders and Mixtures. *Journal of the Transportation Research Board,* No. 1766, pp. 7-14.

(6) Hoare, T.R., and Hesp, S.A.M. (2000) Low-Temperature Fracture Testing of Asphalt Binders: Regular and Modified Systems. *Journal of the Transportation Research Board,* No. 1728, pp. 36-42.

(7) Anderson, D.A., Champion-Lapalu, L., Marasteanu, M.O., LeHir, Y.M., Planche, J.P. and Martin, D. (2001) Low-Temperature Thermal Cracking of Asphalt Binders as Ranked by Strength and Fracture Properties. *Journal of the Transportation Research Board,* No. 1766, pp. 1-6.

(8) Hesp, S.A.M., Iliuta, S., Marasteanu, M.O., Masliwec, T., and Tam, K.K. (2004) Field validation study of low-temperature performance grading tests for asphalt binders. *Transportation Research Record: Journal of the Transportation Research Board*, in press.

(9) Hesp, S.A.M. (2003) An Improved Low-Temperature Asphalt Binder Specification Method. Final Report, NCHRP-IDEA Contract 84 and Ministry of Transportation Ontario Contract 9015-A-000190, December 2003.